71-9239

Westinghouse

Westinghouse Electric Company
Nuclear Fuel
Columbia Fuel Site
P.O. Drawer R
Columbia, South Carolina 29250
USA

U. S. Nuclear Regulatory Commission
Attn: Mr. E. William Brach, Director
Spent Fuel Project Office
Office of Nuclear Material Safety and Safeguards
United States Nuclear Regulatory Commission
Washington DC, 20555-0001

Direct tel: (803) 647-3552
Direct fax: (803) 695-3964
e-mail: kentna@westinghouse.com

Your ref:
Our ref: NRC-02-005

February 14, 2002

Mr. Brach:

Subject: Docket No. 71-9239, Additional Information for the Application for Timely Renewal of MCC Shipping Container, Package Identification USA/9239/AF

Westinghouse Electric Company hereby submits additional information pursuant to the license renewal for the MCC package. Included are two copies of Revision 10 to the Consolidated License Application for the MCC, which supersedes the Consolidated License Application, submitted in November. Revision 10 contains all changes previously incorporated through the supplements that are listed in the Certificate of Compliance. Also included are the following:

- The March 24, 1997 revision request contained justification information for revising the Gd_2O_3 absorber plate inspection requirements. This justification has been added to Appendix 1-6.
- Administrative corrections to Chapter 6 and Appendix 1-6. Both have been changed to reflect the correct enrichment above which double Gd plates are required. The enrichment will be corrected from 4.75wt% to 4.65 wt%.

In addition, the tables that were included in the October 19, 2001 submittal showing the bases for the License Drawing revisions is resubmitted. Explanations have been added for Note L on MCCL301, and Notes M and N on MCCL401.

Westinghouse again thanks you for your attention to this matter. If you have any questions, please call the undersigned at (803) 647-3552.

Sincerely,

WESTINGHOUSE ELECTRIC COMPANY

Norman A Kent

Norman A. Kent
Licensing
Nuclear Fuel Transport

NMSS/Public

Administrative Corrections to License Drawings

1. MCC-3 License Drawing Revision

MCCL301 series License drawings (Revision 6) have been revised to better identify safety-related items that appear on the drawings. Note that the Bill of Material was moved to new sheet 4 of 4.

Item	Name	Sheet	Balloon Location
60	Base	2 of 4	Zone F2 at Section C-C
61	Upright	2 of 4	Zone F2 at Section C-C
62	Axle	1 of 4	Zone C1
63	Pin	1 of 4	Zone B2
64	Standard Hex Nut	1 of 4	Zone C2
65	Ball Lock Pin	1 of 4	Zone D2
66	Flat Head Screw	1 of 4	Zone G2
67	Pillow Block	1 of 4	Zone C1
68	Lock Nut	1 of 4	Zone G2
69	Drive Rivet	1 of 4	Zone G3
Note L	Pertains to the base (#60) and internal cross frame (#61).		

2. MCC-4 License Drawing Revision

MCCL401 series License drawings (Revision 9) have been revised to better identify safety-related items that appear on the drawings. Note that, due to an administrative error, the MCCL401 series drawings were first revised (Revision 8) to include these administrative corrections, and then revised again (Revision 9) to reference the appropriate Engineering Change Notice. Also, please note that the Bill of Material was moved to new sheet 5 of 5.

Item	Name	Sheet	Balloon Location
65	Base	4 of 5	Zone B2 at Detail A
66	Upright	4 of 5	Zone B2 at Detail A
67	Axle	2 of 5	Zone C1
68	Drive Rivet	4 of 5	Zone B2 at Detail A
69	Pillow Block	2 of 5	Zone C1
70	Top Cross Frame	3 of 5	Zone D8
Note M	Pertains to the horizontal absorber plates. Indicates that they may be added to the package.		
Note N	Pertains to the upright (#66).		

FIGURE WITHHELD UNDER 10 CFR 2.390

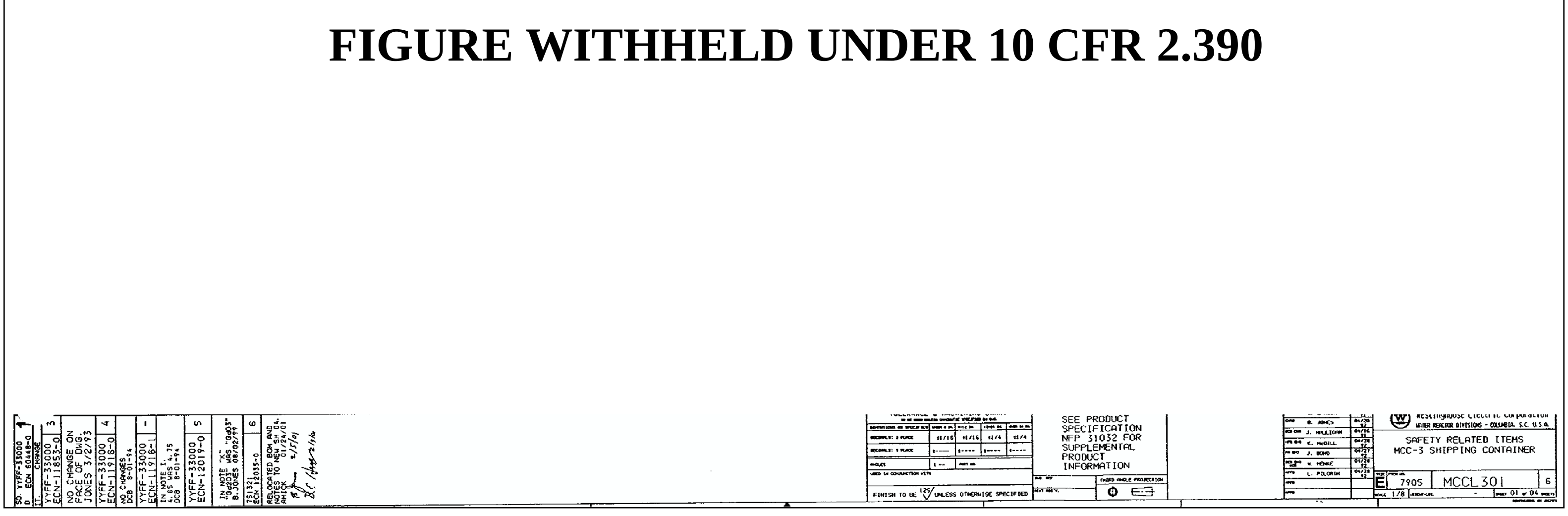

FIGURE WITHHELD UNDER 10 CFR 2.390

TOLERANCE & MACHINING CHART				
DIMENSIONS AS SPECIFIED	OVER 1 IN.	OVER 6 IN.	OVER 30 IN.	OVER 24 IN.
DECIMALS: 2 PLACE	±1/16	±1/16	±1/4	±1/4
DECIMALS: 3 PLACE	±.---	±.---	±.---	±.---
ANGLES	± --			
FINISH TO BE 125 UNLESS OTHERWISE SPECIFIED				

SEE PRODUCT SPECIFICATION NFP 31032 FOR SUPPLEMENTAL PRODUCT INFORMATION

THIRD ANGLE PROJECTION

APVD.	C. LAWSON	04/14 72
CHKD	B. JONES	04/20 72
DES BY	J. HALLIGAN	04/16 72
DWG BY	K. McDILL	04/28 72
TRACED	J. BOND	04/27 72
MCL BK NO.	H. MONGE	04/28 72
APPD	L. PILGRIM	04/28 72

Westinghouse Electric Corporation
WATER REACTOR DIVISIONS - COLUMBIA S.C. U.S.A.

SAFETY RELATED ITEMS
MCC-3 SHIPPING CONTAINER

FROM NO.		
7905	MCCL 301	6

SCALE 1:4 WEIGHT LBS. – SHEET 02 OF 04 SHEETS
DIMENSIONS IN INCHES

FIGURE WITHHELD UNDER 10 CFR 2.390

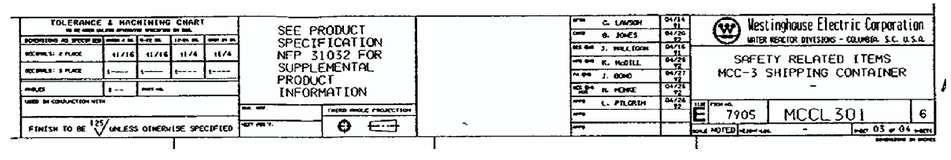

NOTE:
A. B.O. FROM CONTAINER RESEARCH CORPORATION.
B. SKIDS AND STABILIZERS INCLUDED ON BASE WELDMENT (ITEM 01) ARE NOT SAFETY RELATED.
C. B.O. FROM ELASTIC STOP NUT CORP.. OF AMERICA, UNION. N.J.OR APPROVED EQUAL.
D. TWO UNISTRUT RETAINING BRACKETS (ITEMS 12.05 & 06) ON THE BOTTOM SIDE OF THE BOTTOM CLAMP MAY BE OMITTED IF THE CLAMP IS TOO CLOSE TO THE END OF THE UNISTRUT CHANNEL (ITEM 34).
E. ASTM A165 OR APPROVED EQUAL.
F. 1010-1020 CARBON STEEL
G. ASTM-A36
H. MINIMUM YIELD STRENGTH 30,000 PSI
I. FOR ASSEMBLIES WITH ENRICHMENTS GREATER THAN 4.65 BUT LESS THAN 5.00 AN ADDITIONAL ABSORBER PLATE (ITEM 55) WILL BE INCORPORATED INTO THE HORIZONTAL SURFACE OF THE SKIN. (ITEMS 26 & 51)
J. B.O. FROM UNISTRUT CORP. WAYNE. MI. OR APPROVED EQUAL.
K. EACH CONTAINER IS EQUIPPED WITH ABSORBER PLATES MADE FROM CARBON STEEL COATED WITH Gd_2O_3. STL. DIMENSIONS 160.06 X 7.25 X .035.
L. ASTM A500 OR APPROVED EQUAL.

BILL OF MATERIAL

REQ'D. 04	REQ'D. 03	REQ'D. 02	REQ'D. 01	ITEM	GROUP NOTE	IDENT CLASS	PART NAME	(SIZE) REFERENCE INFORMATION	MATL SIZE CODE PART NUMBER OR REF DWG
		-	1	01	A		BASE WELDMENT RCC-3/MCC-3	1010-1020 CS	-
		-	1	02	A		COVER WELDMENT RCC-3/MCC-3	1010-1020 CS	-
		-	30	03	E		T-BOLT	.500-13-2A X 2.00 LG.	-
		-	30	04	E		HEX. NUT	.500-13-2B C.S.	-
		-	AR	05	C/J		STUD NUT	P-2381-S-EG	-
		-	AR	06	C/D		ELASTIC STOP NUT	.500-13 CAT. #79-NE-083	-
		-	4	07	C		ELASTIC STOP NUT	.375-16 CAT. #79-NE-66	-
		-	1	08	F		CLAMP CHANNEL	-----	-
		-	4	09	F		HEX. HD. BOLT	.375-16 UNC X 1.5 LG. C.S.	-
		-	2	10			BALL LOCK PIN TOP CLOSURE	CAT. #CL-8-BLP-2.50-S	-
		-	4	11	F		HEX. HD. BOLT	.500-13 UNC X 4.5 LG. C.S.	-
		-	AR	12	D/J		BRACKET	UNISTRUT RETAINING	-
		-	AR	13			CLAMP FRAME	ASTM A240, TYPE 304	-
		-	AR	14	H		PRESSURE PAD	CARBON STEEL	-
		-	AR	15			SWING BOLT (GRID PRESSURE PAD)	ASTM A36 .500-13 UNC-2A X 4.25	-
		-	AR	16			HEX. NUT	.500-13 AISI 18-8 SS	-
		-	AR	17	F		PIN	CLAMP FRAME/SIDE PIVOT	-
		-	AR	18			BALL LOCK PIN CLAMP FRAME/TOP PIVOT	CAT. #CL-7-BLPT-2.50-S-C	-
		-	AR	19			TOP PIVOT MOUNT	ASTM A36	-
		-	AR	20			SIDE PIVOT MOUNT	ASTM A36	-
		-	AR	21	F		PIN	PAD/SWING BOLT/SNUBBER	-
		-	AR	22			SNUBBER	TOP-ASTM A36	-
		-	AR	23	K		ABSORBER PLATE	------------	-
		-	AR	24			SNUBBER	UPPER SIDE ASTM A36	-
		-	AR	25			SNUBBER	LOWER SIDE ASTM A36	-
		-	1	26	F		SKIN	SUPPORT FRAME	-
		-	2	27	F		RAIL	SUPPORT FRAME TOP RAIL	-
		-	1	28	F		SUPPORT PLATE	SUPPORT FRAME BOTTOM SUPPORT	-
		-	1	29	F		BASE PLATE	SUPPORT FRAME BOTTOM SUPPORT	-
		-	2	30	F		GUSSET	SUPPORT FRAME BOTTOM SUPPORT	-
		-	1	31	F		BASE	TOP CROSS FRAME	-
		-	1	32	F		CROSS FRAME UPRIGHT	TOP CROSS FRAME	-
		-	4	33	F		CLEVIS HALF	TOP CROSS FRAME	-
		-	2	34	J		UNISTRUT CHANNEL (SIDE)	CAT.#P5000 1.625 X 1.357 X.105 THK.	-
		-	1	35	J		UNISTRUT CHANNEL (CENTER)	CAT.#P5000 1.625 X 1.357 X.105 THK.	-
		-	4	36	F		FLAT HD. CAP SCREW	.500-13 UNC X 3.50 LG. C.S.	-
		-	2	37	F		SOC. HD. CAP SCREW	.500-13 UNC X 4.00 LG.	-
		-	1	38	F		SOC. HD. CAP SCREW	.625-11 UNC X 2.00 LG.	-
		-	42	39			BLIND FASTNER (CENTER UNISTRUT)	.25 DIA. FLUSH CS	-
		-	2	40	F		GUSSET	TOP CLOSURE MTG. BRKT.	-
		-	2	41	F		SUPPORT TUBE (1.5 X 2.5 X .25)	TOP CLOSURE MTG. BRKT.	-
		-	2	42	F		PLATE	TOP CLOSURE MTG. BRKT.	-
		-	1	43	F		PRESSURE BAR (1.0 X 1.5 X 13.5)	TOP CLOSURE ASSY.	-
		-	1	44	F		PRESSURE BAR (1.0 X 1.5 X 13.5)	TOP CLOSURE ASSY.	-
		-	1	45	F		PRESSURE BAR (1.0 X 1.5 X 13.5)	TOP CLOSURE ASSY.	-
		-	1	46	F		PRESSURE BAR (1.0 X 1.5 X 13.5)	TOP CLOSURE ASSY.	-
		-	4	47	F		PIN .500 Ø	TOP CLOSURE ASSY.	-
		-	2	48	F		HINGE ANGLE 2 X 2 X .188	TOP CLOSURE CORNER ASSY.	-
		-	8	49	F		HINGE PLATE	TOP CLOSURE CORNER ASSY.	-
		-	6	50	F		FLAT HEAD SCREW	.500-13 UNC X 2.50 LG.	-
		-	1	51	F		SKIN	SUPPORT FRAME	-
		-	2	52	F		HEX. BOLT (CLAMP CHANNEL)	.500-13 UNC-2A X 5.00 LG. C.S.	-
		-	1	53	F		BASE	BOTTOM CROSS FRAME	-
		-	1	54	F		UPRIGHT	BOTTOM CROSS FRAME	-
		-	AR	55	I		ABSORBER PLATE	OPTIONAL	-
		-	AR	56			FLAT HD. SCREW #8 X 1.00	CARBON STEEL	-
		-	AR	57	C		LOCK NUT	79 NM-82	-
		-	AR	58			FLAT HD. SCREW #12 X 1.00	CARBON STEEL	-
		-	AR	59	C		LOCK NUT	79 NM-124	-
		-	6	60	L		BASE	INTERMEDIATE CROSS FRAME	-
		-	6	61	L		UPRIGHT	INTERMEDIATE CROSS FRAME	-
		-	1	62	G		AXLE	CARBON STEEL	-
		-	14	63	G		PIN	INTERNALS	-
		-	4	64			STD HEX NUT	.500-13 CS	-
		-	2	65			BALL LOCK PIN	CL-7-BLPT-2.55-C	-
		-	70	66			FLAT HEAD SCREW	#8-1.00LG CS	-
		2	2	67	G		PILLOW BLOCK	BOTTOM CROSS FRAME	-
		-	70	68			LOCK NUT	79NM82	-
		-	28	69			DRIVE RIVET	CAT NO 38-608-09-91	-

NOTES

1. ALL STRUCTURAL GRIDS ARE RESTRAINED BY A CLAMPING FRAME ASSEMBLY.
2. SEE PRODUCT SPECIFICATION PDSHIP00 FOR ADDITIONAL REQUIREMENTS.
3. MCC-3 CONTAINERS CONVERTED FROM RCC3 DESIGN ARE TO BE INSPECTED PER OCI MCC 938609. ALL NEW PARTS WILL BE FABRICATED AND INSPECTED PER W APPROVED QUALITY ASSURANCE PLAN. (NRC APPROVAL NO. 0708. APPROVED 10/29/90)
4. NEW MCC-3 CONTAINERS (NOT CONVERTED) ARE TO BE FABRICATED AND INSPECTED PER W APPROVED QUALITY ASSURANCE PLAN. (NRC APPROVAL NO. 0708. APPROVED 10/29/90.)
5. WELDING SHALL BE PER MIL-STD-248. WESTINGHOUSE PS82121GA-GB IS EQUAL. SPECIFICATIONS EQUAL OR BETTER MAY BE USED IF APPROVED BY WESTINGHOUSE.

SHIPPING CONTAINER ESTIMATED WEIGHT: 4244# MAX. EMPTY
7544# MAX. LOADED

TOLERANCE & MACHINING CHART				
DIMENSIONS AS SPECIFIED	UNDER 6 IN.	6-12 IN.	12-24 IN.	OVER 24 IN.
DECIMALS: 2 PLACE	±1/16	±1/16	±1/4	±1/4
DECIMALS: 3 PLACE	±----	±----	±----	±----
ANGLES	± --	PART NO.		
USED IN CONNECTION WITH				
FINISH TO BE 125 UNLESS OTHERWISE SPECIFIED				

SEE PRODUCT SPECIFICATION NFP 31032 FOR SUPPLEMENTAL PRODUCT INFORMATION

DWG. REF.
NEXT ASS'Y.
THIRD ANGLE PROJECTION

DFTR	C. LAWSON	04/14/91
CHKD	B. JONES	04/20/92
	J. HALLIGAN	04/18/91
	K. McDILL	04/28/92
	J. BOND	04/27/92
	H. HENKE	04/28/92
APPD	L. PILGRIM	04/28/92
APPD		
APPD		

Westinghouse Electric Corporation
WATER REACTOR DIVISIONS - COLUMBIA, S.C. U.S.A.

SAFETY RELATED ITEMS
MCC-3 SHIPPING CONTAINER

SIZE E | FSCM NO. 7905 | MCCL301 | 6

SCALE 1/8 | WEIGHT LBS. - | SHEET 04 OF 04 SHEETS

DIMENSIONS IN INCHES

CADAM DRAWING DO NOT REVISE MANUALLY

SO. YYFF-33000
D ECN 60448-0
IT. CHANGE
751321
ECN 12035-0
6
ADDED ITEMS 60-69, GR 02 AND NOTE L. AMICK 01/24/01

FIGURE WITHHELD UNDER 10 CFR 2.390

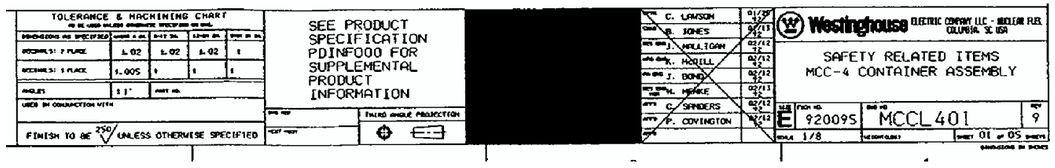

FIGURE WITHHELD UNDER 10 CFR 2.390

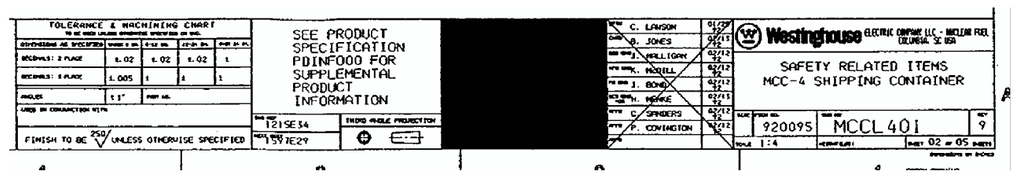

FIGURE WITHHELD UNDER 10 CFR 2.390

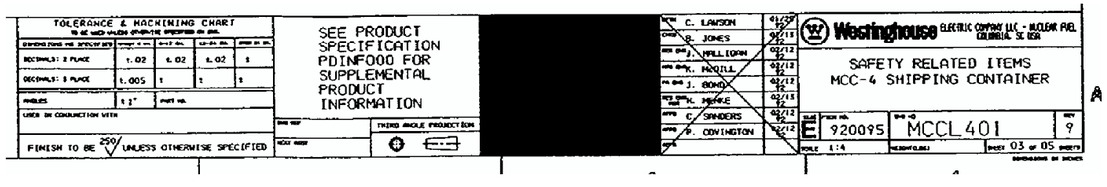

FIGURE WITHHELD UNDER 10 CFR 2.390

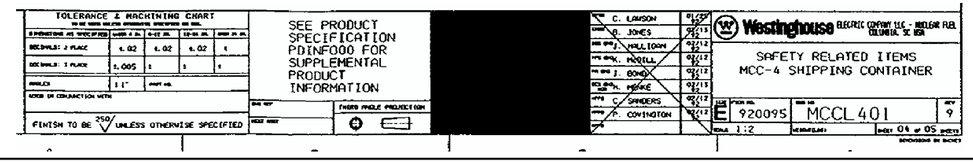

FIGURE WITHHELD UNDER 10 CFR 2.390

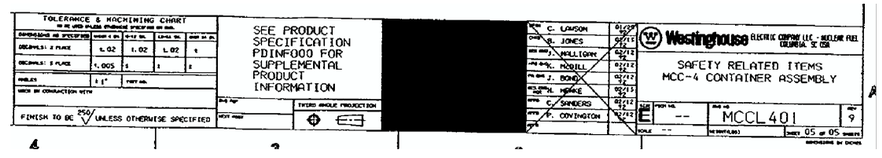

FIGURE WITHHELD UNDER 10 CFR 2.390

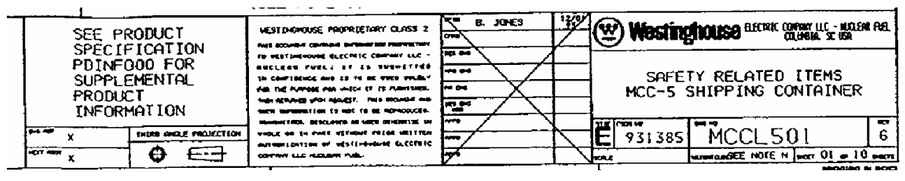

FIGURE WITHHELD UNDER 10 CFR 2.390

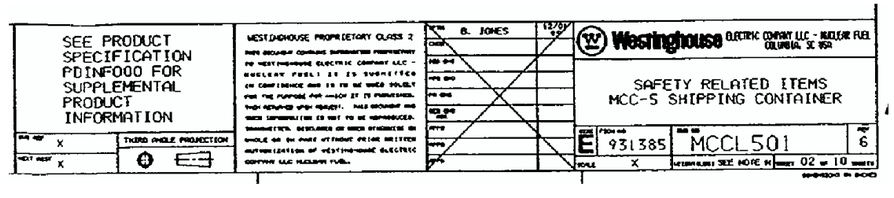

FIGURE WITHHELD UNDER 10 CFR 2.390

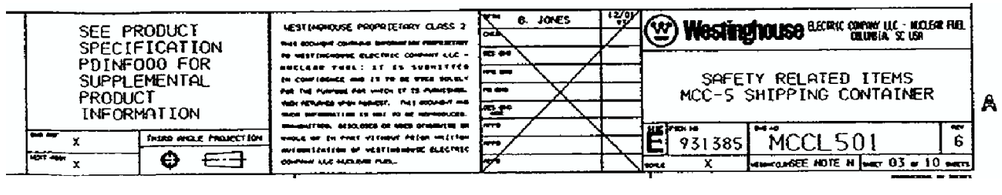

FIGURE WITHHELD UNDER 10 CFR 2.390

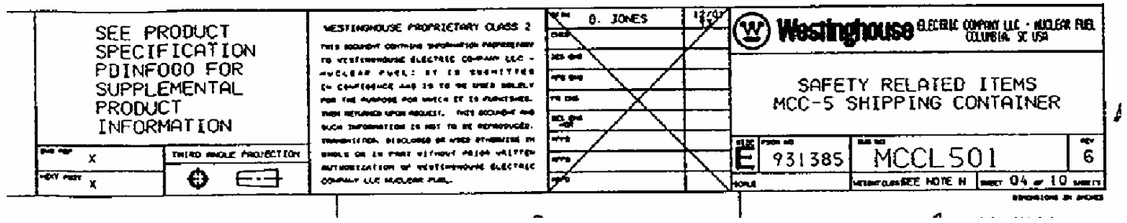

FIGURE WITHHELD UNDER 10 CFR 2.390

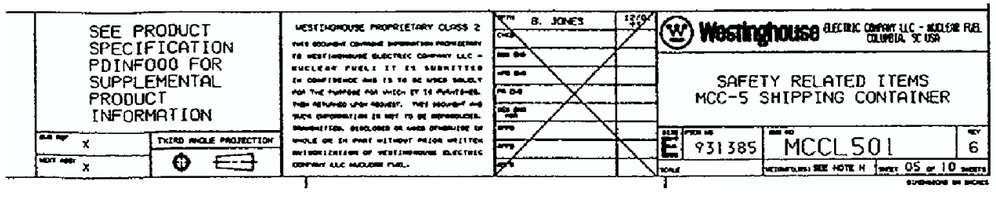

FIGURE WITHHELD UNDER 10 CFR 2.390

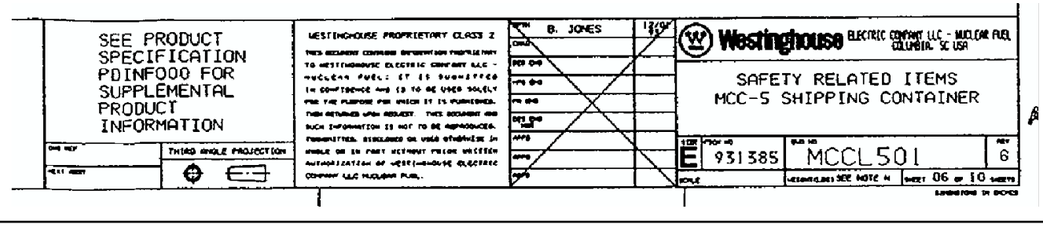

FIGURE WITHHELD UNDER 10 CFR 2.390

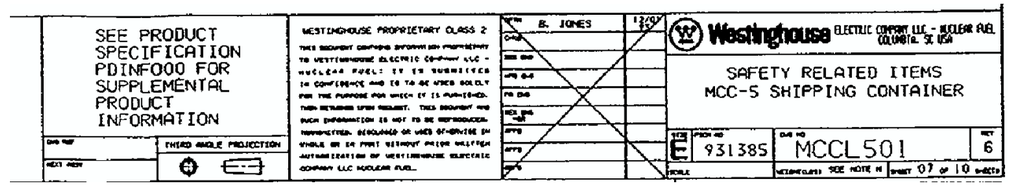

FIGURE WITHHELD UNDER 10 CFR 2.390

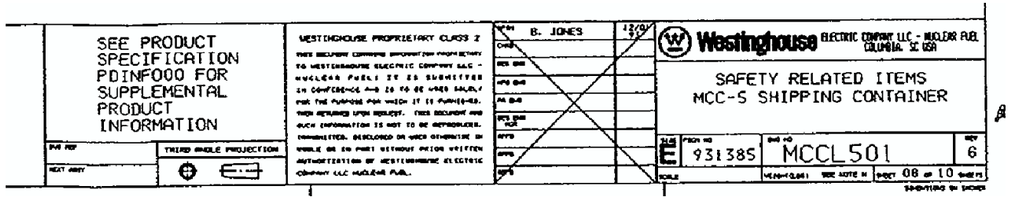

FIGURE WITHHELD UNDER 10 CFR 2.390

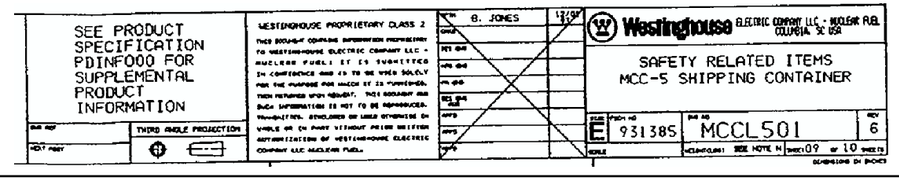

FIGURE WITHHELD UNDER 10 CFR 2.390

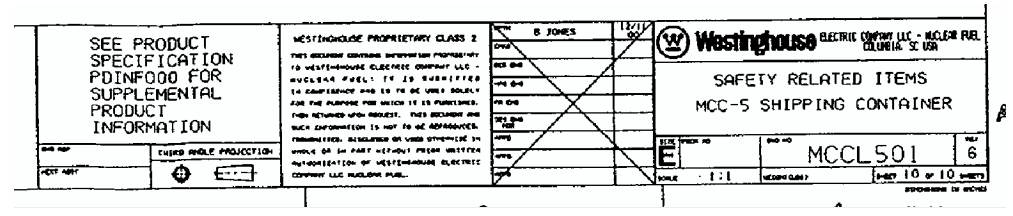

WESTINGHOUSE ELECTRIC COMPANY LLC
NUCLEAR FUEL

APPLICATION FOR APPROVAL OF PACKAGING OF FISSILE RADIOACTIVE MATERIAL (MCC SHIPPING CONTAINERS)

PACKAGE IDENTIFICATION NUMBER USA/9239/AF

Initial Submittal: January 1, 1991
Renewal: February 15, 2002
Expiration: March 31, 2007

U. S. NUCLEAR REGULATORY COMMISSION

DOCKET 71-9239

TABLE OF CONTENTS

TABLE OF CONTENTS

TABLE OF CONTENTS

MCC LICENSE
EFFECTIVE DATE OF REVISIONS

CHAPTER	REVISION	EFFECTIVE DATE
TOC	10	2/15/02
1	10	2/15/02
2	10	2/15/02
3	10	2/15/02
4	10	2/15/02
5	10	2/15/02
6	10	2/15/02
7	10	2/15/02
8	10	2/15/02
APPENDIX	**REVISION**	**EFFECTIVE DATE**
1-1	10	2/15/02
1-2	10	2/15/02
1-3	10	2/15/02
1-4	10	2/15/02
1-5	10	2/15/02
1-6	10	2/15/02
1-7	10	2/15/02
2-1	10	2/15/02
2-2	10	2/15/02
2-3	10	2/15/02
2-4.1	10	2/15/02
2-4.2	10	2/15/02
2-4.3	10	2/15/02
2-4.4	10	2/15/02
2-4.5	10	2/15/02
2-5	10	2/15/02
6-1	10	2/15/02
6-2	10	2/15/02

MCC LICENSE
EFFECTIVE DATE OF REVISIONS

Submittal Date	Reason	NRC Certificate	DOT Certificate (Corresponding NRC CoC)
15 FEB 02	License Renewal. All sections set to Revision 10 Revised Appendix 1-6 to include technical justification contained in Mar 24, 1997 submittal.		

CHAPTER 1: GENERAL INFORMATION

1.1 INTRODUCTION

The Modified Core Component [MCC(-#)] package is to be used for transporting up to two low-enriched uranium fuel assemblies for light water power reactor cores. The nominal number of packages per shipment is to be six. The package classification is to be Fissile Class I.

1.2 PACKAGE DESCRIPTION

1.2.1 PACKAGING

1.2.1.1 MCC-3 Container

Designation - MCC-3 Shipping Container.
Gross Weight - 7544 pounds.
Fabrication - The design and fabrication details for MCC-3 series shipping containers are given in Equipment Specification Addendum E-MCC-676498 and Westinghouse drawing MCCL301; which are included in Appendices 1-1 and 1-2, respectively to this application.
Coolants - Not applicable.

1.2.1.2 MCC-4 Container

Designation - MCC-4 Shipping Container.
Gross Weight - 10,533 pounds.
Fabrication - The design and fabrication details for MCC-4 series shipping containers are given in Equipment Specification Addendum E-MCC-953511 and Westinghouse drawing MCCL401; which are included in Appendices 1-1 and 1-2, respectively to this application.
Coolants - Not applicable.

1.2.1.3 MCC-5 Container

Designation - MCC-5 Shipping Container.
Gross Weight - 10,533 pounds.
Fabrication - The design and fabrication details for MCC-5 series shipping containers are given in Equipment Specification Addendum E-MCC-953511 and Westinghouse drawing MCCL501; which are included in Appendices 1-1 and 1-2, respectively to this application.
Coolants - Not applicable.

1.2.2 OPERATIONAL FEATURES

Not applicable.

1.2.3 CONTENTS OF PACKAGING

1.2.3.1 MCC-3 Container - Contents Description

Identification and Enrichment of Special Nuclear Material (SNM) - The SNM will be unirradiated uranium enriched up to 5 w/o in the isotope U-235. Nominal weight-percent quantities of principal radionuclides, at maximum enrichment, are -- ^{234}U: 0.044; ^{235}U: 5.000; ^{236}U: 0.004; ^{238}U: 94.952. Radionuclide quantity details are included in Appendix 1-3 to this application.

Form of SNM - The SNM will be in the form of clad fuel assemblies. In the clad form, the assemblies will not disruptively react or decompose at the Accident Thermal Condition. No chips, powders, or solutions will be offered for transport in this packaging. Specific data on maximum assembly parameters are included in Appendix 1-4 to this application.

Neutron Absorbers, etc. - For fuel assemblies containing enrichments greater than the limiting enrichment dictated by the limiting reactivity value, integral assembly neutron absorbers may be included as necessary to meet the limit. Specific information concerning such absorbers is included in Appendix 1-5 to this application. Neutron absorber plates, consisting of carbon steel, with Gd_2O_3 affixed to each side of the plate, are mounted in the packaging. Two permanently mounted plates are installed such that they are between the contained fuel assemblies. Additional such plates may be installed beneath the contained fuel assemblies, as required to meet the limiting reactivity value. The installation is such that the presence of the neutron absorber plates may be readily detected by visual examination. Specific information concerning the Gd_2O_3 neutron absorber plates is included in Appendix 1-6 to this application.

Maximum Weight of Fissile Contents - 51.2 Kg ^{235}U.

Maximum Net Weight of Contents - 3300 pounds.

Maximum Decay Heat - Not applicable.

The contents will be loaded in such a fashion that if the package were to be flooded

and subsequently drained, any water which may have penetrated the contents would drain simultaneously.

1.2.3.2 MCC-4 Container - Contents Description

The contents description for the MCC-3 container is directly applicable to the MCC-4 container, except as follows:

Maximum Weight of Fissile Content - 59.7 Kg ^{235}U.
Maximum Net Weight of Contents - 3870 pounds.

1.2.3.3 MCC-5 Container - Contents Description

The contents description for the MCC-3 container is directly applicable to the MCC-5 container, except as follows:

There are Gd_2O_3 neutron absorber plates which are permanently installed in the MCC-5 container: the two, previously described, which are installed between the two assemblies; and segmented plates which are installed under the strongback. Additional vee-shaped plates may be installed beneath the contained fuel assemblies as required to meet the limiting reactivity value.

Maximum Weight of Fissile Content - 52 Kg ^{235}U.
Maximum Net Weight of Contents - 3700 pounds.

The MCC-5 package is essentially identical in design and size as the MCC-4 package, but with several minor notable differences. The significance of these minor differences is addressed in Sections 6 and 7, and Appendices 1-1, 1-2, 2-1, 2-5, 6-1, and 6-2. A specific list of the minor differences is provided in Appendix 1-7, Design Comparison of the MCC-5 Package to the MCC-4 Package.

1.3 APPENDIX

The following are appended to this application:

Appendix 1-1: Container Equipment Specifications.
Appendix 1-2: Container Drawings.
Appendix 1-3: Radionuclide Quantities.
Appendix 1-4: Fuel Assembly Parameters.
Appendix 1-5: Assembly Neutron Absorber Specifications.
Appendix 1-6: Gd_2O_3 Neutron Absorber Plates Specifications.
Appendix 1-7: Design Comparison of the MCC-5 Package to the MCC-4 Package.

CHAPTER 2: STRUCTURAL EVALUATION

2.1 STRUCTURAL DESIGN

2.1.1 Discussion

The design of the MCC series of unirradiated fuel shipping containers is basically the same for all models. The fundamental differences between models are length and weight. All containers consist of a container shell (base and cover) and an internals assembly. Positive closure of the shell base and cover is accomplished by means of high strength bolts. The number of bolts is proportional to the length of the container, thus maintaining the loading per bolt at a nominal value that is well below the bolt's ultimate strength. Both the shell design and bolts have been subjected to the drop conditions of 10CFR71 without failure. Therefore, these designs are more than adequate to withstand the loads experienced during normal conditions of transport. See the Westinghouse container drawings, for details of these designs, which are included as Appendix 1-2 to this application.

2.1.2 Design Criteria

The design of the MCC Series of containers complies with structural requirements of 10CFR71. This is accomplished through the application of design criteria which permits no yielding of the container shell under a static loading of 5 times the weight of the loaded package, and no yielding of the internals assembly under static loadings of 6 times the expected maximum weight of the package contents.

The MCC container design has been demonstrated to comply with the hypothetical drop accident conditions of 10CFR71. An MCC container, loaded to 100 percent of expected maximum weight of contents, was subjected to the drop conditions. This drop test did not produce a configuration more reactive than that analyzed in the criticality evaluation.

Since the containers are fabricated from carbon steel, the following yield stress values are used:

Tensile Yield Stress:	30000 psi
Shear Yield Stress:	15000 psi
Weld Shear Yield:	13600 psi

2.2 WEIGHTS AND CENTERS OF GRAVITY

The weights and centers of gravity for the MCC containers are tabulated and presented in Appendix 2-1 to this application.

2.3 MECHANICAL PROPERTIES OF MATERIALS

The structural materials used in the MCC series of containers consists of AISI 1010-1020, ASTM A36, ASTM A240, and ASTM A283 steels. Mechanical properties for ASTM materials are found in the respective ASTM Specifications; mechanical properties for the AISI 1010-1020 material is section 2.1.2 of this chapter. Material properties of the load suspension system are provided in Appendix 2-2 to this application.

2.4 GENERAL STANDARDS FOR ALL PACKAGES

2.4.1 Chemical and Galvanic Reactions

The MCC container is fabricated from structural steel, and the fuel assemblies are fabricated from stainless steels and zircaloy; thus, no potential exists for chemical or galvanic reactions to occur.

2.4.2 Positive Closure

The MCC container is positively closed by means of high strength bolts which require use of tools and deliberate action to facilitate their removal. The number, type, and size of these bolts is provided on the drawings included in Appendix 1-2 to this application.

2.4.3 Lifting Devices

The lifting attachments that are a structural part of the MCC container shell are designed with a minimum safety factor of 4 against yielding when used to lift the loaded container in the intended manner.

2.4.4 Tiedown Devices

Tiedown attachments that are a structural part of the MCC container shell are designed to be capable of withstanding a static force applied to the center of gravity of the loaded container having:

(1) A vertical component of 2 times the weight of the loaded container;

(2) A horizontal component, along the transport vehicle forward direction, of 10 times the weight of the loaded container; and,

(3) A horizontal component, in the transverse direction, of 5 times the weight of the loaded container.

2.5 STANDARD FOR TYPE B AND LARGE QUANTITY PACKAGING

Not Applicable.

2.6 NORMAL CONDITIONS OF TRANSPORT

The performance requirements specified in Subpart F of 10 CFR 71 for normal conditions of transport are met by the MCC containers. This regulatory compliance is demonstrated in the following subsections where each normal condition is addressed and shown to meet the applicable regulatory criteria. Detailed supporting information can be found in Appendix 2-3.

2.6.1 Heat

Chapter 3 of this application concludes that the normal heat conditions specified in 10 CFR 71.71(c)(1) will have negligible effects on the MCC containers.

2.6.1.1 Summary of Pressures and Temperatures

There is no pressure seal in the MCC containers. Therefore, there is no pressure build up within the container. The unirradiated fuel assemblies under the required 10CFR71 sun conditions develop temperatures of less than 200 °F for the components of the MCC containers.

2.6.1.2 Differential Thermal Expansion

The differential thermal expansion for the MCC containers is negligible. The greatest differential is between the outer shell and the internals -- 0.188 inches. This differential creates very little stress as it is accommodated by the vibration isolators. Details can be found in Appendix 2-3.

2.6.1.3 Stress Calculations

Due to the lack of hard restraints within the container and the fact that it does not have pressure seals, the package will not develop any significant stresses due to normal conditions of transport for heat per section 71.71(c)(1) of 10 CFR 71.

2.6.1.4 Comparison with Allowable Stresses

The heat conditions of 10CFR71.71(c)(1) do not create any significant stresses within the package. Therefore, allowable stress limits are not exceeded.

2.6.2 Cold

The cold conditions specified will not adversely affect the performance of the package. Due to the materials of construction and the dimensions of the material's cross section, brittle fracture is not a concern.

2.6.3 Pressure

Since the package is not sealed against pressure, there can not be any significant differential pressure. However, information presented in Appendix 2-3 demonstrates that the package could withstand the differential pressure described in 10 CFR 71.71 if the containers were sealed.

2.6.4 Vibration

Analyses presented in Appendix 2-3 demonstrate that the package has a sufficient margin of safety to resist the loads imposed by shock and vibration incident to normal conditions of transport per 10 CFR 71.71 (c)(5).

2.6.5 Water Spray

The water spray requirement of 10 CFR 71.71(c)(6) will have no effect on the MCC containers since the exterior is constructed of steel.

2.6.6 Free Drop

The MCC containers weigh less than 11,000 lbs (5,000 kg). The 30-foot drop required in the Hypothetical Accident conditions section 10 CFR 71.73 (c)(1) is substantially more than the required free drop of four feet by 10 CFR 71(c)(7). Section 2.7.1 demonstrates the containers' survivability and bounds the free drop requirements of 10 CFR 71.71 (c)(7). Due to the nature of the payload, any event that would come close to approximating the free drop would cause the containers to be completely re-examined before continuing in service.

2.6.7 Corner Drop

The MCC containers are fabricated mainly of steel and exceed 110 pounds gross weight. Therefore, the corner drop test requirement of 10 CFR 71.71 (c)(8) is not applicable.

2.6.8 Penetration

The penetration test of a 13-lb steel rod dropped 40 inches has insufficient energy to effect the performance of the package. The test will have a negligible effect on the

steel outer shell and will not have any effect on the containers ability to maintain a sub-critical geometry.

2.6.9 Compression

The compressive load requirement of 10 CFR 71.71 (c) (9) is easily met by the MCC containers. Details of the analysis can be found in Appendix 2-3.

2.7 HYPOTHETICAL ACCIDENT CONDITIONS

The performance criteria specified in Subpart E of 10 CFR 71 are met when the MCC containers are subjected to the hypothetical accident conditions specified in 10 CFR 71.73. The packages' ability to meet the design criteria discussed in Section 2.1.2 for the various accident conditions is discussed below. Detailed evaluations for the various conditions is presented in Appendix 2-4.1. Results of full scale testing of a container is presented in Appendix 2-4.3.

The basic criteria for the container is that, in a post-accident condition, integrity and spacing for criticality safety purposes must be met. The shell must stay attached (integrity) -- both to assure that contained assemblies can only be exposed to full-density water (i.e., flooding) and not partial-density water (e.g., water sprays); and, to prevent the clamp frames from lining up side-by-side such that spacing requirements between two containers would be compromised. Further, the fuel and gadolinium absorber plates must remain restrained (integrity); and, container damage dimensions must not be such that spacing requirements between two containers would be compromised.

2.7.1 Free Drop

10 CFR 71.73 (c)(1) of Subpart F requires that a package withstand a drop from a height of 30-feet (9 meters) onto a flat, essentially unyielding, horizontal surface. The package is to strike the surface in a position for which maximum damage is expected. To evaluate which position would cause the most damage several positions were considered. The side drop with the top down was considered to cause the greatest loads per clamp frame, which could cause a failure of the clamp frame, or the connections, in such a manner that the fuel would be free. The other condition that could have the same effect would be the side drop on the corner of the clamp frames. To maximize the damage in this orientation, an oblique drop that would create high loads due to slapdown was considered. The other orientation of interest was the side drop on the closure flange. This orientation would create the greatest loadings on the closure T-bolts. Failure of sufficient bolts to allow the bottom (containing internals) to separate from the cover was the concern.

It is shown in Appendix 2-4 that for all orientations the containers have an adequate margin of safety against either the fuel assemblies becoming free or the outer shell separating from the container. These margins were confirmed by full-scale testing. The details of the evaluation and confirmatory testing can be found in Appendix 2-4.

2.7.1.1 End Drop

The end drop does not impose any load on the MCC containers that will cause the fuel to separate from the clamp frames or separate the closure. Therefore, the end drop does not influence the criticality spacing of the package. Supporting evaluations can be found in Appendix 2-4.1.

2.7.1.2 Side Drops

2.7.1.2.1 Side Drop onto Container Top

The restraint of the fuel and the necessary spacing is maintained in this orientation. The clamp frame and snubber assembly adequately hold the fuel and easily maintain the spacing. This is demonstrated in the evaluation shown in Appendix 2-4.1. Confirmation of the evaluation is found in the testing of the package described in Appendix 2-4.3.

2.7.1.2.2 Side Drop with Slapdown onto Internal Clamp Frames

The oblique drop, which puts the greatest load onto the clamp frames, imparts significant damage on both the external shell and the internals. This damage is localized, allowing redundancy in the container design to maintain restraint of the fuel in the clamp frame and within the external package. Details of this evaluation are in Appendix 2-4.1. Justification of the impact angle is located in Appendix 2-4.2. Confirmation testing results are in Appendix 2-4.3.

2.7.1.2.3 Side Drop onto Package Closure

The side drop onto the package closure imparts the greatest separation moments to the package closure. The evaluation in Appendix 2-4.1 demonstrates that the package closure has adequate margin to keep the outer shell together. Due to the construction of the package, various mechanisms apply loads to the closure T-bolts during the impact. These are evaluated in detail in Appendix 2-4.1. Confirmation of the adequacy of the closure was demonstrated by full scale testing discussed in Appendix 2-4.3.

2.7.1.3 Corner Drop

The corner drop event will impart loads into the container that will result only in localized damage that does not influence the overall criticality spacing which is of concern. The actual loads imparted into the components of concern are bounded by the side impacts and the oblique drop.

2.7.1.4 Oblique Drops

The results of the oblique drop evaluation are covered in Section 2.7.1.2.2. Details of the evaluation can be found in Appendix 2-4.1. Justification for the angle of impact evaluated is in Appendix 2-4.2. Conformational testing results are located in Appendix 2-4.3.

2.7.1.5 Summary of Results

The evaluations of the various drop orientations, and the resulting damage, demonstrates that the containers have adequate margin to maintain restraint of the fuel and integrity of the closure, to maintain spacing between adjacent fuel assemblies. Significant localized damage occurs that does not influence the overall spacing. Further discussion of the damage can be found in Appendix 2-4.

2.7.2 Puncture

Due to the localized nature of the puncture impact, the pin puncture will not change the ability of the container to maintain the criticality spacing of the fuel assemblies. In addition, due to the redundancy in the containers' design, any single component that could be destroyed by the puncture event, such as a clamp frame or connection, would not change the effectiveness of the package. Therefore, the puncture event described in 10 CFR 71.73(2) is not a controlling condition for the MCC containers.

2.7.3 Thermal

The thermal evaluation of the MCC containers for the hypothetical accident heat condition is discussed in Chapter 3.

2.7.3.1 Summary of Pressure and Temperatures

The accident case pressure is assumed to be 0 psig since the container is not sealed. The fuel rods are designed to withstand a maximum temperature of 2,200 °F without substantial damage. During the accident fire condition, it is assumed that all combustible components are burned away.

2.7.3.2 Differential Thermal Expansion

Because of the thin components and the isolation of the internal structure from the external structure, the accident case thermal loads will not develop thermal gradients of a sufficient magnitude to result in significant thermal stress.

2.7.3.3 Stress Calculations

Due to the construction of the MCC containers, there are no significant stresses developed by the thermal gradients.

2.7.3.4 Comparison with Allowable Stresses

The negligible stresses are significantly lower than any of the allowable stresses.

2.7.4 Water Immersion

Since the MCC containers are not sealed against pressure, there will not be any significant differential pressure with the water immersion loads defined in 10 CFR 71.73(5). The water immersion will have little effect on the container or payload.

2.7.5 Summary of Damage

The most significant damage to the package comes from the free drop and the thermal event. Portions of the clamp frames and closure T-bolts are damaged and become ineffective. Since the system is highly redundant, sufficient clamp frames and closure T-bolts remain intact in all cases to provide restraint of the fuel assemblies and maintain closure. Details of the damage to the packages from the drop events can be found in Appendix 2-4. It is assumed that the accident thermal load will burn away all combustible material in the package, including the shock mounts. This assumption allows the internal structure (with the restrained fuel) to contact the outer shell, but remain within the outer shell. The upper and lower external shell assemblies stay together, retaining the fuel inside. The gadolinium plates within the internal structure will remain intact and maintain their relative position to the fuel.

2.8 SPECIAL FORM

Not applicable.

2.9 FUEL RODS

Fuel rod cladding is considered to provide containment of radioactive material under both normal and accident test conditions. Discussion of this cladding, and its ability to maintain sufficient mechanical integrity to provide such containment, is described in Chapter 4, "Containment," of this application.

2.10 APPENDIX

The following are appended to this application:

Appendix 2-1: Container Weights and Centers of Gravity
Appendix 2-2: Container Load Suspension System
Appendix 2-3: Calculations and Evaluations Relating to Assessment of Normal Conditions of Transport
Appendix 2-4: Calculations and Evaluations Relating to Assessment of Hypothetical Accident Conditions
Appendix 2-5: Structural Calculations and Evaluations Relating to the Assessment for Transportation of VVER 1000 Fuel.

CHAPTER 3: THERMAL EVALUATION

The MCC container is limited to use for transporting unirradiated, low enriched uranium, nuclear reactor core assemblies. Therefore, thermal engineering design of the packaging, per se, is not necessary. The fuel rods, that contain the radioactive material, are designed to withstand temperatures of 1204°C (2200°F) without substantial damage. All combustible components of the container internals (e.g., the shock mounts) are postulated to have burned away for the criticality evaluation.

CHAPTER 4: CONTAINMENT

4.1 CONTAINMENT BOUNDARY

The MCC container is limited to use for transporting unirradiated, low enriched uranium, nuclear reactor core assemblies. The radioactive material, bound in sintered pellets having very limited solubility, has minimal propensity to suspend in air. These pellets are further sealed into cladding, to form the fuel rod portion of each assembly. The principal containment boundary for the MCC container is the fuel rod cladding. Design and fabrication details for this cladding are given in Appendix 1-4 to this application.

4.2 REQUIREMENTS FOR NORMAL CONDITIONS OF TRANSPORT

The nature of the contained radioactive material, and the structural integrity of the fuel rod cladding and container shell, are such that there will be no release of radioactivity under normal conditions of transport.

4.3 CONTAINMENT REQUIREMENTS FOR THE HYPOTHETICAL ACCIDENT CONDITION

The nature of the contained radioactive material, and the integrity of the fuel rod cladding and container shell, are such that there will be no substantial release of radioactivity under hypothetical accident conditions. It is estimated that, as a result of the puncture condition, the maximum radioactive material released from damaged fuel rods might be some 450 equivalent ceramic pellets, which represents some 4000 grams of uranium with a maximum specific activity of 2.8×10^{-6} curies/gram.

4.4 APPENDIX

The following is appended to this application:

Appendix 1-4: Fuel Assembly Parameters.

CHAPTER 5: SHIELDING EVALUATION

The MCC container is limited to use for transporting unirradiated, low enriched uranium, nuclear reactor core assemblies. Therefore, shielding design of the packaging, per se, is not necessary. Typical maximum dose equivalent rates are 2.0 millirem per hour, at any point on the external surface of the container, and 0.8 millirem per hour at one meter from the external surface of the container.

CHAPTER 6: CRITICALITY EVALUATION

6.1 DISCUSSION AND RESULTS

The contents of an MCC container are to be so limited that, for contained fuel assemblies having a ^{235}U enrichment up to and including five weight-percent (5 wt% ^{235}U), the limiting K_{eff}, with bias and uncertainties included at the 95-percent confidence level, will not exceed 0.95 -- in the most reactive credible configuration, moderated by water to the most reactive credible extent, and closely reflected by water on all sides. Also considered are the effects of fuel pin gap flooding and annular fuel blankets. No consideration of dispersible material is required, since the contents are limited to clad ceramic fuel forms.

A primary objective of the criticality evaluation is to determine: (1) What is the limiting enrichment (wt% ^{235}U) for two fuel assemblies, without added assembly neutron absorbers, to be shipped in an MCC container having only the permanent container neutron absorber plate. For assemblies having greater than this limiting enrichment, up to and including 5 wt% ^{235}U, either additional assembly neutron absorbers (i.e., coated pellets or cluster absorber rods), or additional container neutron absorber plates, are options. Thus, a secondary objective of the criticality evaluation is to determine: (2) When the additional assembly neutron absorber option is selected, what is the minimum number of additional absorber rods, per assembly, or when the additional container neutron absorber plate option is selected, what is the required nature and placement of the additional plates.

Significant criticality engineering design features are incorporated into the MCC container to assure that, in the event of a transport accident, structural integrity is maintained, and the assemblies will remain in a subcritical geometry. These structural features are presented in detail in Appendix 1-1. Briefly, the design assures that the container:

1) will not open along the closure flange,

2) internals will hold the contents in place,

3) neutron absorber plates will remain in place; and

4) will not experience any deformation (compression) which would serve to reduce the spacing between adjacent pairs of fuel assemblies to less than the limiting spacing value.

During normal conditions of transport, there will be a minimum of 12-inches of separation between the contents of any two containers. Any number of undamaged, unflooded MCC containers will be subcritical, since unmoderated uranium enriched to 5

wt% or less in ^{235}U is subcritical in any quantity under any conditions. Any number of undamaged but flooded containers will also have a K_{eff} less than or equal to 0.95, since 12-inches of water separation provides isolation between the contents of any two containers; and, if the water external to the container is removed, then the contents will also drain so that the array returns to the unmoderated condition.

The Hypothetical Accident Condition array can be reduced to only two containers, crushed top-to-top, such that the spacing between the pairs of assemblies, aligned parallel to each other, will be reduced to 8.178 inches (8 inches of water plus two shell thicknesses). This array is then assumed to be flooded (since drop tests have demonstrated that damaged containers remain substantially closed, exposure of the contained assemblies to less than full density water is not considered credible; however, calculations are included in Appendix 6-2 which show that subcriticality is also maintained at partial water densities). The heavy structural members of the base and the internal component support structures of the container are assumed to provide sufficient spacing such that any other container(s) in the shipment would be isolated from this combination by a minimum of 12-inches of water. Since only two containers will combine to form the HAC array with a K_{eff} less than or equal to 0.95, and any isolated additional containers can only form similar isolated arrays, any number of the MCC containers will be subcritical under the HAC. That is, the number "N" of undamaged packages, with nothing between the packages, that would be subcritical; and, the number "N" of damaged packages, if each package were subjected to the HAC with interspersed hydrogenous moderation, that would be subcritical -- are both equal to infinity.

The calculations were performed using the AMPX cross-section generation modules, NITAWL-S and XSDRNPMS, and the Monte Carlo code KENO-Va for reactivity determination. The requirement that the fuel be in assemblies in a fixed array assures that these calculations are accurate and directly applicable.

Appendix 6-1 includes a sample KENO input deck and the calculated K_∞ results of the uncontained fuel with attributes identified in Appendix 1-4. Based on these results, the assemblies are classified into three groups; Type A assemblies have uncontained K_∞'s less than 0.936, which encompasses all the 14x14 and 16x16 assembly lattice designs; Type B assemblies have uncontained K_∞'s greater than 0.936 and include all the 15x15 and 17x17 lattice designs; the Type C assembly is the VVER-1000 fuel assembly which has an uncontained K_∞ of 0.9432.

Appendix 6-2 includes sample decks and calculations for contained Type A and B fuel assemblies. For the Type A assemblies, the 14x14 OFA (optimized fuel assembly) is used exclusively for the contained calculations since this assembly was shown to be the most reactive of the Type A designs. The calculations show that Type A assemblies can be shipped with enrichments up to 5.0 wt% without the use of additional assembly neutron absorbers or additional container neutron absorber plates.

For Type B assemblies, the 17x17 OFA is used exclusively for the contained calculations since this assembly was shown to be more reactive than the other Type B designs. As with Type A assemblies, Type B assemblies can also be shipped without the use of additional neutron absorbers provided the enrichments are restricted to 4.65 wt% or less. For Type B assemblies with enrichments greater than 4.65 wt%, additional neutron absorbers are required. Any of the following types and numbers of absorbers have been shown to be acceptable:

1) Assembly IFBA Rods: A minimum of 32 nominally (1X) loaded fuel rods are required in each assembly, each with a minimum coating length of 108 inches. For increased IFBA loadings (1.5X, 2X, etc.), the number of loaded fuel rods required can be reduced by the ratio of the increased loading to the nominal loading.

2) Assembly Absorber Rods: A minimum of 4 absorber rods are required in each assembly. The rods can be Pyrex BA, WABA, or Ag-In-Cd designs with a minimum length of 108 inches. The rods must be positioned within the assemblies in a symmetric pattern about the assembly center guide tube.

3) Container Absorber Plates: A minimum of 2 additional Gadolinia coated absorber plates, having the same specifications as the permanent container absorber plate, are required. The additional plates must be positioned directly below the strongback, underneath each assembly.

For the Type C assembly, the VVER-1000 is used exclusively for the contained calculations. The Type C assembly can be shipped without the use of additional neutron absorbers provided the enrichments are restricted to 4.80 wt% or less. For the Type C assembly with an enrichment greater than 4.80 wt%, additional neutron absorbers, described below, are required. It should be noted that the MCC-5 container used for the VVER-1000 assembly has permanent absorber plates between the assemblies, just as the MCC-3 and MCC-4 containers do, and permanent absorber plates under the strongback.

Any of the following types and numbers of absorbers have been shown to be acceptable:

1) Assembly IFBA rods: A minimum of 24 nominally (1X) coated fuel rods are required in each assembly, each with a minimum coating length of 108 inches. With increased IFBA loadings (1.5X, 2X, etc.), the number of loaded fuel rods required can be reduced by the ratio of the increased loading to the nominal loading.

2) Assembly Absorber Rods: A minimum of 4 absorber rods are required in each assembly. The rods can be WABA or Ag-In-Cd designs with a minimum length of 108 inches. The rods must be positioned within the assemblies in a symmetric

pattern about the assembly center guide tube.

3) Guide Support Absorber Coating: A minimum coating of 0.027 grams of Gd_2O_3/cm^2 on the underside of the guide supports is required. The guide supports sit on the strongback and are located between the grid supports.

6.2 PACKAGE FUEL LOADING

The MCC container fuel loading configurations and parameters for normal transport conditions are included in Appendix 1-4 to this application. The configurations and parameters for the Hypothetical Accident Condition are included in Appendix 6-2 to this application.

6.3 MODEL SPECIFICATION

6.3.1 DESCRIPTION OF CALCULATIONAL MODEL

Figures 6-1 and 6-2 present a geometric description of the criticality model for the unpackaged fuel assembly evaluation, with a 17x17 OFA assembly and a VVER-1000 assembly shown respectively. The attributes of these fuel assembly designs, as well as all the other fuel assembly designs, are described in Appendix 1-4. In the unpackaged fuel assembly evaluation, each assembly is modeled as infinite in length and surrounded by 6-inches of water. The boundary conditions for all surfaces are conservatively chosen to be fully reflective (zero current), which precludes any neutron leakage from the array. With reflective boundary conditions, the calculation model actually represents an infinite array of single assemblies separated from each other by 12 inches of water. However, since twelve inches of water is sufficient to effectively isolate each assembly from its neighbors, the reactivity of the infinite array is the same as the reactivity of a single assembly.

FIGURE 6-1

UNPACKAGED 17 OFA FUEL ASSEMBLY MODEL

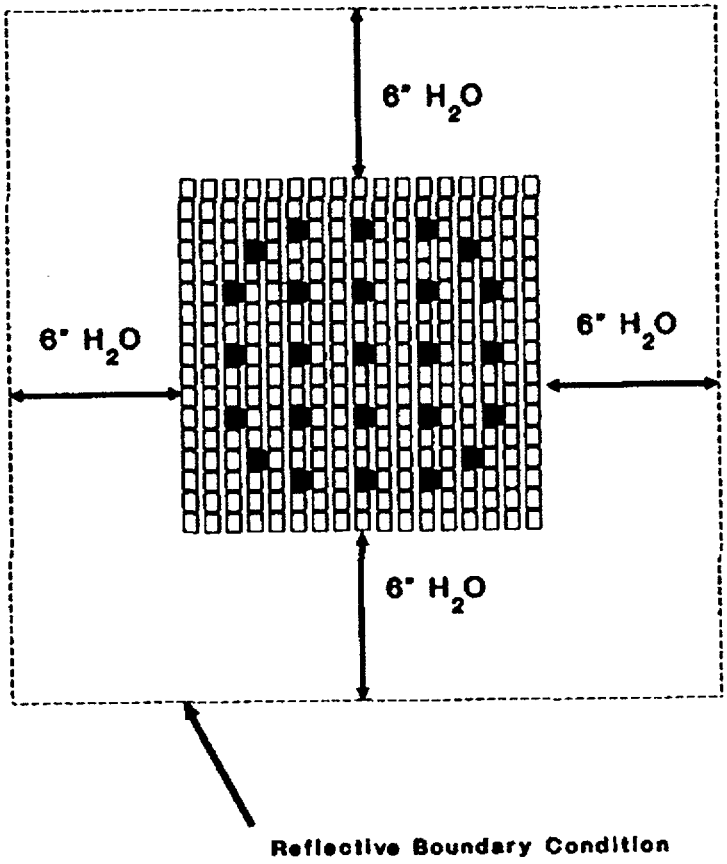

FIGURE 6-2

DIAGRAM OF KENO UNCONTAINED VVER-1000 ASSEMBLY MODEL

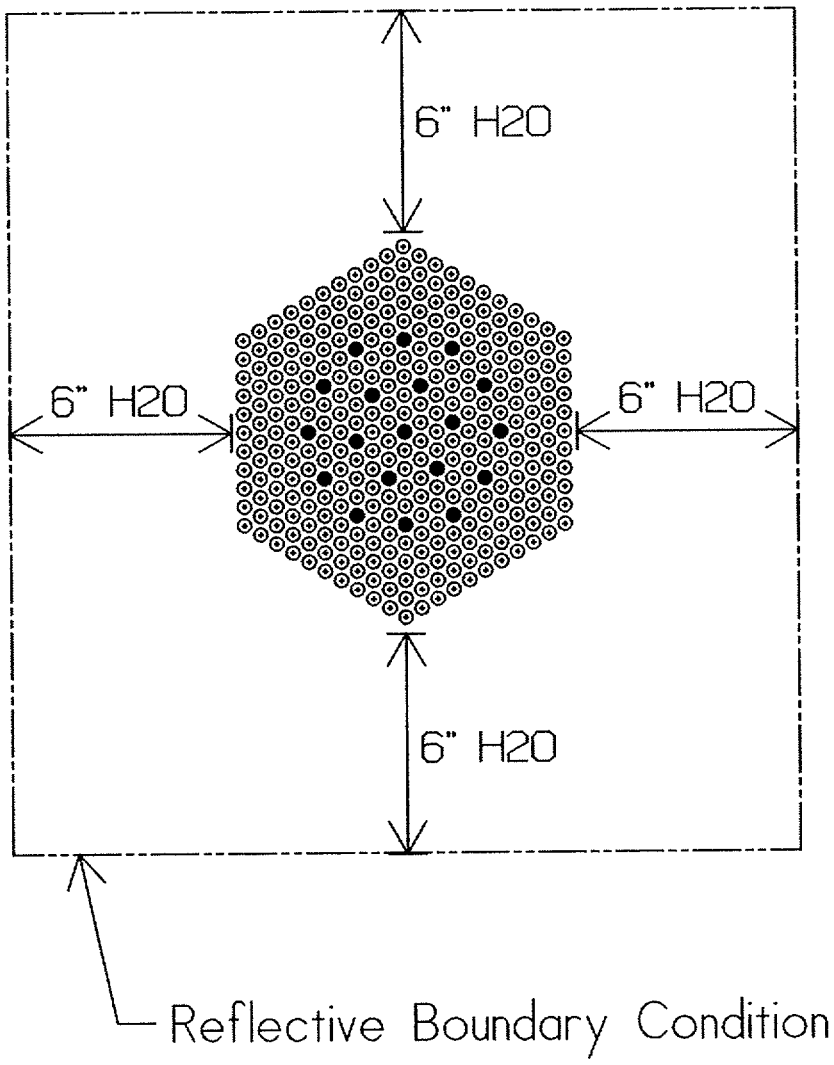

⊕ : Fuel Rod (312 Rods/Assy)

● : Thimble and Instrument Locations

The KENO calculational model based on Figure 6-1 uses only two geometry units to model the unpackaged fuel assembly. One unit describes the fuel rod cell, which contains an explicit geometric representation of a fuel pellet, gap, cladding, and surrounding water. The other unit describes the thimble tube cell, which has water both inside and outside of the tube. The KENO calculation model based on Figure 6-2 uses five geometry units. The first two units describe the top and bottom of a fuel rod cell. The next two units describe the top and bottom of a modified thimble tube cell. The thimble tube has been modified to fit correctly into the fuel assembly array model. The last unit is an empty water cell used to create a square assembly array in KENO. The fuel rod cells and thimble tube cells are positioned in an array to create a triangular pitch equal to the VVER-1000 fuel assembly. In modeling the fuel, the UO_2 atom density is calculated by assuming a UO_2 density that is 96.5% of theoretical (10.96 g/cc); pellet densities actually encountered typically range from 94.5% to 95.5% of theoretical. No pellet dishing fraction or chamfering is modeled, which conservatively increases the number of ^{235}U atoms by about 1.2%, depending on the specific pellet type. No credit is taken for the presence of naturally occurring ^{234}U or ^{236}U, nor is any credit taken for assembly structural material that does not extend the full length of the assembly (i.e., grids, top and bottom nozzle, etc.). These combined assumptions result in a very conservative model of a fuel assembly.

Figure 6-3 shows the package configuration for Normal Conditions of Transport for Square Lattice Fuel Assemblies and Figure 6-4 shows the package configuration for Normal Conditions of Transport for VVER-1000 Fuel Assemblies. Since more than 6 inches of water is present between any assembly edge and the interior surface of the package shell, the assemblies in any single container will be isolated from the assemblies in nearby containers by at least 12 inches of water. Therefore, similar to the unpackaged assemblies, the reactivity of an infinite array of packages under Normal Conditions of Transport would be the same as the reactivity of any single package.

Figure 6-5 presents the Hypothetical Accident Conditions of Transport package configuration and its criticality model for square lattice fuel. For the HAC, two crushed packages are aligned top-to-top such that an array of four assemblies is created, with the assemblies in the lower container separated from the assemblies in the upper container by 8 inches of water. To simplify the calculational model, reflective boundary (zero current) conditions are employed at the vertical centerline within the container and at the horizontal interface between the lower and upper containers. In this way, the array of four assemblies is appropriately simulated, yet the model input is reduced to a representation of only one assembly. For conservatism, reflective boundary conditions are also used at the outer edges of the two crushed packages, which precludes any neutron leakage from the array. Since at least 12 inches of water separates each grouping of four assemblies in this model, the results for the infinite array are the same as for a single cluster of four assemblies. For certain higher enriched assemblies (Type B with enrichments greater than 4.75 wt%), added neutron absorbers are used to maintain K_{eff} less than 0.95. The additional absorbers can be placed within the assemblies (IFBA,

Pyrex BA, WABA, or Ag-In-Cd rods) or placed external to the assemblies as part of the container (Gd absorber plates). Each absorber type is described by a nominal density and manufacturing tolerance at the 95% confidence level. For calculational purposes, the modeled absorber number densities are reduced from nominal by a factor to account for the 95% manufacturing tolerance, and by an additional 25% for added conservatism.

Figure 6-6 presents the Hypothetical Accident Conditions of Transport package configuration and its criticality model for VVER-1000 Fuel Assemblies. The model is similar to the square lattice model in its conservative approximation on boundary conditions (zero current). The model has an added horizontal Gadolinia absorber underneath the strongback. As with the Type B assemblies, the VVER-1000 assemblies require added neutron absorbers at higher enrichments in order to maintain K_{eff} less than 0.95. The additional absorbers can be placed within the assemblies (IFBA, WABA, or Ag-In-Cd) or placed external to the assemblies as part of the container (Gd coated guide supports). Each absorber type is described by a nominal density and manufacturing tolerance at the 95% confidence level. For calculational purposes, the modeled absorber number densities are reduced from nominal by a factor to account for the 95% manufacturing tolerance, and by an additional 25% for added conservatism.

FIGURE 6-3

NORMAL CONDITIONS OF

TRANSPORT CONFIGURATION AND MODEL

FOR SQUARE LATTICE FUEL

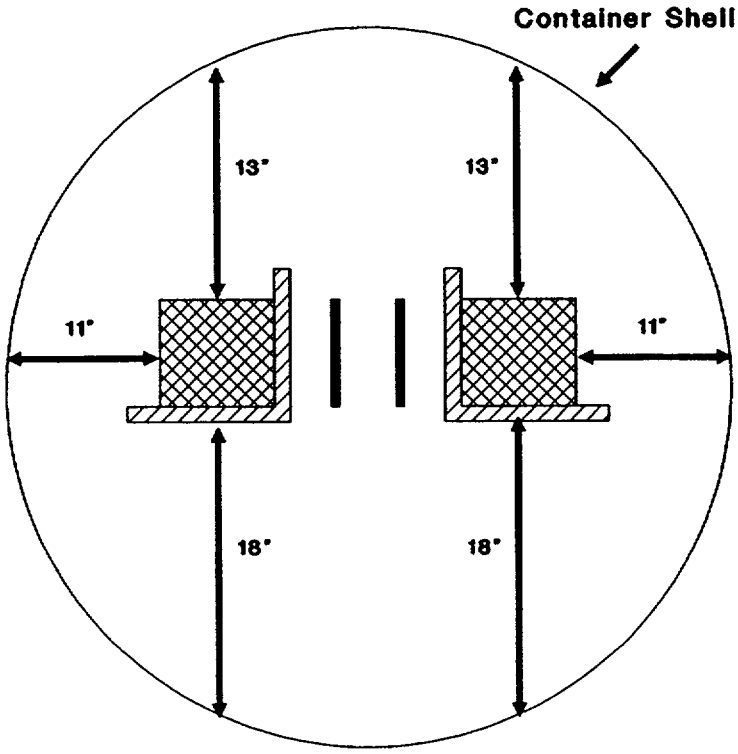

FIGURE 6-4

NORMAL CONDITIONS OF

TRANSPORT CONFIGURATION AND MODEL

FOR VVER-1000 FUEL

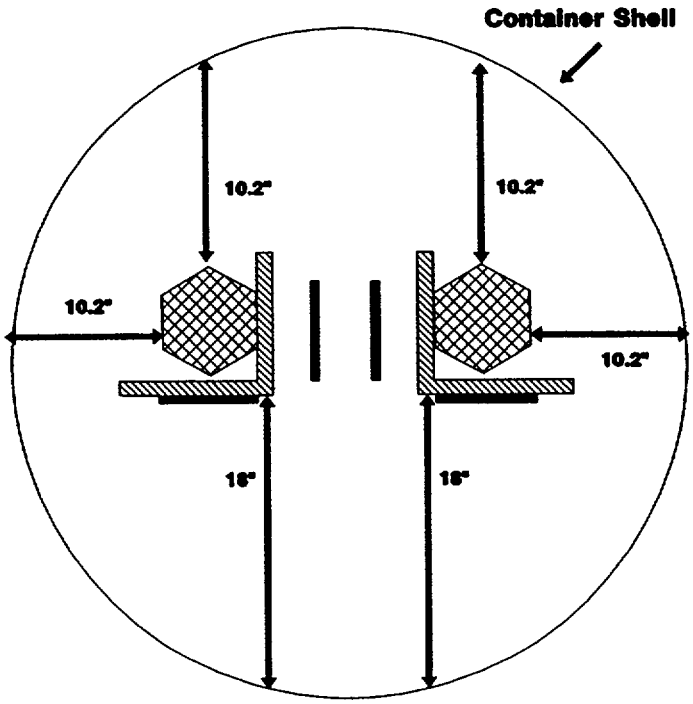

FIGURE 6-5

HYPOTHETICAL ACCIDENT CONDITION

CONFIGURATION AND MODEL

FOR SQUARE LATTICE FUEL

FIGURE WITHHELD UNDER 10 CFR 2.390

FIGURE 6-6

HYPOTHETICAL ACCIDENT CONDITION
CONFIGURATION AND MODEL FOR VVER-1000 ASSEMBLY

FIGURE WITHHELD UNDER 10 CFR 2.390

In summary, the criticality calculations for uncontained and contained fuel assemblies incorporate many conservatisms, including:

1) Reflective boundary conditions on all peripheral surfaces to preclude any neutron leakage from the array;

2) Fuel pellets modeled at 96.5% theoretical density with no dishing or chamfering, and no credit taken for naturally occurring ^{234}U and ^{236}U;

3) Fuel assemblies modeled without grids, top and bottom nozzles, etc.;

4) Neutron absorber densities reduced by manufacturing tolerances, and an additional 25% safety factor;

5) Fuel assemblies modeled intact, ignoring that HAC testing results in crushed assemblies that would have lower reactivities.

The above conservatisms result in conservative calculations of reactivity.

6.3.2 PACKAGE REGIONAL DENSITIES

Densities (g/cc) for all materials used in the calculational models for uncontained and contained analyses are presented in Figure 6-7. Atomic number densities (atoms/barn-cm) for constituent nuclides in all materials used for calculational models for uncontained and contained analyses are presented in Figure 6-8. Fissionable isotopes are considered to be at their most reactive credible concentration, assuming 5 wt% ^{235}U. These are the number densities used in all KENO calculations.

6.4 CRITICALITY CALCULATION

6.4.1 CALCULATIONAL OR EXPERIMENTAL METHOD

The current Westinghouse design method, which insures the criticality safety of fuel assemblies in the shipping container, starts with 227 energy group cross-sections generated from ENDF/B-V data. AMPX system codes, NITAWL-S and XSDRNPMS, are used for cross-section library processing. The NITAWL-S program performs the self-shielded resonance cross-section corrections that are appropriate for each particular geometry (The Nordheim Integral Treatment is used). Energy and spatial weighting of the cross-sections are performed by the XSDRNPMS program, which is a one-dimensional transport theory code. XSDRNPMS cell models are generated for fuel cells and for representative absorber cells. Cross-sections for IFBA coated fuel are prepared by placing the ^{10}B material from the absorber in the clad region of the cell.

FIGURE 6-7

MATERIAL DENSITIES FOR KENO CALCULATIONS

REGION	MATERIAL	DENSITY
Fuel	UO_2	10.576 g/cc
Cladding & Guide Tube	Zircaloy	6.55 g/cc
Container Components	Carbon Steel	7.87 g/cc
Moderation And Reflection	Water	1.0 g/cc
IFBA Neutron Absorber	ZrB_2	1.06875 g/cm^2
Absorber Rods	Ag-In-Cd	10.17 g/cc
Absorber Rods	Borosilicate-Pyrex	2.3 g/cc
Absorber Rods	WABA	3.68 g/cc
Permanent And Additional Neutron Absorber Plates	Gd_2O_3	0.02 g/cm^2

FIGURE 6-8

LISTING OF KENO MATERIAL NUMBER DENSITIES

REGION	ISOTOPE	MATERIAL ID	NUMBER DENSITY
UO_2 FUEL	^{235}U	92235	0.0011942
	^{238}U	92238	0.022404
	^{16}O	8016	0.047196
ZIRCALOY CLAD	ZIRC	40302	0.043326
ZIRCALOY CLAD WITH ZrB	ZIRC	40302	0.043326
	^{10}B	5010	0.0001644
WATER	H	1001	0.066854
	O	8016	0.033427
CARBON STEEL	Fe	26000	0.0842011
	C	6012	0.0004728898
	^{55}Mn	25055	0.0003887064
	P	15031	0.00005807008
	S	16032	0.00006642906
ABSORBER PLATE	O	8016	0.009810529
	^{152}Gd	64152	0.0000130807
	^{154}Gd	64154	0.0001373474
	^{155}Gd	64155	0.0009679722
	^{156}Gd	64156	0.001347313
	^{157}Gd	64157	0.001026835
	^{158}Gd	64158	0.001622008
	^{160}Gd	64160	0.001425792
BOROSILICATE-PYREX	^{10}B	5010	0.0006837358
	^{11}B	5011	0.003862628
	O	8016	0.045331
	Na	11023	0.000880
	Al	13027	0.000680
	Si	14000	0.018040
WABA	^{10}B	5010	0.001914
	^{11}B	5011	0.012084
	C	6012	0.003772
	O	8016	0.039580
	Al	13027	0.026387

FIGURE 6-8 (cont)

LISTING OF KENO MATERIAL NUMBER DENSITIES

REGION	ISOTOPE	MATERIAL ID	NUMBER DENSITY
Ag-In-Cd	^{107}Ag	47107	0.017551
	^{109}Ag	47109	0.016305
	Cd	48000	0.001941
	^{113}In	49113	0.000254
	^{115}In	49115	0.005648

Cross-sections for structural materials are obtained by introducing trace material amounts into the moderator region of the cell. This procedure does not produce any bias in the results due to the fineness of the energy group structure. These multigroup cross-section sets are then used as input to KENO Va, which is a three dimensional Monte Carlo theory program designed for reactivity calculations.

6.4.2 FUEL LOADING OR OTHER CONTENTS LOADING OPTIMIZATION

The geometric capabilities of KENO are used to provide essentially exact representations of actual fuel assembly and shipping container geometries. All uncontained assembly calculations are performed in two dimensional geometry, which conservatively ignores the benefits of axial leakage. For contained Type A fuel assemblies (14x14 and 16x16 designs), calculations are also performed in two dimensions. For contained Type B assemblies (15x15 and 17x17 designs), a conservative three dimensional geometry is used. The three dimensional calculations assume an active fuel stack height of 168 inches, which is conservative, since the majority of Type B fuel assembly designs are considerably shorter than 168 inches. Reflection is used at the fuel axial centerline to minimize problem size and complexity. Within the container, 5.08 inches of water is modeled at the assembly end, followed by the thin container shell and a reflective boundary condition. For contained Type C fuel asemblies (VVER-1000 design), calculations are performed with a conservative three dimensional geometry. The three dimensional calculations assume an active fuel stack height of 142.91 inches. Reflection is used a the fuel axial centerline to minimize problem size and complexity. Within the container, 6.0 inches of water is modeled at the assembly end, followed by the thin container shell and a reflective boundary conditions. This geometry model conservatively ignores the benefits of additional spacing between the fuel rod plenum and the additional neutron absorption by the top and bottom assembly structure. Where applicable, fuel pin gap flooding and annular fuel blankets are included in the calculations. When additional within-assembly neutron absorbers are required, the absorbers are modeled assuming an axial length of 108 inches, centered about the axial assembly midplane. Typically, absorbers are significantly longer than the assumed 108 inch minimum, thereby adding additional conservatism. For IFBA absorbers, the ^{10}B is modeled within the clad region of the fuel cell, which is consistent with the standard Westinghouse reactor core design methodology.

6.4.3 CRITICALITY RESULTS

Appendix 6-1 includes the KENO input decks and K_{eff} results for the Monte Carlo criticality analysis of single fuel assemblies having attributes described in Appendix 1-4. Appendix 6-2 includes the KENO input decks and K_{eff} results for the Monte Carlo criticality analyses of the MCC shipping container under infinite array Normal Condition of Transport and Hypothetical Accident Conditions.

The Hypothetical Accident Condition evaluations were performed assuming infinite array geometry, therefore these results bound the infinite array Normal Condition of Transport calculations.

For the MCC shipping container using permanent Gd_2O_3 absorber plates, under infinite array Hypothetical Accident Conditions, it has been calculated that the final K_{eff} with bias and uncertainties at the 95% confidence level is less than 0.95 for the following conditions:

1) Type A fuel assemblies (14x14 and 16x16 designs) with maximum enrichments up to 5.0 wt%; or,

2) Type B fuel assemblies (15x15 and 17x17 designs) with maximum enrichments up to 4.65 wt%; or,

3) Type B fuel assemblies (15x15 and 17x17 designs) with maximum enrichments above 4.65 wt%, up to 5.0 wt%, using one of the following additional absorber options:

   a) Assembly IFBA Rods: A minimum of 32 nominally (1X) loaded fuel rods in each assembly, each with a minimum coating length of 108 inches. For increased IFBA loadings (1.5X, 2X, etc.), the number of loaded fuel rods required can be reduced by the ratio of the increased loading to the nominal loading.

   b) Assembly Absorber Rods: A minimum of 4 absorber rods in each assembly. The rods can be Pyrex BA, WABA, or Ag-In-Cd designs with a minimum length of 108 inches. The rods must be positioned within the assemblies in a symmetric pattern about the assembly center guide tube.

   c) Container Absorber Plates: A minimum of 2 additional Gadolinia coated absorber plates, having the same specifications as the permanent container absorber plates, are required. The additional plates must be positioned directly on the strongback (top or bottom), underneath each assembly.

4) The Type C fuel assembly (VVER-1000) with maximum enrichments up to 4.8 wt%; or,

5) The Type C fuel assembly (VVER-1000) with maximum enrichments above 4.8 wt%, up to 5.0 wt%, using one of the following additional absorber options:

   a) Assembly IFBA rods: A minimum of 24 nominally (1X) coated fuel rods are required in each assembly, each with a minimum coating length of 108 inches. With increased IFBA loadings (1.X, 2X, etc.), the number of

loaded fuel rods required can be reduced by the ratio of the increased loading to the nominal loading.

b) Assembly Absorber Rods: A minimum of 4 absorber rods are required in each assembly. The rods can be WABA or Ag-In-Cd designs with a minimum length of 108 inches. The rods must be positioned within the assemblies in a symmetric pattern about the assembly center guide tube.

c) Guide Plate Absorber Coating: A minimum coating of 0.027 grams of Gd_2O_3 per cm^2 on the underside of the guide plates is required. The guide plates sit on the strongback and are located between the grid supports.

6.4.4 REFERENCES

1. Ford III, W.E., et. al.; CSRL-V: PROCESSED ENDF/B-V 227-NEUTRON-GROUP AND POINTWISE CROSS-SECTION LIBRARIES FOR CRITICALITY SAFETY, REACTOR, AND SHIELDING STUDIES; NUREG/CR-2306; June 1982.

2. Greene, N.M., et. al.; AMPX: A MODULAR CODE SYSTEM FOR GENERATING COUPLED MULTIGROUP NEUTRON-GAMMA LIBRARIES FROM ENDF/B; ORNL-TM-3706; March 1976.

3. Petrie, L.M., Landers, N.F.; KENO Va - AN IMPROVED MONTE CARLO CRITICALITY PROGRAM WITH SUPERGROUPING; NUREG/CR-0200; December 1984.

6.5 CRITICAL BENCHMARK EXPERIMENTS

6.5.1 BENCHMARK EXPERIMENTS AND APPLICABILITY

The criticality calculation method and cross-section values are verified by comparison with critical experiment data for fuel assemblies similar to those for which the shipping container is designed. This benchmarking data is sufficiently diverse to establish that the method bias and uncertainty will apply to shipping container conditions which include strong neutron absorbers and large water gaps.

A set of 32 critical experiments has been analyzed using the above method to demonstrate its applicability to criticality analysis and to establish the method bias and uncertainty. The benchmark experiments cover a wide range of geometries, materials and enrichments; ranging from relatively low enriched (2.35, 2.46, and 4.31 wt%), water moderated, oxide fuel arrays, separated by various materials (B_4C, aluminum, steel, water, etc) that simulate LWR fuel shipping and storage conditions; to dry, harder

spectrum, uranium metal cylinder arrays at high enrichments (93.2 wt%), with various interspersed materials (Plexiglas and air). Comparison with these experiments demonstrates the wide range of applicability of the method.

6.5.2 DETAILS OF THE BENCHMARK CALCULATIONS

All experiments were modeled without complication. Material densities and geometries were taken directly from the references. No critical experiments were eliminated on the basis of anomalous results.

6.5.3 RESULTS OF THE BENCHMARK CALCULATIONS

Descriptions and results of the 32 critical experiments as executed on a CRAY XMP computer are provided in Figure 6-9; benchmark calculation statistics are given in Figure 6-10. These results are appropriate for all calculations performed prior to January 1, 1994.

The 32 low enriched, water-moderated experiments result in an averabe KENO Va K_{eff} of 0.9933. Comparison with the average measured experimental K_{eff} of 1.0007 results in a method bias of 0.0074. The standard deviation of the bias value is 0.0013 ΔK. The 95/95 one-sided tolerance limit factor for 32 values is 2.20. Thus, there is a 95 percent probability with a 95 percent confidence level that the uncertainty in reactivity, due to the method, is not greater than 0.0029 ΔK.

Descriptions and results of the 32 critical experiments as executed on an HP-735 series workstation are provided in Figure 6-ll; benchmark calculation statistics are given in Figure 6-12. These results are appropriate for all calculations performed after January 1, 1994.

The 32 low enriched, water-moderated experiments result in an average KENO Va K_{eff} of 0.9930. Comparison with the average measured experimental K_{eff} of 1.0007 results in a method bias of 0.0077. The standard deviation of the bias value is 0.0013 ΔK. The 95/95 one-sided tolerance limit factor for 32 values is 2.20. Thus, there is a 95 percent probability with a 95 percent confidence level that the uncertainty in reactivity, due to the method, is not greater than 0.0030 ΔK.

The results of even higher enrichment benchmark experiments show that the criticality method can correctly predict the reactivity of a hard spectrum environment, such as the optimum moderation scenario often considered in fresh rack and shipping cask designs. However, the results of such higher enrichment benchmarks are not incorporated into the criticality method bias because the enrichments are well beyond the range of typical applications. Basing the method bias solely on the 32 low enriched benchmarks results in a more appropriate and more conservative bias.

FIGURE 6-9

BENCHMARK CRITICAL UO_2 ROD LATTICE EXPERIMENTS USING A CRAY XMP COMPUTER

Critical Number	Enrichment ^{235}U wt%	Reflector Material	Separating Material	Soluble Boron (ppm)	Measured K_{eff}	KENO Reactivity $K_{eff} \pm 1\sigma$
1	2.46	water	water	0	1.0002	0.9966 ± 0.0024
2	2.46	water	water	1037	1.0001	0.9914 ± 0.0019
3	2.46	water	water	764	1.0000	0.9943 ± 0.0019
4	2.46	water	B_4C pins	0	0.9999	0.9871 ± 0.0022
5	2.46	water	B_4C pins	0	1.0000	0.9902 ± 0.0022
6	2.46	water	B_4C pins	0	1.0097	0.9948 ± 0.0021
7	2.46	water	B_4C pins	0	0.9998	0.9886 ± 0.0021
8	2.46	water	B_4C pins	0	1.0083	0.9973 ± 0.0021
9	2.46	water	water	0	1.0030	0.9966 ± 0.0021
10	2.46	water	water	143	1.0001	0.9973 ± 0.0021
11	2.46	water	stainless steel	514	1.0000	0.9992 ± 0.0020
12	2.46	water	stainless steel	217	1.0000	1.0031 ± 0.0021
13	2.46	water	borated aluminum	15	1.0000	0.9939 ± 0.0022
14	2.46	water	borated aluminum	92	1.0001	0.9882 ± 0.0022
15	2.46	water	borated aluminum	395	0.9998	0.9854 ± 0.0021
16	2.46	water	borated aluminum	121	1.0001	0.9848 ± 0.0022
17	2.46	water	borated aluminum	487	1.0000	0.9892 ± 0.0021
18	2.46	water	borated aluminum	197	1.0002	0.9944 ± 0.0022
19	2.46	water	borated aluminum	634	1.0002	0.9956 ± 0.0020
20	2.46	water	borated aluminum	320	1.0003	0.9893 ± 0.0020
21	2.46	water	borated aluminum	72	0.9997	0.9900 ± 0.0020
22	2.35	water	borated aluminum	0	1.0000	0.9980 ± 0.0024
23	2.35	water	stainless steel	0	1.0000	0.9933 ± 0.0022
24	2.35	water	water	0	1.0000	0.9920 ± 0.0024
25	2.35	water	stainless steel	0	1.0000	0.9877 ± 0.0022
26	2.35	water	borated aluminum	0	1.0000	0.9912 ± 0.0022
27	2.35	water	B_4C	0	1.0000	0.9921 ± 0.0021
28	4.31	water	stainless steel	0	1.0000	0.9968 ± 0.0023
29	4.31	water	water	0	1.0000	0.9963 ± 0.0027
30	4.31	water	stainless steel	0	1.0000	0.9950 ± 0.0026
31	4.31	water	borated aluminum	0	1.0000	0.9952 ± 0.0025
32	4.31	water	borated aluminum	0	1.0000	1.0006 ± 0.0024

FIGURE 6-10

BENCHMARK CALCULATION STATISTICS
FOR A CRAY XMP COMPUTER

Number of Experiments	32
Average Measured K_{eff} (K_m)	1.0007
Average KENO Va K_{eff} (K_c)	0.9933
KENO Va Bias (K_m - K_c)	0.0074
Bias Standard Deviation (s)	0.0013
One Sided Tolerance Factor for 95/95 (k)	2.20
95/95 Bias Uncertainty (ks)	0.0029

FIGURE 6-11

BENCHMARK CRITICAL UO_2 ROD LATTICE EXPERIMENTS USING AN HP-735 WORKSTATION

Critical Number	Enrichment ^{235}U wt%	Reflector Material	Separating Material	Soluble Boron (ppm)	Measured K_{eff}	KENO Reactivity $K_{eff} \pm 1\sigma$
1	2.46	water	water	0	1.0002	0.9935 ± 0.0023
2	2.46	water	water	1037	1.0001	0.9936 ± 0.0019
3	2.46	water	water	764	1.0000	0.9946 ± 0.0019
4	2.46	water	B_4C pins	0	0.9999	0.9877 ± 0.0022
5	2.46	water	B_4C pins	0	1.0000	0.9884 ± 0.0022
6	2.46	water	B_4C pins	0	1.0097	1.0013 ± 0.0022
7	2.46	water	B_4C pins	0	0.9998	0.9957 ± 0.0023
8	2.46	water	B_4C pins	0	1.0083	0.9991 ± 0.0021
9	2.46	water	water	0	1.0030	0.9966 ± 0.0023
10	2.46	water	water	143	1.0001	0.9971 ± 0.0020
11	2.46	water	stainless steel	514	1.0000	0.9986 ± 0.0020
12	2.46	water	stainless steel	217	1.0000	0.9941 ± 0.0021
13	2.46	water	borated aluminum	15	1.0000	0.9923 ± 0.0022
14	2.46	water	borated aluminum	92	1.0001	0.9885 ± 0.0021
15	2.46	water	borated aluminum	395	0.9998	0.9842 ± 0.0021
16	2.46	water	borated aluminum	121	1.0001	0.9847 ± 0.0021
17	2.46	water	borated aluminum	487	1.0000	0.9852 ± 0.0020
18	2.46	water	borated aluminum	197	1.0002	0.9920 ± 0.0021
19	2.46	water	borated aluminum	634	1.0002	0.9892 ± 0.0020
20	2.46	water	borated aluminum	320	1.0003	0.9946 ± 0.0020
21	2.46	water	borated aluminum	72	0.9997	0.9877 ± 0.0022
22	2.35	water	borated aluminum	0	1.0000	0.9935 ± 0.0013
23	2.35	water	stainless steel	0	1.0000	0.9957 ± 0.0012
24	2.35	water	water	0	1.0000	0.9979 ± 0.0024
25	2.35	water	stainless steel	0	1.0000	0.9896 ± 0.0024
26	2.35	water	borated aluminum	0	1.0000	0.9884 ± 0.0023
27	2.35	water	B_4C	0	1.0000	0.9902 ± 0.0023
28	4.31	water	stainless steel	0	1.0000	0.9906 ± 0.0025
29	4.31	water	water	0	1.0000	0.9899 ± 0.0023
30	4.31	water	stainless steel	0	1.0000	1.0001 ± 0.0025
31	4.31	water	borated aluminum	0	1.0000	1.0007 ± 0.0025
32	4.31	water	borated aluminum	0	1.0000	1.0009 ± 0.0025

FIGURE 6-12

BENCHMARK CALCULATION STATISTICS
FOR AN HP-735 WORKSTATION

Number of Experiments	32
Average Measured K_{eff} (K_m)	1.0007
Average KENO Va K_{eff} (K_c)	0.9930
KENO Va Bias (K_m - K_c)	0.0077
Bias Standard Deviation (s)	0.0013
One Sided Tolerance Factor for 95/95 (k)	2.20
95/95 Bias Uncertainty (ks)	0.0030

The final equation for all K_{eff} calculations is defined as follows:

$$Final\ K_{eff} = K_{nom} + B_{meth} + \sqrt{(Ks_{nom})^2 + (Ks_{meth})^2}$$

where,

Final K_{eff} is the calculated K_{eff} with bias and all uncertainties included at the 95 percent confidence level;

K_{nom} is the average K_{eff} generated from Keno Va;

B_{meth} is the bias associated with the Keno methodology established from comparison with critical experiments;

Ks_{nom} is the 95/95 uncertainty on the KENO calculation result;

Ks_{meth} is the 95/95 uncertainty associated with the KENO method bias.

6.5.4 REFERENCES

4) N. M. Baldwin, "Critical Experiments Supporting Close Proximity Water Storage of Power Reactor Fuel," B&W-1484-7, July 1979.

5) S. R. Bierman and E. D. Clayton, "Criticality Separation Between Subcritical Clusters of 2.35 wt% 235U Enriched UO2 Rods in Water with Fixed Neutron Poisons," PNL-2438, Pacific Northwest Laboratory, October 1977.

6) S. R. Bierman and E. D. Clayton, "Criticality Experiments with Subcritical Clusters of 2.35 wt% and 4.31 wt% 235U Enriched UO2 Rods in Water at a Water-to-Fuel Volume Ratio of 1.6," PNL-3314, Pacific Northwest Laboratory, July 1980.

7) S. R. Bierman and E. D. Clayton, "Critical Separation Between Subcritical Clusters of 4.29 wt% 235U Enriched UO2 Rods in Water with Fixed Neutron Poisons," PNL-2615, Pacific Northwest Laboratory, August 1979.

8) J. T. Thomas, "Critical Three-Dimensional Arrays of U(93.2) Metal Cylinders," Nuclear Science and Engineering, Volume 52, pages 350-359, 1973.

6.6 APPENDIX

The following are appended to this application:

Appendix 1-1 Container Equipment Specifications

Appendix 1-4 Fuel Assembly Parameters

Appendix 6-1 Evaluation Of the Nuclear Criticality Safety Of Unpackaged Fuel Assemblies

Appendix 6-2 Evaluation Of the Nuclear Criticality Safety Of Packaged Fuel Assemblies

CHAPTER 7: ROUTINE SHIPPING CONTAINER UTILIZATION SUMMARY OPERATING PROCEDURES

The following information contains the significant events relating to the routine use of fuel assembly shipping containers. Complete detailed instructions are outlined within the individual plant operating procedures and quality control instructions pertinent to each specific operation.

7.1.0 Receive fuel assembly shipping container.

7.1.1 Unload the shipping container from the truck.
7.1.2 Report any obvious damage to supervisor.
7.1.3 Prepare a container identification route card.

7.2.0 Clean shipping container.

7.2.1 Use soap or a suitable detergent and water to clean the container.
7.2.2 Hose down the container and direct a high pressure water stream around the flange area.
7.2.3 Move the container into the building and open.
7.2.4 Inspect for water leaks in the flange area.

7.3.0 Refurbish shipping container.

7.3.1 Repair any water leaks found and remove excess water from container.
7.3.2 Check container shell closure fasteners and repair damaged or rusted fasteners. Lubricate fasteners and torque.
7.3.3 Paint repaired and damaged paint areas on the container with Dupont Imron paint.
7.3.4 Inspect container support frame clamp pads and repair if necessary.

7.4.0 Prepare container for fuel assembly loading.

7.4.1 Configure fuel assembly clamping frame.
7.4.2 Place and secure spacer blocks in container as needed.
7.4.3 Configure top closure jack screws.
7.4.4 Install absorber plates specific to the fuel assembly types to be loaded. For enrichments greater than 4.65% (for MCC-3 and MCC-4) or 4.80% (for MCC-5), an additional set of gadolinium plates is required.

1. MCC-3 and MCC-4 containers have vertical gadolinium absorber plates installed between the fuel assemblies, which must be in place for all enrichments of fuel assemblies. For enrichments greater than 4.65 wt%, additional segmented horizontal absorber plates are installed beneath the strongback per note I of drawing MCCL301 and note M of drawing

MCCL401.

2. The MCC-5 containers have both the vertical and segmented horizontal absorber plates, as described above for the MCC-3 and MCC-4 containers, permanently installed per note M of drawing MCCL501; these plates must be in place for all enrichments of fuel assemblies. For enrichments greater than 4.80 wt%, additional absorber plates which are shaped to conform to the vee-shape of the fuel assemblies are installed on the upper side of the strongback between the grid support blocks per note P of drawing MCCL501.

7.4.5 Repair or replace as necessary the container gasket.
7.4.6 Configure and place shock mounts.
7.4.7 Verify that accelerometers are sealed, calibrated, and not tripped. Replace if required.

7.5.0 Inspection.

7.5.1 Verify that the container interior and exterior are clean, well painted, and in good condition.
7.5.2 Verify that the required internal hardware is present and in good working condition.
7.5.3 Verify that the required decals, license plates, labels, stencil markings, etc. are present and legible.
7.5.4 Verify that the required absorber plates are properly installed.
7.5.5 Verify that outstanding QCDN's and FOR's have been cleared prior to release for loading.

7.6.0 Fuel assembly loading.

7.6.1 Open shipping container.
7.6.2 Visually verify that correct shipping container absorber plates are installed prior to loading fuel assemblies. (See Section 7.4.4).
7.6.3 Configure and place outriggers.
7.6.4 Extend lateral cross bars and secure to support pads.
7.6.5 Run jacking nuts toward pressure pads as far as possible.
7.6.6 Open clamping frames and top closure assemblies.
7.6.7 Place and secure support frame in vertical position. Each clamping frame on the support frame side to be loaded shall be opened as far as possible. The associated pressure pads shall be retracted as far as the jacking nut.
7.6.8 Place the fuel assembly in the support frame.
7.6.9 Adjust the alignment of bottom, middle and top clamping frames to associated fuel assembly grids.
7.6.10 Close the bottom, middle and top clamping frames around the fuel assembly and tighten the frame fastener nuts.

7.6.11 Snug the bottom, middle and top clamping frame pressure pads against the fuel assembly grid in order. The side pressure pad shall be snugged before the top pressure pad in each case.

7.6.12 Load the second fuel assembly in a similar manner.

7.6.13 Verify the absence of debris on and in the container shell lower subassembly. Remove debris as required.

7.6.14 Release stabilizing bars and lock in storage position.

7.6.15 Lower support frame into horizontal position.

7.6.16 Release cross bars. Retract and lock in storage configuration.

7.6.17 Retract and secure the outriggers.

7.6.18 Close the remaining clamping frames around the fuel assembly and tighten their clamping frame fastener nuts.

7.6.19 Pull plastic wrapper through the gap between pressure pads so that only a single layer encloses the grid.

7.6.20 Align pressure pads with grids such that grid springs are not visible along either long side of the pressure pad.

7.6.21 Torque the jacking nuts starting with the bottom clamping frame and working up the fuel assembly.

7.6.22 Close and secure top closure assemblies.

7.6.23 Check all fasteners and plastic wrapper for correct configuration.

7.6.24 Engage shock mount frame swing bolts with support frame clamp pads and tighten nut until it is "snug-tight". Turn nut an additional one-half turn.

7.7.0 Inspection

7.7.1 Verify that the fuel assemblies and core components have been released and the proper component is being shipped with the assembly.

7.7.2 Verify that the plastic is installed correctly.

7.7.3 Verify that the enrichment of the fuel assemblies loaded into each container does not exceed the applicable maximum permissible per Section 7.4.4.

7.7.4 Verify that the fuel assemblies are properly oriented in the container.

7.7.5 Verify the number of shock mounts is correct and accelerometers are sealed, calibrated and not tripped.

7.7.6 Verify that clamps, shock mount frame swing bolts, etc. are tightened.

7.7.7 Verify general cleanliness and absence of debris on container internals, fuel assembly, plastic wrapper, container flange and container shell lower subassembly prior to closing the container.

7.7.8 Verify placement and integrity of shipping container gasket.

7.8.0 Close shipping container.

7.8.1 Verify that the cover flange is free of debris and place cover on container.

7.8.2 Tighten container closure fasteners to secure cover.

7.8.3 Install one approved tamper proof security seal on each end of the container.

7.9.0 Inspection

7.9.1 Verify that the container lid is properly seated and all closure bolts are present.
7.9.2 Verify that outriggers are present.

7.10.0 Truck loading of shipping containers.

7.10.1 Place shipping container on trailer equipped to permit chaining down of container.
7.10.2 Center and place container lengthwise on trailer.
7.10.3 Secure containers to trailer bed with stops.
7.10.4 Chain containers to trailer using "come along" tighteners and chains of 3/8 inch minimum diameter.

7.11.0 Regulatory

7.11.1 Conduct direct alpha surveys on both the containers and the accessible areas of the flatbed.
7.11.2 Perform the removable alpha and beta-gamma external smear surveys on both the containers and the accessible areas of the flatbed. If any single alpha measurement exceeds 220 dpm/100cm^2 or beta-gamma measurement exceeds 2200 dpm/100cm^2, notify Regulatory Engineering for instructions on decontamination.

7.12.0 Inspection

7.12.1 Verify that containers are properly stacked and secured.
7.12.2 Verify that required Health Physics, Radioactive and any other placards or labels have been properly placed.
7.12.3 Verify that two tamper proof security seals have been properly placed on each container.

CHAPTER 8: ACCEPTANCE TESTS, MAINTENANCE PROGRAM AND RECERTIFICATION PROGRAM

8.1 ACCEPTANCE TESTS

MCC Shipping Containers may be acquired by Westinghouse as newly constructed containers, individual parts assembled on site into new containers or conversion of RCC to MCC containers. In each instance, all critical parts and materials are obtained from qualified suppliers. These suppliers are routinely evaluated for compliance under the plant's quality surveillance program. Additionally, each container is subjected to both direct and statistical quality control inspections prior to first use. Should unacceptable components be found, they are replaced or repaired before the container is released for use.

8.2 MAINTENANCE PROGRAM

Every container is processed through routine refurbishment activities prior to each use. The specifics of each phase of the program are described below.

8.2.1 Clean the container and check for leaks.
8.2.2 Visually inspect the exterior and interior for obvious defects and repair or replace as necessary.
8.2.3 Inspect the cork surface and repair or replace as necessary.
8.2.4 Inspect the internal components and safety significant nuts, bolts, and pins, for obvious defects and repair or replace as necessary.
8.2.5 Visually inspect the gadolinium absorber plates and corresponding tamper seal.
8.2.6 Visually inspect safety significant welds, flanges, and markings.
8.2.7 Q.C. Inspect and release prior to use.

8.3 RECERTIFICATION PROGRAM

On a periodic basis (not to exceed five years), containers will be inspected to verify the existing configuration to drawing requirements. Quality control Instructions and Mechanical Operating Procedures will define the specific inspection requirements. Safety related components as identified in approved verification plans will be inspected for compliance to key drawings characteristics and for correct configuration on the container. A detailed visual inspection will be conducted of the visible side of the gadolinium absorber plates. Personnel will:

8.3.1 Visually inspect to verify that no more than seven (7) square inches total area of coating is missing.
8.3.2 Verify no single area greater than one (1) square inch of coating is missing.
8.3.3 Visually verify that the coating is not flaking off or blistering.

These plates will be repaired or replaced if defects are found.

Documentation relating to these inspections, repairs, part replacements, etc. will be produced and subsequently maintained via the existing plant records program.

APPENDIX 1-1

CONTAINER EQUIPMENT SPECIFICATIONS

EQUIPMENT SPECIFICATION ADDENDUM

E-MCC-676498

MCC-3 shipping containers differ from Specification E-676498 containers in the design of the clamping frame assemblies that secure the contained fuel assemblies within the package internals. The MCC-3 clamping frame assemblies include the following modified features:

- SNUBBERS have been incorporated into the grid pressure pad systems, to limit displacement of contained fuel assemblies in event of severe shipping container impact conditions.
- The ductility of the grid pad SWING BOLTS have been increased, such that they will plastically deform and dissipate energy in event of severe shipping container impact conditions.
- The CLAMPING FRAMES have been designed with increased strength, to prevent yielding in event of severe shipping container impact conditions.

These MCC-3 parts are shown in detail in the following:

PART NAME	DRAWING MCCL301 ITEM NO.
SNUBBER	22, 24, 25
SWING BOLT	15
CLAMPING FRAME	13

EQUIPMENT SPECIFICATION ADDENDUM

E-MCC-953511

MCC-4 shipping containers differ from Specification E-953511 containers in the design of the clamping frame assemblies that secure the contained fuel assemblies within the package internals. The MCC-4 clamping frame assemblies include the following modified features:

- SNUBBERS have been incorporated into the grid pressure pad systems, to limit displacement of contained fuel assemblies in event of severe shipping container impact conditions.
- The ductility of the grid pad SWING BOLTS have been increased, such that they will plastically deform and dissipate energy in event of severe shipping container impact conditions.
- The CLAMPING FRAMES have been designed with increased strength, to prevent yielding in event of severe shipping container impact conditions.

These MCC-4 parts are shown in detail in the following:

PART NAME	DRAWING MCCL401 ITEM NO.
SNUBBER	42, 43, 44
SWING BOLT	35
CLAMPING FRAME	33

EQUIPMENT SPECIFICATION ADDENDUM

E-MCC-953511

MCC-5 shipping containers differ from Specification E-953511 containers in the design of the clamping frame assemblies that secure the contained fuel assemblies within the package internals. The MCC-5 clamping frame assemblies include the following modified features:

- SNUBBERS have been incorporated into the grid pressure pad systems, to limit displacement of contained fuel assemblies in event of severe shipping container impact conditions.
- The ductility of the grid pad SWING BOLTS have been increased, such that they will plastically deform and dissipate energy in event of severe shipping container impact conditions.
- The CLAMPING FRAMES have been designed with increased strength, to prevent yielding in event of severe shipping container impact conditions.

These MCC-5 parts are shown in detail in the following:

PART NAME	DRAWING MCCL501 ITEM NO.
SNUBBER	42, 43, 44, & 46
SWING BOLT	35
CLAMPING FRAME	33

APPENDIX 1-2

CONTAINER DRAWINGS

LIST OF LICENSE DRAWINGS

SAFETY RELATED ITEMS MCC-3 SHIPPING CONTAINER

MCCL301, SHEET 01 OF 04
SHEET 02 OF 04
SHEET 03 OF 04
SHEET 04 OF 04

SAFETY RELATED ITEMS MCC-4 SHIPPING CONTAINER

MCCL401, SHEET 01 OF 05
SHEET 02 OF 05
SHEET 03 OF 05
SHEET 04 OF 05
SHEET 05 OF 05

SAFETY RELATED ITEMS MCC-5 SHIPPING CONTAINER

MCCL501, SHEET 01 OF 10
SHEET 02 OF 10
SHEET 03 OF 10
SHEET 04 OF 10
SHEET 05 OF 10
SHEET 06 OF 10
SHEET 07 OF 10
SHEET 08 OF 10
SHEET 09 OF 10
SHEET 10 OF 10

FUEL ASSEMBLY CROSS SECTIONAL VIEWS

6481E15, SHEET 01 OF 01

APPENDIX 1-3

RADIONUCLIDE QUANTITIES

RADIONUCLIDE QUANTITIES

Figure 1 provides a five year history of Uranium isotopic measurements at the Columbia Fuel Fabrication Facility. The isotopes of interest in this figure are ^{234}U and ^{236}U. Only these two isotopes are plotted since ^{235}U and ^{238}U are relatively fixed. The ^{234}U levels have been constant over the five year period while ^{236}U levels have varied significantly. The variance in ^{236}U levels is of little concern due to its low specific activity. However, ^{234}U levels are expected to be consistent since it is present in natural uranium and is therefore enriched along with ^{235}U. The isotope ^{234}U accounts for 70-80 percent of the specific activity of low enriched uranium. Data for 1990 indicate a ^{234}U average of 8700 ug/g^{235}U and a ^{236}U average of 750 ug/g^{235}U.

Figure 2 is constructed using the average values given above to calculate the specific activity of uranium at various enrichments. The specific activity is calculated by multiplying the isotopic concentration by its specific activity. The basic equation used in these calculations is presented in Figure 2. The predicted specific activity at 5.0 wt% ^{235}U enrichment is 2.8 uCi/gU. This calculated value is conservative with respect to published values.

RADIONUCLIDE QUANTITIES
URANIUM ISOTOPICS
U234 AND U236

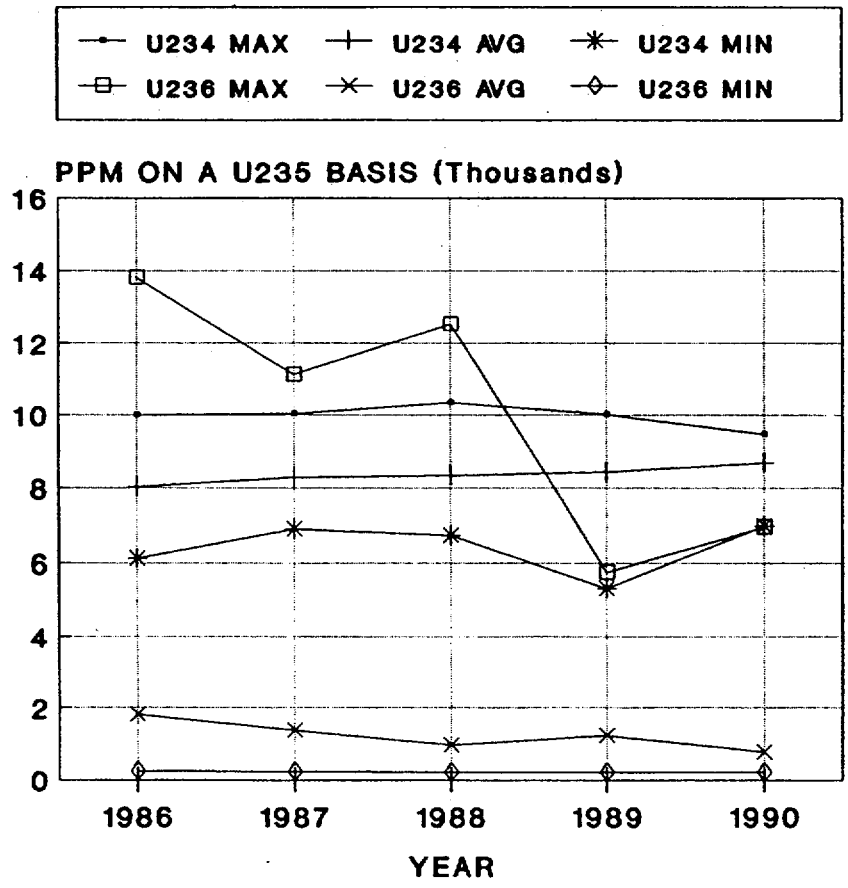

FIGURE 2

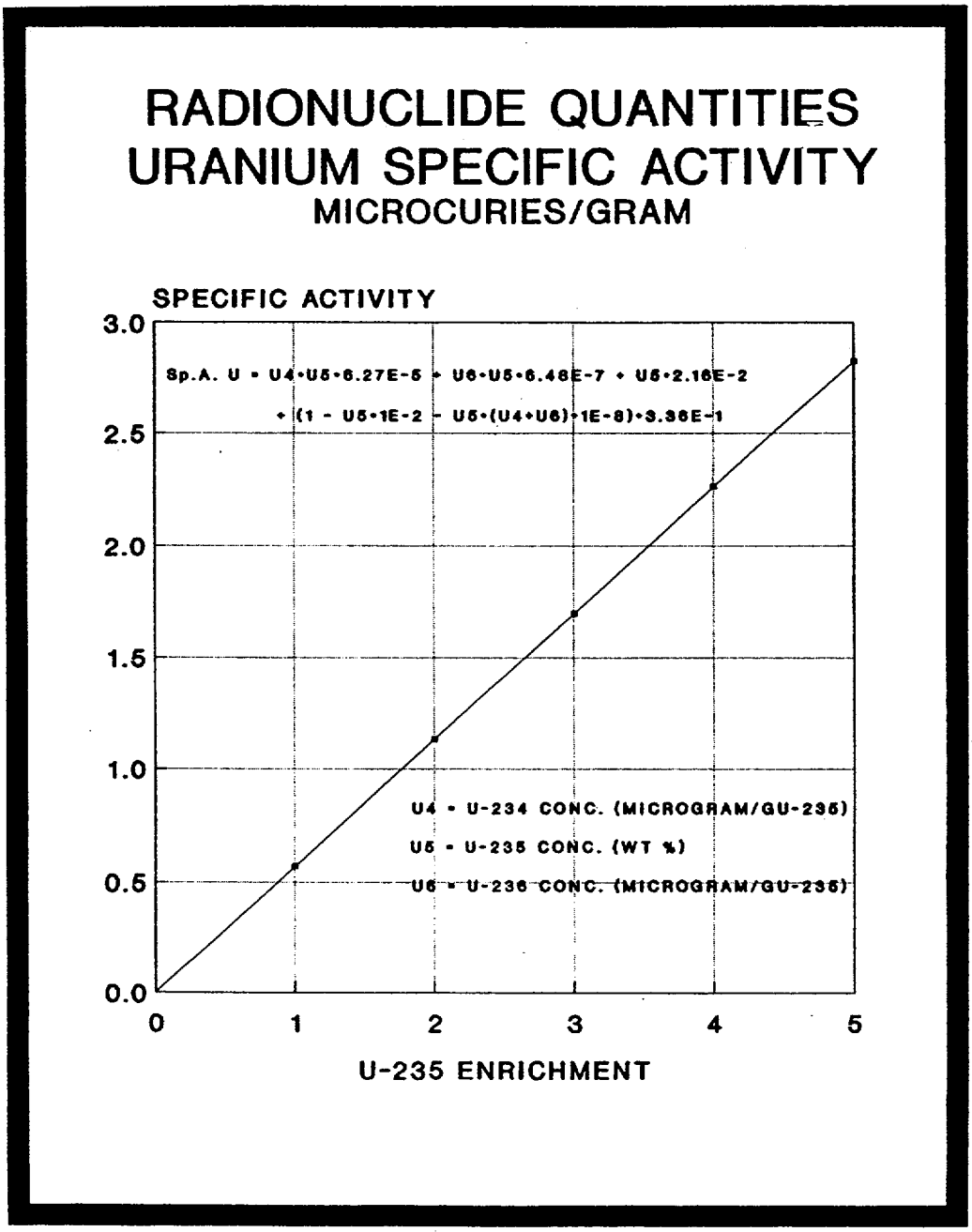
RADIONUCLIDE QUANTITIES
URANIUM SPECIFIC ACTIVITY
MICROCURIES/GRAM
SPECIFIC ACTIVITY
Sp.A. U = U4•U5•6.27E-5 + U6•U5•6.48E-7 + U5•2.16E-2
+ (1 - U5•1E-2 - U5•(U4+U6)•1E-8)•3.36E-1
U4 = U-234 CONC. (MICROGRAM/GU-235)
U5 = U-235 CONC. (WT %)
U6 = U-236 CONC. (MICROGRAM/GU-235)
3.0
2.5
2.0
1.5
1.0
0.5
0.0
0
1
2
3
4
5
U-235 ENRICHMENT

APPENDIX 1-4

FUEL ASSEMBLY PARAMETERS

FUEL ASSEMBLY PARAMETERS

The attached tables are the fuel assembly parameters for 14X14, 15X15, 16X16, 17X17, and VVER-1000 fuel types to be transported in the MCC fuel shipping container. The parameters indicated are used in the Criticality Analysis section to support uncontained and contained fuel assembly calculations. All parameters are used in the criticality analysis section except for the fuel stack length which is assumed to be infinite except in the 3D calculations performed for square lattice fuel involving IFBA and all VVER-1000 fuel assemblies in containers. Assembly reactivities are provided to indicate the highest reactivity fuel (17X17 W-OFA) to be used in the HAC model for the criticality calculations. The tabulated reactivity values assume an enrichment of 5 wt%, moderation by water to the most reactive credible extent, and close reflection by water on all sides. Fuel assembly cross-sectional views are provided on Westinghouse Drawing 6481E15, Sheet 1 of 1. The assemblies are identified by design origin with location identified for all fuel rods, instrument tubes (IT), and guide tubes (GT or thimbles). The instrument tube is a single tube centrally located and surrounded by the guide tubes.

TABLE 1-4.1

FUEL ASSEMBLY PARAMETERS
14 X 14 TYPE FUEL ASSEMBLY

Fuel Assembly Description	14 X 14	14 X 14	14 X 14	14 X 14	14 X 14	14 X 14
Fuel Assembly Type	W-STD	422 V+	W-OFA	CE-1	CE-2	W-SS
Nominal Pellet Diameter	0.3659	0.3659	0.3444	0.3765	0.3805	0.3835
Annular Pellet Inner Diameter	N/A	0.183	0.172	N/A	N/A	N/A
Nominal Clad Thickness	0.0243	0.0243	0.0243	0.0280	0.0260	0.0165
Clad Material	ZIRC	ZIRLO	ZIRC	ZIRC	ZIRC	SS-304
Nominal Clad Outer Diameter	0.4220	0.4220	0.4000	0.4400	0.4400	0.4220
GT Diameter	0.5390	0.5260	0.5260	1.1110	1.1110	0.5355
GT Thickness	0.0170	0.0170	0.0170	0.0380	0.0380	0.0120
GT Material	ZIRC	ZIRLO	ZIRC	ZIRC	ZIRC	SS-304
IT Diameter	0.4220	0.4220	0.3990	1.1110	1.1110	0.5355
IT Thickness	0.0240	0.0240	0.0235	0.0380	0.0380	0.0120
IT Material	ZIRC	ZIRLO	ZIRC	ZIRC	ZIRC	SS-304
Maximum Stack Length	145	145	145	145	145	145
Nominal Assembly Envelope	7.756	7.751	7.756	8.110	8.110	7.756
Kg's 235U/ Assembly	21	21	19	22	23	23
Nominal Lattice Pitch	0.5560	0.5560	0.5560	0.5800	0.5800	0.5560
Assembly K∞	0.9124	0.9134	0.9359	0.9296	0.9350	0.8859

(1) Fuel assembly parameters identified on Westinghouse Drawing 6481E15.
(2) Non-specified dimensions are units of inches.
(3) Nominal 8.0-inch annular pellet zones are at top and bottom of fuel rod.

TABLE 1-4.2
FUEL ASSEMBLY PARAMETERS
15 X 15 TYPE FUEL ASSEMBLY

Fuel Assembly Description	15 X 15	15 X 15	15 X 15
Fuel Assembly Type	W-STD	W-OFA	B&W
Nominal Pellet Diameter	0.3659	0.3659	0.3659
Annular Pellet Inner Diameter	0.183	0.183	0.183
Nominal Clad Thickness	0.0243	0.0243	0.0243
Clad Material	ZIRC	ZIRC	ZIRC
Nominal Clad Outer Diameter	0.4220	0.4220	0.4220
GT Diameter	0.5460	0.5330	0.5330
GT Thickness	0.0170	0.0170	0.0170
GT Material	ZIRC	ZIRC	ZIRC
IT Diameter	0.5460	0.5330	0.5300
IT Thickness	0.0170	0.0170	0.0450
IT Material	ZIRC	ZIRC	ZIRC
Maximum Stack Length	145	145	145
Nominal Assembly Envelope	8.418	8.418	8.528
Kg's ^{235}/U Assembly	24	24	24
Nominal Lattice Pitch	0.5630	0.5630	0.5680
Assembly K_∞	0.9632	0.9615	0.9599

(1) Fuel assembly parameters identified on Westinghouse Drawing 6481E15.
(2) Non-specified dimensions are units of inches.
(3) Nominal 8.0-inch annular pellet zones are at top and bottom of fuel rod.

TABLE 1-4.3
FUEL ASSEMBLY PARAMETERS
16 X 16 TYPE FUEL ASSEMBLY

Fuel Assembly Description	16 X 16	16 X 16
Fuel Assembly Type	W-STD	CE
Nominal Pellet Diameter	0.3225	0.3250
Annular Pellet Inner Diameter	0.155	N/A
Nominal Clad Thickness	0.0225	0.0250
Clad Material	ZIRC	ZIRC
Nominal Clad Outer Diameter	0.3740	0.3820
GT Diameter	0.4710	0.9800
GT Thickness	0.0180	0.0400
GT Material	ZIRC	ZIRC
IT Diameter	0.4710	0.9800
IT Thickness	0.0180	0.0400
IT Material	ZIRC	ZIRC
Maximum Stack Length	145	151
Nominal Assembly Envelope	7.763	8.122
Kg's ^{235}U Assembly	22	23
Nominal Lattice Pitch	0.4850	0.5060
Assembly K_∞	0.9055	0.9302

(1) Fuel assembly parameters identified on Westinghouse Drawing 6481E15.
(2) 16x16 CE Fuel Design to be shipped only in MCC-4.
(3) Non-specified dimensions are units of inches.
(4) Nominal 8.0-inch annular pellet zones are at top and bottom of fuel rod.

TABLE 1-4.4
FUEL ASSEMBLY PARAMETERS
17 X 17 TYPE FUEL ASSEMBLY

Fuel Assembly Description	17 X 17			17 X 17			17 X 17
Fuel Assembly Type	W-STD(Note 5)			W-STD/XL(Note 5)			W-OFA(Note 4)
Nominal Pellet Diameter	0.3225			0.3225			0.3088
Annular Pellet Inner Diameter	0.155			0.155			0.155
Nominal Clad Thickness	0.0225			0.0225			0.0225
Clad Material	ZIRC			ZIRC			ZIRC
Nominal Clad Outer Diameter	0.3740			0.3740			0.3600
Maximum Stack Length	145			169			145
Nominal Assembly Envelope	8.418			8.418			8.418
Kg's ^{235}U Assembly	24			28			22
Nominal Lattice Pitch	0.4960			0.4960			0.4960
	GT1	GT2	GT3	GT1	GT2	GT3	
GT Diameter	0.4820	0.4820	0.4740	0.4820	0.4820	0.4740	0.4740
GT Thickness	0.0160	0.0200	0.0160	0.0160	0.0200	0.0160	0.0160
GT Material	ZIRC	ZIRC	ZIRC	ZIRC	ZIRC	ZIRC	ZIRC
IT Diameter	0.4820	0.4820	0.4740	0.4820	0.4820	0.4740	0.4740
IT Thickness	0.0160	0.0200	0.0160	0.0160	0.0200	0.0160	0.0160
IT Material	ZIRC	ZIRC	ZIRC	ZIRC	ZIRC	ZIRC	ZIRC
Assembly K_∞	0.9541	0.9530	0.9536	0.9541	0.9530	0.9536	0.9644

(1) Fuel assembly parameters identified on Westinghouse Drawing 6481E15.
(2) 17x17 XL Fuel Design to be shipped only in MCC-4.
(3) Non-specified dimensions are units of inches.
(4) Nominal 8.0-inch annular pellet zones are at top and bottom of fuel rod.
(5) Nominal 10.25-inch annular pellet zones at top and bottom of 17x17 STD/XL

TABLE 1-4.5

FUEL ASSEMBLY PARAMETERS
VVER-1000 TYPE FUEL ASSEMBLY

Fuel Assembly Description	VVER-1000
Nominal Pellet Diameter	0.3088
Nominal Clad Thickness	0.0225
Clad Material	ZIRC
Nominal Clad Outer Diameter	0.3600
GT Diameter	0.4740
GT Thickness	0.0160
GT Material	ZIRC
IT Diameter	0.4740
IT Thickness	0.0160
IT Material	ZIRC
Maximum Stack Length	144
Kg ^{235}U Assembly	26
Nominal Lattice Pitch	0.5020
Assembly K_∞	0.9432

(1) Fuel assembly parameters identified on Westinghouse Drawing 6481E15.
(2) VVER-1000 fuel design to be shipped only in MCC-5 containers.
(3) Non-specified dimensions are units of inches.

APPENDIX 1-5

ASSEMBLY NEUTRON ABSORBER SPECIFICATIONS

ASSEMBLY NEUTRON ABSORBER SPECIFICATIONS

I. INTEGRAL FUEL BURNABLE NEUTRON ABSORBERS (IFBA)

INTRODUCTION

In the Hypothetical Accident Condition (HAC) test of Integral Fuel Burnable Absorber rods, a conclusion was drawn that indicated the ZrB_2 maintained its relative design configuration. Therefore, two (2) undamaged fuel assemblies -- having ZrB_2 coated pellets intact within zircaloy fuel rod cladding -- in the relative MCC container design configuration, were modeled for the Nuclear Safety Analysis.

DESIGN

A zirconium diboride (ZrB_2) coating is deposited onto the cylindrical portion of a uranium dioxide (UO_2) pellet by a sputtering system. This coating process is conducted in a cryogenicly pumped vacuum chamber housing a rotating drum. The coating process is conducted at a temperature range of 1300-1470°F for twelve (12) hours. Planar Magnetron cathodes mounted both within and outside of the rotating drum permit coating of the cylindrical surface of the UO_2 pellets nearly all around, simultaneously.

Each batch of pellets produced is identified as a specific coater lot. Extensive testing of each coater lot is necessary from a quality standpoint to ensure that the ZrB_2 has adhered to the pellet.

INTEGRITY

In order to demonstrate that the effectiveness of the ZrB_2 coating will not be reduced under the Hypothetical Accident Conditions (HAC) prescribed in 10CFR71, a drop test, thermal test, and water immersion test were conducted using two simulated fuel rods.

The test consisted of dropping the fuel rods from a height of 30 feet onto a flat, horizontal, essentially unyielding surface; heating rods to a temperature of 1475°F followed by water quenching; and immersion in water for at least 8 hours.

The test specimens consisted of 18.5 inch long fuel rods containing a (nominally) six (6) inch long stack of ZrB_2 coated fuel pellets and a 4.2 inch long uncoated fuel pellet stack in a (nominally) 0.360 inch diameter tube. A nominal plenum length of 7.525 inches with a standard 4G helical spring was used to simulate the hold down. The test rods were pressurized with helium to 200 psig, the standard pressure for IFBA rods.

Coated fuel stacks were weighed prior to rod fabrication. After welding, the rods were helium leak tested and the girth and seal welds were ultrasonically inspected to assure the integrity of the

welds. The pellet stacks were x-rayed, and the coated zone location was determined by active gamma scanning. Figure 1 illustrates the test rod configuration. Average boron loading on pellets was analytically determined using coated pellets from the same lot as those used in the test rods.

The drop test consisted of dropping one test rod on the bottom (pellet) end, and a second rod on the holddown spring end, from a height of 30 feet onto a half (1/2) inch thick steel plate that rested on a concrete floor. After the drop test, both rods were helium leak tested to confirm that the rod integrity was not lost. Subsequently, the test rods were placed in a muffle furnace preheated to 1475°F for 30 minutes. Although the average temperature at the center of the furnace was as specified (based on thermocouple indications), the back end of the furnace was 150°F higher. This higher temperature caused the cladding to balloon, which resulted in a creep rupture type failure of the cladding in a 2 inch section. Subsequent water (68°F) immersion for a period of no less than 8 hours resulted in water ingress into the rods. The condition made the test more severe than that specified in 10CFR71 and, therefore, the results are considered to be conservative.

After completion of water immersion, both test rods were x-rayed to determine the condition of the pellet stacks. X-ray inspection showed that the pellet stacks were intact in both the test rods. In the first rod, dropped on the bottom (pellet) end, considerable pellet fragmentation was observed. In the second rod, dropped on the holddown spring end, the coated and uncoated stacks were intact with only a small amount of fragmentation in the uncoated section.

Next, the first rod was gamma scanned to locate the ZrB_2 coated pellet zone. Gamma scan results illustrated in Figure 2 showed that the drop, thermal, and water immersion tests did not affect the ZrB_2 coating adherence to the pellets. The coating effectively stayed in position. The differences in the delayed gamma counts before and after the test (Figure 2) are due to normal equipment and test uncertainties. The second rod could not be properly gamma scanned because of problems encountered in transporting it through the gamma scanner due to its bowed condition.

The test rods were subsequently sectioned to remove the pellet stacks and perform ceramographic examination of the coated pellets. Since the pellet stack in the second rod could be removed intact, the pellets were dried and weighed, and the weight was compared to the pre-test weight. Results are presented in Table 1. Adherence of the ZrB_2 coating to the pellet was determined from ceramography, and analytical measurement of boron on tested and control pellets from the same coater lot. Table 2 shows a comparison of the measured boron loading on coated pellets from the test rods with that on pellets which had not undergone testing. The test results are within the normal process variability as defined in Table 3. A similar ceramographic comparison is illustrated in Figure 3.

FIGURE 1

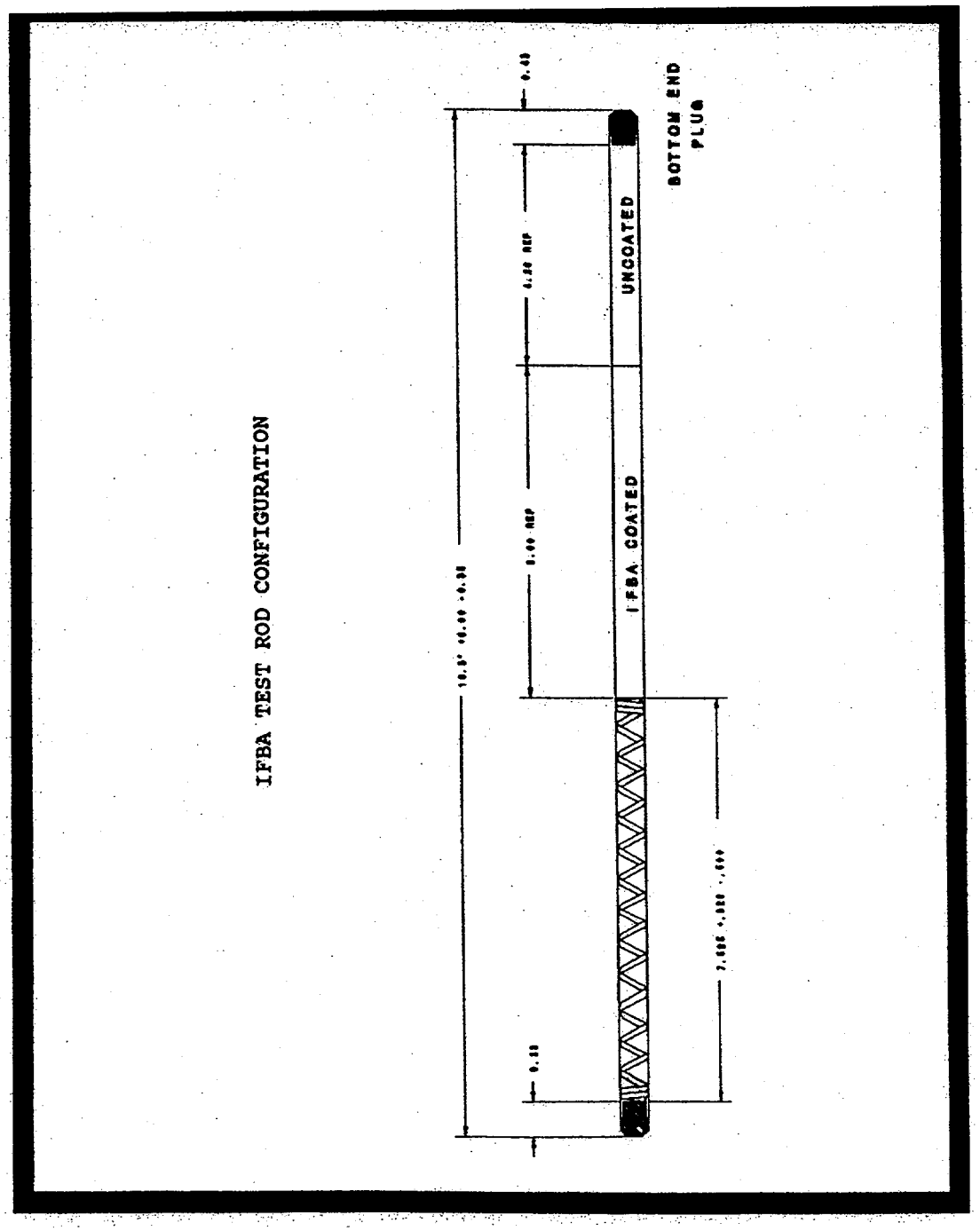
IFBA TEST ROD CONFIGURATION
BOTTOM END PLUG
UNCOATED
IFBA COATED

FIGURE 2

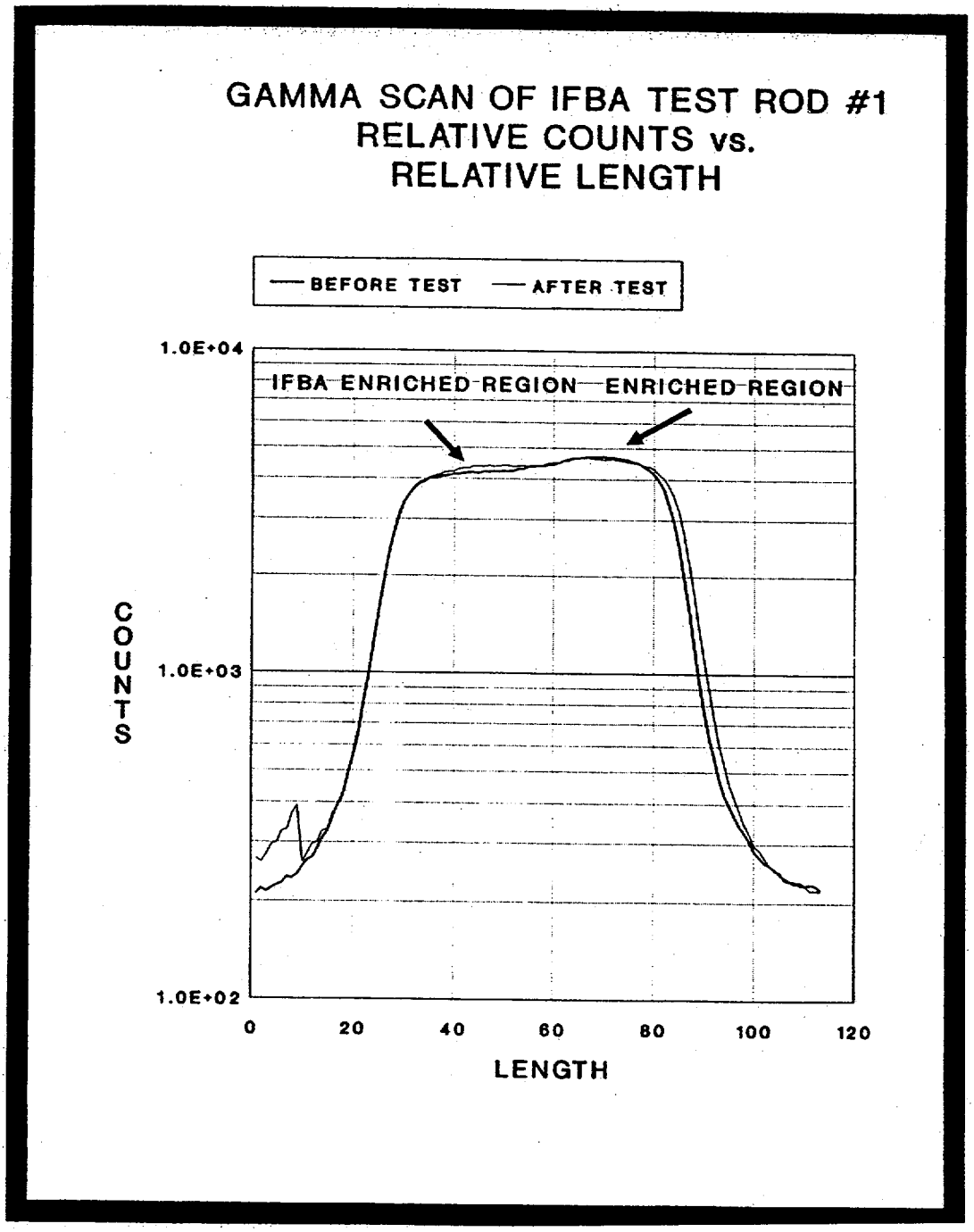
GAMMA SCAN OF IFBA TEST ROD #1
RELATIVE COUNTS vs.
RELATIVE LENGTH
BEFORE TEST
AFTER TEST
IFBA ENRICHED REGION
ENRICHED REGION
1.0E+04
1.0E+03
1.0E+02
COUNTS
0
20
40
60
80
100
120
LENGTH

TABLE 1

Stack Length and Weight Measurements

Rod No.	Stack Type	Stack Length, inches	Stack Weight, grams	
			Before	After
1	coated	6.203	78.8938	N/A
	uncoated	4.140	N/A	N/A
2	coated	6.179	78.5416	78.5413
	uncoated	4.110	N/A	N/A

N/A - Not Measured

TABLE 2

BORON LOADING MEASUREMENTS[1]

Test No	Control Pellets Boron, mg/inch	Tested Pellets Boron, mg/inch
1	7.39 ± 0.11	---
2	7.49 ± 0.11	---
3	---	7.04 ± 0.11
4	---	7.43 ± 0.11

1. These values are within the normal process variability defined in Table 3.

TABLE 3

IFBA VARIABILITY (Percent)

Item	σ_{SPEC} [1]	σ_{CE} [2]	σ_{BE} [3]	BASIS
Pellets	25	12	12	These values are on individual pellet weight gain data collected over 3 years and on group pellet chemistry data required as part of the product specification.
Strings	--	10	7.0	Inferred from the pellet distribution. These are conservative values since they assume no mixing during overturn operation or due to the dimension differences between the fixtures and the receiving trays.
Coater[4]	2.5	2.5	2.0	Each run is measured with a 96 pellet sample. The expected error of this estimate is 1.2% so the true values will be less than estimated. The best estimate value accounts for mixing to ± 3%.
Rods[5]	--	4.8	3.5	The standard deviations are estimated from the statistical convolution of the variability of the strings and the variability of the coater. Gamma scanner results show that the standard deviation of the rods is less than 5% which includes the large uncertainty of the scanner.
Assembly	1.5	1.9	1.5	Assembly variability is measured for each contract. The rod channels are checked before rod loading and, if necessary, rod mixing is used to ensure assemblies meet this criterion.

1. Product specification of the standard deviation.
2. Conservative estimate of the standard deviation.
3. Best estimate of the standard deviation.
4. $(\sigma^2_{string}/6 + \sigma^2_{coater})^{1/2}$
5. $(\sigma^2_{coater}/2 + \sigma^2_{rod}/48)^{1/2}$

FIGURE 3

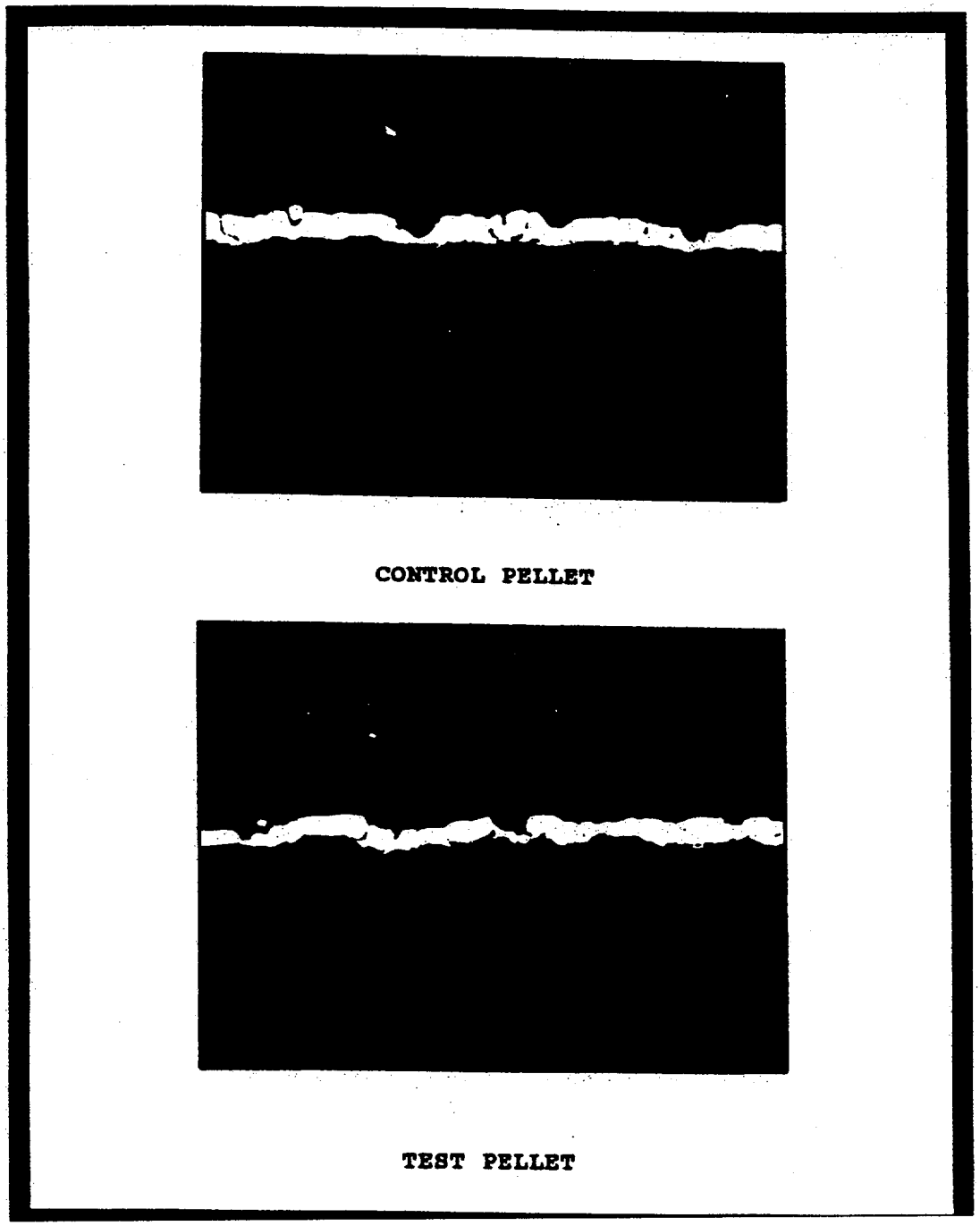

CONTROL PELLET

TEST PELLET

The test results conclusively proved that the ZrB_2 coating stayed on the pellets, and that the pellet stacks (although fragmented) did not move within the rod, thus demonstrating the effectiveness under the hypothetical accident conditions.

NUCLEONICS

IFBA Loading Uncertainty

The pellet coating process produces pellets that vary in the amount of ZrB_2 coating deposited. Pellets on the outside of the coating fixture receive less material than the ones on the inside because of shadowing by the fixture supports. Consequently, since there is no attempt to keep track of where the pellets end up, the result is a pseudo pellet variability. The specification calls for the standard deviation of the pellet loading to be less than 25%. Actually, the coaters produce material with a standard deviation of 12%. These values are based on several years worth of measurements of individual pellets by a weight gain technique, and by continuing analyses of each coater run by chemical analysis.

While this pellet variability seems large, it does not result in large variability in either the IFBA rods or in the assemblies containing IFBA. The reason is that there are large numbers of IFBA pellets in each rod (about 300) and still larger numbers in an assembly (greater than 10000). Thus, because of random mixing effects, the variability of rods or assemblies is slight.

Actually, mixing of pellets is not completely random and, consequently, the results of the mixing that does occur is not quite as good as might be expected from the above. For one, the pellets from an individual coater run are not thoroughly mixed so the effective mixing in a rod is decreased. Second, the pellets in a region (coater run to coater run) are not thoroughly mixed so that the assemblies will tend to vary because the coater runs vary.

Table 4 gives a description of the actual mixing process and conservatively estimates the IFBA rod variability. The result is a standard deviation of 4.8%. Gamma scan measurements of the rods show a standard deviation of 5%. For instance, the gamma scanner estimates the U-235 rod variability to be 2.5%, whereas, from more accurate sources it is known to be less than 1%. The scanner precision is statistical in nature and is therefore driven by the low count rate produced in the activation process.

A more important variability than the rods, is the variability of the assembly loading. This is more important because it affects the overall reactivity of the assembly. The variability of the rods only slightly affects the reactivity of the assembly because the statistical combination of rods with variable loading tends to cancel the effect of high and low rods. (Note this is not true for strong poisons which can only have reduced worth as a result of variability.)

TABLE 4
MIXING MECHANISMS

1. When the pellet fixtures from the coater are unloaded, the first operation is to get them onto a receiving tray. This tray is placed upside down on the fixture and the fixture is overturned. There is some mixing of rows in this operation since frequently pellets end up on top of each other or roll to locations different than the one they were in while in the coater.

2. Chipped or other reject pellets are removed at this stage by manufacturing. Filling the vacancies left introduces a slight amount of mixing.

3. Since the fixtures are 17 to 18 rows wide, and the trays they are to be placed on in the pellet cart are 25 rows wide, there has to be considerable rearranging of rows of pellets in this process to get the number of rows to match. This operation is done by hand and in a happenstance manner which is dictated by the state that the person doing the mixing finds the receiving tray after overturning. This state will be different from overturning to overturning.

4. Once the pellets get on the 25 row trays about 150 pellets are removed by Quality Assurance (QA) for sampling. The largest portion (96) of these pellets are used to determine the average coater loading. Others are used to check for hydrogen, coating adherence, etc. QA also removes any pellets that do not meet the visual specification. Again, the vacancies introduced increase mixing slightly.

5. At this stage the pellets are in 20 inch strings on the pellet trays. For ease of analysis, these strings are assumed to have been together in the coater as a continuous string. This is a conservative assumption since the required handling (as described in the steps above) produces considerable mixing. This is the second conservative assumption in the mixing analysis.

In addition, since these strings are about 20 inches long, they must contain at least one section of pellets from an end of the fixture or a section of pellets from next to one of the vertical support bars. This means that no string can contain only pellets from the middle of the fixture. No string can contain just high loading pellets.

6. The strings of pellets on these trays are then measured for length and loaded onto separate trays by the collator for later loading into rods. Since a typical IFBA stack length is 120 inches and since the trays hold stacks of about 20 inches, it takes about 6 lengths of pellets from 6 different trays to make up one IFBA stack. Since the stacks on the trays are in no particular order with respect to their position in the coater they will be loaded into rods in a pseudo random manner.

7. Assuming the mixing described above (but excluding the important additional mixing during the fixture overturn and tray loading operations), randomly loaded pellet strings that have a standard deviation of about 10%, taken from coater runs that are varying by about 2.5%, produce a rod population that is varying by about 5% in boron content [$(10/\text{sqrt}(6))^2+2.5^2=4.8^2$]. This sum of squares is permissible since the variability of the rods due to the variability of the pellet strings [10/sqrt(6)] is independent of the variability of the rods due to the coater variability of 2.5%. This estimate that the rod variability is less than 5% is conservative for several reasons:

   a) The pellet string variability will be less than 10%. This number assumes no mixing of the pellets during the overturn operation. Since much of the variability of the strings is the result of the low outside rows in the fixtures, any mixing of these pellets will reduce the variability of the strings. Since the pellet variability is about 12%, the 10% pellet string variability assumption is conservative (there are about 50 pellets in a string).

   b) The effective number of strings in a rod will be greater than 6. Since the tray and fixture length and width are different, the strings of pellets on a tray are not likely to be composed of a continuous string of pellets from a fixture. Thus, most pellet strings on the trays will themselves be composed of two or more pellet strings from the fixtures.

   c) The effective coater variability will be less than 2.5%. A coater mixing process was introduced in March of 1989 where any coater run outside " 3% of nominal is mixed with another coater run so that the average of the two is within "3%. The mixing process guarantees that approximately half of the pellets in each rod come from each of the two coater runs. Thus, on a rod basis, the coater runs will effectively vary less than the 2.5% assumed.

8. Assembly variability is measured for each contract. The rod channels are checked before rod loading and, if necessary, rod mixing is used to ensure all assemblies meet the specification limit of 1.5%.

Because assembly worth is important in reactor core design, the amount of boron in each assembly is monitored. Each rod is assumed to have an amount of boron in it based on the coater run or runs it came from. The boron from each of the rods in the assembly is added and compared to the amount the assembly should contain. The standard deviation of the percentage differences between nominal and measured values is calculated to assure it is less than 1.5% as defined in the product specification.

Because of coater run variability, this is a difficult value to meet and would be expected to be exceeded occasionally if steps were not taken to reduce the assembly variability. One step taken is to monitor rods in channels before loading into assemblies. If the variability of the rods between channels is too great, the rods in the channels are mixed to form a more uniform population. Since monitoring channels was begun, no contract has exceeded the 1.5% limit on assembly variability.

Another step taken to reduce assembly variability is coater mixing. At the present time coater runs are mixed if they are more than 3% from the contract nominal. They are mixed with another run so that the combined run is within ± 3%. Credit for this is not taken because the specification does not require it. This is an in-house method of ensuring that the 1.5% assembly variability specification is met.

All of these factors which go into making up the assembly boron loading variability are given in Table 4. This table shows the specification requirements on IFBA variability, a conservative estimate of these variabilities, and a best estimate value for the variabilities. The bases for the estimates is also given.

The assembly variability is the pertinent result for criticality work. This variability is a specification quantity and is measured on each contract to be below 1.5%. The boron content in the IFBA rods has been reduced by 5% in analysis of the shipping container. This is conservative for two reasons. First, the 5% value is much larger than the 1.5% limit times the one sided 95/95 uncertainty factor. Second, this is included as a bias by reducing the number of B^{10} atoms in the assembly. If it were to be included as a variability (which it is) instead of as a bias, its resulting effect would be smaller because of statistical convolution with other variable factors of equal or larger magnitude.

Number densities calculated for ^{10}B concentration given above are further reduced 25% to provide an additional safety margin.

Axial Reflector Modeling

Westinghouse models shipping containers as infinite in length because this is convenient and slightly conservative (since credit for axial leakage is ignored). However, since part-length

poisons are to be used, a full 3D model is needed rather than constructing a more conservative infinite model.

Table 5 shows the composition of the material between the fuel stacks. The values in this table

TABLE 5

Structure Between Axial Fuel Stacks

Region	Length, inches	Composition
Fuel Stack	0.0	
End Plug	0.43	30% Zr 70% H_2O
Bottom Nozzle	2.4	20% SS 80% H_2O
Container End Plate	0.75	100% SS
Container Structure	1.5	10% SS 90% H_2O
Center Line	5.08	

assume that two assembly bottoms are lined up, even though assemblies always ride front to back on the truck. This is a considerable conservatism because it excludes the 7 inch plenum region (3 inch, if spring compression is assumed) from separating the two fuel stacks.

Table 5 defines a 5.08 inch distance from the fuel stack to the center line between two fuel stacks, or a 10.16 inch axial spacing between fuel stacks. This is essentially an infinite distance between fuel stacks. This is conservative since the plenum space is excluded.

QUALITY ASSURANCE

IFBA Pellet ZrB_2 Adherence

IFBA pellets are coated with zirconium diboride, ZrB_2, using a Westinghouse patented and qualified sputtering process. This high temperature, high vacuum process applies a dense, mechanically adherent ZrB_2 coating to 17000 to 20000 pellets at a time during one coating cycle. The coating is applied to a nominal thickness of 0.0004 inch as the pellets are rotated while held in a coating fixture bounded with wire.

When the timed coating cycle is complete, all coated pellets are unloaded and placed on trays for visual inspection and sampling. A trained and qualified inspector performs a 100 % visual inspection, discarding all pellets with chips, cracks, discoloration, and other questionable surface anomalies. Sample pellets are randomly selected for boron chemical analysis (mg B^{10} / inch), coating adherence tests (thermal cycle/peel test), metallographic ZrB_2 / UO_2 interface evaluation, and chemical impurities.

The amount of boron present on the coated pellets is determined by a qualified analytical procedure involving removal of the ZrB_2 coating by pyrohydrolysis and boron measurement by titration. Residual boron is determined by emission spectrometry to assure that all boron is removed from the pellets. A NIST No. SRM 951 boric acid standard is used to standardize the titrant. Control standards are analyzed to verify boron recovery through the pyrohydrolysis system. This procedure is performed on 12 groups of eight pellets each for every coating lot of pellets. The average milligrams of boron measured on the 12 groups is multiplied by the percent B^{10} in Boron as determined by ZrB_2 powder mass spectrographic analyses of supplier and Westinghouse overcheck samples. The result is milligrams B^{10}, which is divided by the total length of the 96 pellet sample to achieve milligrams B^{10} per inch.

Adherence testing is performed on a sample of 10 pellets per coating lot. This test takes the form of 10 thermal cycles followed by a tape peel test. This test is performed to assure that the coating adheres to the UO_2. The sample of 10 pellets is cycled from room temperature to 600 EC ten times to simulate start-up and shut down of reactor operation. The cycled pellets are then weighed and peel tested by applying and removing tape to the pellet circumference. The tape

itself must pass an adherence test for stickiness or gripping ability before it is used. After the peel test, pellets are reweighed and disposition is made by determining the amount of coating removed. Less than 0.0008 grams at a 95% confidence limit is the specification. No coating lot has ever failed an adherence test.

A pellet sample from each coating lot is analyzed by emission spectroscopy for metallic impurities. Carbon, nitrogen, and fluorine are also analyzed by other analytical techniques. These analyses are performed to assure that the ZrB_2 coating contains no detrimental impurities. The same analyses were performed on the UO_2 pellets prior to coating as a condition of their release.

IFBA Pellet Location In Fuel Rod

The next precaution taken to assure that ZrB_2 coated pellets are present in the fuel is computerized, robotic stack collation. For each rod design, (three zone - natural / coated / natural, or five zone - natural / enriched / coated / enriched / natural) a software program is loaded into a process control computer at the pellet collation station. This program instructs a pair of robots. The robots are located inside a ring of pellet tray carts which contain the necessary pellet types to fabricate the desired rod design. At the computer's command one robot picks up the appropriate tray of pellets (25 rows) and positions it so that the other robot may measure and remove the correct lengths of pellets. The tray handling robot then puts the tray back and proceeds to place another tray in position for pellet length measurements and removal. This process is repeated until 25 measured, and correctly zoned, pellet stacks are located on special capture row trays for continued processing. It is important to note that there is no way for pellets to escape from the capture row trays once they are loaded.

After IFBA pellets are loaded into tubes, the resultant rods are pressurized, seal welded, and inspected by passive gamma scanning. The purpose of this inspection is to verify that correct uranium enrichment is present, and that no deviant uranium enrichment pellets are mixed in with the stack.

The final inspection to assure that ZrB_2 pellets are present as desired is a neutron activated gamma scan of the finished rods. This calibrated procedure is performed on 100 % of all rods fabricated at Columbia. This inspection has the capability of discriminating a single coated pellet which may be mixed into an uncoated pellet zone. Each rod containing coated pellets is inspected for correct zone lengths (natural, enriched, or coated) and plenum length. The active gamma scanner inspection is done by activating the uranium with neutrons as the rod passes by a Californium source. The resultant gamma activity is measured for each zone and compared with standard rod activity levels recorded in a process control computer.

IFBA Rod Location In Fuel Assembly

Boron bearing rods are known as Integral Fuel Burnable Absorber (IFBA) rods. There are four separate actions which assure that IFBA rods are in their correct positions within a fuel assembly.

The first step in assuring correct IFBA rod position in the assembly is in loading the magazine. The magazine is a fixture used to stage rods prior to assembly loading. Templates are placed over the end of the magazine which will only permit rods to be loaded into certain positions within the magazine. Templates have been prepared and are selected according to the drawing number of the particular assembly being loaded. The assembly drawing number specifies the particular pattern of IFBA type rods to be used in the assembly. After loading IFBA type rods into the magazine, the template is removed and the standard rods are inserted into the remaining positions in the magazine.

The second step in assuring correct IFBA rod position in the assembly is in the inspection of the loaded magazine. The IFBA rods each have an identifying mark on the top end plug. Quality control (QC) Inspection verifies that the IFBA rods and the standard rods are in their correct positions based on a visual inspection of the top end plugs in the magazine.

The third step in assuring correct rod position in the assembly is the entry of assembly-rod data into the Rod Accountability and Monitoring (RAMS) real-time computer system. The system is pre-loaded with a list of the correct assembly id's for that region, and the correct rod loading pattern for the assemblies. Unique rod identifications are scanned into the RAMS real-time system using barcode reader devices. The computer system records the correct pattern of standard and IFBA rods for each assembly. It recognizes the rod type scanned and compares the location for that rod with acceptable locations for rods of that type. If the rod is in an acceptable location, the transaction accepts; if not, the transaction is rejected and the operator is instructed to check the pattern and make corrections if necessary. If any alterations to the rods loaded in the magazine are required, the corrected magazine is reinspected.

The fourth step in assuring correct rod position in the fuel assembly occurs when the data collected by the real-time computer system is transmitted to the batch database and updated. As in the real-time system, rod patterns for each assembly are preloaded into the computer's memory. The rod location which comes in with each rod transaction is compared to the location table to determine if the rod type is correct for that particular location. If the rod's position is correct, the transaction updates; if not, the transaction suspends and a warning message is generated to alert the area engineers to investigate and resolve the problem.

CONTROL OF CONTAINER USAGE

Verification that required assemblies in fact contain Integral Fuel Burnable Absorber (IFBA) rods is based on procedural controls traceable to visual confirmation of the top end plug identification mark when the assembly is fabricated. Applicable process specifications, operating procedures, and quality control instructions contain explicit guidance on requirements for IFBA rods in assemblies to be placed in MCC containers that might not have the optional container neutron absorber plates installed.

ASSEMBLY NEUTRON ABSORBER SPECIFICATIONS

II. SILVER - INDIUM - CADMIUM ROD CONTROL CLUSTER NEUTRON ABSORBERS (RCCA)

INTRODUCTION

In the Hypothetical Accident Condition (HAC) test of Rod Control Cluster Absorber rods, a conclusion was drawn that indicated the rods maintained their relative design configuration. Therefore, two (2) undamaged fuel assemblies -- having RCCA rods intact within the assembly -- in the relative MCC container design configuration, were modeled for the Nuclear Safety Analysis.

DESIGN

The Silver-Cadmium-Indium rod control clusters are essentially strong neutron absorbers contained within a stainless steel cladding. Control rod clusters typically consist of 16 to 24 rods attached to an apparatus for insertion into a fuel assembly. The chemical compositions for the Ag-In-Cd alloy are described in the following table:

Element	Product Analysis	
	Min Wt%	Max Wt%
Ag	79.5	80.5
In	14.75	15.25
Cd	4.75	5.25

The above material is typically classed as nominal Ag, 15 In, 5 Cd alloy. This material has a density of 10.17 g/cm^3 at room temperature and a melting point of 1472 °F (800 °C).

The alloys are fabricated as either cast or wrought bar. The cylindrical surface of the bar is essentially a smooth finish, free from cracks, laps, seams, slivers, blisters and other surface imperfections which due to their nature, degree, or extent will interfere with the use of the material. The end product is free of oxides, grease, oil, residual lubricants, polish material, and any other extraneous materials. The dimension for the cylindrical material is specified on applicable engineering drawings.

Each batch of material is identified as a specific lot. Extensive testing of each lot is necessary from a quality standpoint to ensure that dimensional tolerances are exact, the chemical compositions are correct, and that the bars are within specified weight tolerances.

INTEGRITY

In order to demonstrate that the effectiveness of the silver control rod will not be reduced under Hypothetical Accident Conditions (HAC) prescribed in 10CFR71, a drop test was performed using simulated rods. Lead, which has similar mechanical properties to that of Ag-In-Cd, was used in three drop tests in the MCC container.

The drop tests clearly indicated that the control rods will maintain their integrity and relative design configuration within the assembly. The thermal and mechanical properties of the alloy clearly show that the rods would be effective neutron absorbers after a 1475 °F thermal test coupled with water quenching and immersion.

NUCLEONICS

The rod dimensions vary with the fuel design in which they are to be contained, however, the minimum dimensions are assumed in the nuclear design. These dimension are 0.329 in. o.d. silver rod, in a 0.367 in. o.d. stainless steel tube, with an absorber length of 142 in.

The dimensions on the silver rod described above are used in the actual criticality model. This is acceptable since the fabrication tolerances are very strict for use in reactor environments. The minimum chemical compositions described in the above table are used in the actual criticality analysis. Number densities calculated from the minimum chemical compositions are further reduced 25% to provide an additional safety margin. The actual number of absorber rods required for each assembly is described in the Nuclear Safety Analysis.

QUALITY ASSURANCE

Each bar is inspected in accordance with written quality assurance procedures. Inspections conducted include visual appearance of the material finish, dimensions with calibrated equipment and weighing (cast bars only).

Two bars per lot minimum are sampled at random and analyzed to ensure that the material is within specification tolerances. Lots consist of all bars of the same nominal cross-section, condition and finish that are produced from the same heat, processed in the same manner, and presented for inspection at the same time.

Samples are also taken to show that there is no chemical heterogeneity between final rods. All samples are chemically or spectrographically examined. Traceability of each bar by heat is maintained through packaging and shipping.

The vendor who will fabricate the alloy bar has a quality assurance plan approved by Operations Product Assurance. Vendors will be qualified in accordance with WCAP 7800.

CONTROL OF CONTAINER USAGE

Verification that required assemblies in fact contain Rod Control Cluster absorber (RCCA) rods is based on procedural controls and visible confirmation of installation when the assembly is loaded into the container. Applicable process specifications, operating procedures, and quality control instructions contain explicit guidance on requirements for RCCA's in assemblies without sufficient Integral Fuel Burnable Absorber (IFBA) rods to provide the required margin of safety, and/or in assemblies to be placed in MCC containers that might not have the optional container neutron absorber plates installed.

ASSEMBLY NEUTRON ABSORBER SPECIFICATIONS

III. BOROSILICATE GLASS NEUTRON ABSORBERS (Glass Pyrex)

INTRODUCTION

In the Hypothetical Accident Condition (HAC) test of Borosilicate Glass Absorber rods, a conclusion was drawn that indicated the rods maintained their relative design configuration. Therefore, two (2) undamaged fuel assemblies -- having Glass Pyrex rods intact within the assembly -- in the relative MCC container design configuration, were modeled for the Nuclear Safety Analysis.

DESIGN

The Borosilicate Glass Neutron Absorber rod control clusters are essentially strong annular neutron absorbers contained within an inner and outer stainless steel cladding. Control rod clusters typically consist of 16 to 24 rods attached to an apparatus for insertion into a fuel assembly. The nominal chemical compositions for the Glass are described in the following table:

Chemical Composition	
Oxide	Weight %
Silica (SiO_2)	80.5
Boron Trioxide (B_2O_3)	12.5
Alumina (Al_2O_3)	3
Sodium Oxide (Na_2O)	4

The boron contained in B_2O_3 is natural without being depleted or enriched in ^{10}B isotope (18.5 ± 0.5 wt%). The density of the glass is 2.23 ± 0.01 g/cc at room temperature. The acceptable range for B_2O_3 material is ± 0.2. The material has a softening point of 1502 °F (817 °C). The Glass is purchased in the form of tubing supplied free of internal stresses, tension, and compression.

The cylindrical surface of each glass rod is essentially a smooth finish, that is visually inspected for imperfections, crushed surfaces, knots, stones, chips, scuffs and scratches and cleanliness.

The dimension of the cylindrical material is specified on applicable engineering drawings.

Each batch is identified as a specific lot. Extensive testing of each lot is necessary from a quality standpoint to ensure that dimensional tolerances are exact, the chemical compositions are correct and that the rods are within the specified density.

INTEGRITY

In order to demonstrate that the effectiveness of the glass control rod will not be reduced under Hypothetical Accident Conditions (HAC) prescribed in 10CFR71, a drop test was performed using simulated rods. Lead, which has similar mechanical properties to that of Borosilicate glass, was used in three drop tests in the MCC container.

The drop tests clearly indicated that the control rods will maintain their integrity and relative design configuration within the assembly. The thermal and mechanical properties of the glass clearly show that the rods would be effective neutron absorbers after a 1475 °F thermal test coupled with water quenching and immersion.

NUCLEONICS

The rod dimensions vary with the fuel design in which they are to be contained, however, the minimum dimensions are assumed in the nuclear design. These dimension are 0.336 in. and 0.190 in. inner and outer diameters, respectively, for the glass in a 0.381 in. o.d. stainless steel tube with an absorber length of 142 in.

The dimensions on the glass rod described above are used in the actual criticality model. This is acceptable since the fabrication tolerances are very strict for use in reactor environments. The minimum chemical compositions described in the above table are used in the actual criticality analysis. The minimum B_2O_3 wt% of 12.3 is further reduced by 25% to provide for an additional safety margin. The actual number of absorber rods required for each assembly is described in the Nuclear Safety Analysis.

QUALITY ASSURANCE

Each rod is inspected in accordance with written quality assurance procedures. Inspections conducted include visual appearance of the material finish, dimensions with calibrated equipment to a 95% confidence level, and weighing for density verification.

One tube per lot minimum is sampled at random and analyzed to ensure that the B_2O_3 material is

within specification tolerances. Lots consist of all tubes of the same nominal cross-section, condition and finish that are produced from the same heat, processed in the same manner, and presented for inspection at the same time.

All samples are chemically or spectrographically examined. Traceability of each tube by heat is maintained through packaging and shipping.

The vendor who will fabricate the glass tube has a quality assurance plan approved by Operations Product Assurance. Vendor will be qualified in accordance with WCAP 7800.

CONTROL OF CONTAINER USAGE

Verification that required assemblies in fact contain Glass Pyrex absorber rods is based on procedural controls and visible confirmation of installation when the assembly is loaded into the container. Applicable process specifications, operating procedures, and quality control instructions contain explicit guidance on requirements for Glass Pyrex rods in assemblies without sufficient Integral Fuel Burnable Absorber (IFBA) rods to provide the required margin of safety, and/or in assemblies to be placed in MCC containers that might not have the optional container neutron absorber plates installed.

ASSEMBLY NEUTRON ABSORBER SPECIFICATIONS

IV. WET ANNULAR BURNABLE NEUTRON ABSORBERS (WABA)

INTRODUCTION

In the Hypothetical Accident Condition (HAC) test of Wet Annular Burnable Absorber rods, a conclusion was drawn that indicated the rods maintained their relative design configuration. Therefore, two (2) undamaged fuel assemblies -- having WABA rods intact within the assembly -- in the relative MCC container design configuration, were modeled for the Nuclear Safety Analysis.

DESIGN

The Wet Annular Burnable Neutron Absorber rod control clusters are essentially strong annular neutron absorbers contained within an inner and outer stainless steel cladding. Control rod clusters typically consist of 16 to 24 rods attached to an apparatus for insertion into a fuel assembly. The nominal chemical compositions for the Glass are described in the following table:

Chemical Composition	
Oxide	Weight %
Silica (SiO_2)	80.5
Boron Trioxide (B_2O_3)	12.5
Alumina (Al_2O_3)	3
Sodium Oxide (Na_2O)	4

The boron contained in B_2O_3 is natural without being depleted or enriched in ^{10}B isotope (18.5 ± 0.5 wt%). The density of the glass is 2.23 ± 0.01 g/cc at room temperature. The acceptable range for B_2O_3 material is ± 0.2. The material has a softening point of 1502 °F (817 °C). The Glass is purchased in the form of tubing supplied free of internal stresses, tension, and compression.

The cylindrical surface of each glass rod is essentially a smooth finish, that is visually inspected for imperfections, crushed surfaces, knots, stones, chips, scuffs and scratches and cleanliness. The dimension of the cylindrical material is specified on applicable engineering drawings.

Each batch is identified as a specific lot. Extensive testing of each lot is necessary from a quality standpoint to ensure that dimensional tolerances are exact, the chemical compositions are correct and that the rods are within the specified density.

INTEGRITY

In order to demonstrate that the effectiveness of the WABA rod will not be reduced under Hypothetical Accident Conditions (HAC) prescribed in 10CFR71, a drop test was performed using simulated rods. Lead, which has similar mechanical properties to that of WABA, was used in three drop tests in the MCC container.

The drop tests clearly indicated that the control rods will maintain their integrity and relative design configuration within the assembly. The thermal and mechanical properties of the glass clearly show that the rods will be effective neutron absorbers after a 1475 °F thermal test coupled with water quenching and immersion.

NUCLEONICS

The rod dimensions vary with the fuel design in which they are to be contained, however, the minimum dimensions are assumed in the nuclear design. These dimension are 0.336 in. and 0.190 in. inner and outer diameters, respectively, for the WABA in a 0.381 in. o.d. stainless steel tube with an absorber length of 142 in.

The dimensions on the WABA rod described above are used in the actual criticality model. This is acceptable since the fabrication tolerances are very strict for use in reactor environments. The minimum chemical compositions described in the above table are used in the actual criticality analysis. The minimum B_2O_3 wt% of 12.3 is further reduced by 25% to provide for an additional safety margin. The actual number of absorber rods required for each assembly is described in the Nuclear Safety Analysis.

QUALITY ASSURANCE

Each tube is inspected in accordance with written quality assurance procedures. Inspections conducted include visual appearance of the material finish, dimensions with calibrated equipment

to a 95% confidence level, and weighing for density verification.

One tube per lot minimum is sampled at random and analyzed to ensure that the B_2O_3 material is within specification tolerances. Lots consist of all tubes of the same nominal cross-section, condition and finish that are produced from the same heat, processed in the same manner, and presented for inspection at the same time.

All samples are chemically or spectrographically examined. Traceability of each tube by heat is maintained through packaging and shipping.

The vendor who will fabricate the WABA tubing has a quality assurance plan approved by Operations Product Assurance. Vendors will be qualified in accordance with WCAP 7800.

CONTROL OF CONTAINER USAGE

Verification that required assemblies in fact contain WABA absorber rods is based on procedural controls and visible confirmation of installation when the assembly is loaded into the container. Applicable process specifications, operating procedures, and quality control instructions contain explicit guidance on requirements for WABA rods in assemblies without sufficient Integral Fuel Burnable Absorber (IFBA) rods to provide the required margin of safety, and/or in assemblies to be placed in MCC containers that might not have the optional container neutron absorber plates installed.

APPENDIX 1-6

Gd_2O_3 NEUTRON ABSORBER PLATES SPECIFICATIONS

Gd_2O_3 NEUTRON ABSORBER PLATES SPECIFICATIONS

INTRODUCTION

Gadolinium oxide (Gd2O3), a strong neutron absorber, has been incorporated into an existing industrial cermet (coating similar to porcelain) for use as a neutron absorber plate. This cermet coating, when applied to a carbon steel base, possesses the required nuclear and mechanical characteristics to permit it to be used in the MCC fuel shipping containers.

These cermets are mainly used in applications requiring heat resistant or chemical resistant coatings such as jet exhausts or heat exchangers. Coating a steel base that provides shape and strength is a relatively simple spraying and fusing process which can be performed in a matter of minutes using existing industrial equipment and techniques.

NUCLEONICS

The most effective absorber plate possible is one which is essentially "black" and absorbs all neutrons directed at it. The amount of Gd_2O_3 necessary to analytically achieve this characteristic is 0.020 gm/cm2. This value is elevated by 25% such that a minimum of 0.027 gm/cm2 is set as a design requirement. The number densities used in the criticality calculations for the Gadolinia in the plate coating are based on a coating density of 0.020 grams Gd2O3/cm2. The effects of minor through-holes, to allow for handling and assembly clearance, and welding burn of the coating, have been evaluated and determined to have an insignificant effect on the absorber function of the plates.

Vertical Gadolinium neutron absorber plates are permanently installed in all the MCC shipping containers; segmented horizontal plates are installed in those MCC-3 and MCC-4 containers used to package fuel assemblies whose 235U enrichment is greater than 4.65 wt%, and in all MCC-5 containers. Once segmented horizontal plates are added to an MCC-3 or -4 container, the plates will remain in place in that container. Optional vee-shaped guided absorber plates will be used in the MCC-5 container, in addition to the vertical and horizontal plates, when 235U enrichment of the VVER-1000 assembly is greater than 4.80 wt%.

Although the minimum required concentration of gadolinium oxide is shown to be 0.027 gm/cm2, the original KENO modeling was based on two layers of coating at 75% of this density; hence the design specifications for all vertical plates, and the horizontal plates for the MCC-3 and MCC-4 container, require a minimum of 0.054 gm/cm2. The MCC-5 horizontal and vee-shaped plates are modeled with one layer of coating, or a minimum of 0.027 gm/cm2.

DESIGN

The Hypothetical Accident Condition (HAC) as defined in 10CFR71 requires that subcriticality of fuel assemblies in the shipping containers be demonstrated after, in sequence, a 30-foot free drop of the loaded container, puncture of the shell, exposure to 1475°F for 30 minutes and water immersion for 8 hours.

Since gadolinium oxide (Gd_2O_3) is a refractory ceramic which is similar to aluminum oxide (Al_2O_3) or zirconium oxide (ZrO_2), substitution of Gd_2O_3 for some or all of the Al_2O_3 or ZrO_2 in the finished coating seemed reasonable. Through trial, a coating composition was arrived at which maximized the Gd_2O_3 content while maintaining physical properties comparable to the base cermet industrial coating. Sample absorber plate sections have demonstrated the coating's damage resistance to normal abrasion, high temperature (1475°F), thermal shock (water splash and quench), impact (30-foot free fall), and flexing. Gd_2O_3 absorber plates were also used in three 30-foot drop tests.

The vertical Gd_2O_3absorber plate used in all MCC containers has approximate dimensions of 0.075" x 7.25" x 160" (189" for the MCC-4 and MCC-5 containers). The thickness is composed of 20 gauge (0.035") steel with a combined Gadolinia and Alumina coating. The coating is on both sides of the plate, such that the total coating contains at least 0.054 gm Gd_2O_3/cm2. The assembly is fabricated by overlapping two sections of absorber plate and fusion welding the edges to produce a 160" (189" for XL) long assembly. The 160" assembly will weigh approximately 15 pounds. The vertical Gadolinium neutron absorber plate is used as a permanent feature within all MCC fuel shipping containers.

The segmented horizontal Gd_2O_3 absorber plates are designed such that they can be positioned beneath the strongback between cross-member supports. The width of the horizontal plates is increased to 8.75 inches for the MCC-3 and -4 containers and 9.25 inches for the MCC-5 container. Typical lengths range from 14.08 to 23.00 inches with corresponding weights of 1.9 to 3.1 pounds for the MCC-3 and -4 containers and 2.0 to 3.3 pounds for the MCC-5 container. The thickness is composed of 20 gauge (0.035") steel with a combined Gadolinia and Alumina coating. The coating is on both sides of the plate for the MCC-3 and MCC-4, such that the total coating is at least 0.054 gm Gd_2O_3/cm2. The drawing requirement for the MCC-5 is also 0.054 gm/cm2, although the KENO modeling only requires 0.027 gm/cm2. The horizontal Gadolinium neutron absorber plate sections are used as an optional feature within the MCC-3 and -4 fuel shipping container, and as a permanent feature in the MCC-5 container. However, once an MCC-3 or -4 container has the horizontal plates installed, they will remain in that container permanently.

The horizontal vee-shaped Gd_2O_3 guided absorber plate used for the MCC-5 container is similar to the horizontal plates in terms of segmented lengths; however, these plates are shaped to conform to the surface of the VVER-1000 assembly and are positioned between the strongback and the assembly. The guided absorber plates are positioned between the container internals grid support structure and below the fuel assembly; as such, they do not support the weight of the fuel assembly. This vee-shaped guided absorber plate is thicker (0.060 inches) than the normal vertical and horizontal plates and is coated only on its underside with the normal Gd_2O_3 loading of 0.027 gm/cm2. The plate width is typically 9.24 inches, with a total Gd_2O_3 coated width of approximately 11.06 inches. Typical lengths range from 6.60 to 15.48 inches with corresponding weights of 1.9 to 5.75 pounds. The Gadolinium neutron absorber guide plate sections are used as an optional feature within the MCC-5 shipping container. However, once an MCC-5 container has the guided absorber plates installed, they will remain in that container permanently.

INTEGRITY

Coating Flexibility

The absorber plates are restrained by the container internals once the plates are installed. One side of each vertical plate faces a continuous sheet metal skin. The other side of each plate faces a ladder-like frame of 1.5 inch square tubing spaced approximately every 20-24 inches. Consequently the plate may bow approximately 1.5 inches at the most between any pair of square tubes. A simple simulation of these conditions with a section of full-size absorber plate reveals no noticeable effect except for slight permanent set of the steel backing. Horizontal plates are mounted in direct contact with the underside of the strongback, and cannot flex more than the strongback itself. The guided absorber plates are mounted to the top of the strongback, and cannot flex more than the strongback.

Improper handling of fabricated plates could cause coating damage. Small radius bends (approximately 2") will cause the coating on the compression side of the plate to crack locally and flake. Bends of 4" radius have no noticeable effect on the coating surface or adherence to the metal base. Normal handling can easily accommodate this restriction by use of a strongback or manual support to prevent small radius bends of the plate. Detection of possible coating damage by bending is simple. First, the metal backing will take a permanent set long before the coating is affected. Second, when damage occurs, it causes noticeable flaking and/or loss of material. Expected handling and service of the plates will not exceed their capability to flex without functional impairment.

Coating Impact Resistance

As part of the HAC, three MCC containers containing two plates each were subjected to 30-foot drops. Since the internals suspension system cannot absorb all internal energy, mechanical shock of the internals will occur. Sample plates were also subjected to a 30-foot free drop onto ½ inch steel plate. The plates were dropped, using guide wires, in the flat (plate width horizontal) and guillotine (plate width vertical) configurations. The flat configuration only slightly deformed the metal backing with no obvious coating damage. The guillotine configuration, where the plate dropped on edge, caused local deformation of the plate edge and random flaking of the coating edge up to 1/8" away from the plate edge. The bulk of the coating was unaffected by the severe shock.

As part of the process specification, adhesion tests are performed on production plates to industry standards. These tests allow a process check to verify the consistency of the coating process and that production plates are representative of sample performance.

These tests demonstrated that the coating is capable of withstanding impacts far greater than that expected under accident conditions in its protected location inside the MCC shipping container support frame. Gd_2O_3 plates present in the three drop tests described in Chapter 2 yielded no obvious coating damage.

Coating Abrasion Resistance

The absorber plates which are positioned within and under the support frame, and the guided absorber plates which are mounted on top of the strongback, are not exposed to conditions where abnormal abrasion forces would occur. The edges of the plate do not need to be coated, and purposely are not coated, although the spraying operation will tend to deposit material there. The bottom edge of the vertical absorber plate interfaces with the internals and bears the weight of the plate. Therefore, the edges of the plates which have been coated and fused will be abraded to base metal to eliminate the generation of gadolinium bearing debris and its possible migration from the container during inspection, cleaning, painting, etc.

The sides of the plates see negligible loads and broad contact areas. The coating is not easily affected by distributed loads; a hard, sharp edge tool is necessary to visibly scar the coating surface.

The gadolinium absorber plates installed in containers which were subjected to a 30-ft. drop test were visually examined after a one year period to verify that their condition was comparable to that of original installation. There was no visible evidence of loss of coating. The coating is adequately abrasion resistant to withstand its service environment and maintain its functional capabilities.

High Temperature Integrity

The HAC essentially requires the container and its contents to withstand 1475°F for 30 minutes and subsequent cooldown. Commercially available materials were either inadequate as neutron absorbers or deteriorate upon exposure to 1475°F. The components of the coating are fused at approximately 1530°F during processing. The sides of the plates are oriented vertically during processing; fusing of the coating at these temperatures does not cause the material to flow from its applied configuration. The fusing is more of a limited wetting condition where materials in intimate contact join as compared to brazing, for example, where the braze wets the base material and flows under the effects of gravity and capillary action.

Sample plates were arranged in a muffle furnace to simulate their interface with the shipping container internals and each other. The purpose of the test was to verify that the plate's coating would not be altered by contact with interfacing surfaces such that its functional characteristics were affected. Once arranged, the furnace was turned on, stabilized at 1475°F for three-and-one-half hours and then turned off. The furnace door was opened and the plates removed when the indicated temperature had dropped to approximately 200°F. The plates were not noticeably altered in either case from their pre-test condition.

10CFR71 regulations specify exposure to an environment of 1475°F with an emissivity coefficient of 0.9 and package absorption coefficient of 0.8. Consequently, the package is heated up to its maximum temperature during the 30 minute period. Also, cooling of the package realistically begins as soon as the radiation environment is removed. The test performed is conservative since the plates were held at 1475°F for the entire 30 minute period, as well as the subsequent three-hour period where natural cooling is permitted.

The plates were then individually heated to 1475°F, removed at that temperature and subjected to poured (room temperature) water on one side. The plates were again heated, removed and then quenched in a bucket of room temperature water. The plates did not exhibit any noticeable cracks, flaking or separations. The plates' demonstrated resistance to thermal shock is similar to the industrial cermets and is adequate for any thermal shock the plates could possibly experience in a shipping container.

These tests demonstrated that absorber plates are capable of meeting the required high temperature accident conditions as well as unlikely, severe thermal shock.

Water Exposure

The absorber plate coating, by its characteristic cermet nature, is essentially impervious to water exposure for an eight-hour period. No formal tests are conducted.

QUALITY ASSURANCE

The basic requirement is that at least the design amount of absorber material (0.027g/cm2) is present in any given area. This requires verification first that the absorber material is present and second that the minimum quantities have been deposited.

For all three types of plates, the cermet is composed of 32.5 wt% Gd_2O_3. The distribution of absorber material in a unit thickness of the coating is assumed to be uniform because the extremely fine (1-10 microns) Gd_2O_3 powder and other powder coating components are combined in a water slurry and sprayed onto the metal backing. An analysis by X-ray fluorescence at Westinghouse ARD laboratories, as expected, did not discover any areas in sample absorber plates significantly deficient in Gd_2O_3 compared to other areas (the equipment examined areas the diameter of a dime). This test is not performed on production samples or plates because the nature of the materials and process are unlikely to cause any segregation of materials and, as explained, there will be absorber material in excess of actual design minimum loadings.

Final verification that the neutron absorber Gd_2O_3 is actually in the coating (not Al2O3 or ZrO2 for example), and present in acceptable concentrations, is made using verified standards and a portable elemental analyzer. The analyzer, using the X-ray fluorescence method, verifies that gadolinium is present by measuring the energy of the fluorescing X-rays that are uniquely characteristic of that element. By comparing the intensity of those X-rays to that of verified standards, it can be determined that the minimum density of 0.027 or 0.054 gm Gd_2O_3/cm2 is indeed present.

Process control of the coating composition and minimum thickness will insure that the minimum design loading of Gd_2O_3 is applied to each plate. Use of the analyzer verifies the Gd_2O_3 loading in the end product composition. The analyzer reading will be documented according to the bright yellow identification number stenciled and fused into the coating of each plate.

The standards used to calibrate the elemental analyzer will have a master in Columbia archives for quality control standards. Preservation of the master standard will enable the plates' Gd_2O_3 content to be checked anytime in the future.

The vendor who will fabricate the absorber plates has a quality assurance plan approved by Operations Product Assurance. Vendors will be qualified in accordance to WCAP 8370.

CONTROL OF CONTAINER USAGE

For MCC containers, once an absorber plate, whether vertical, horizontal, or shaped, is installed, it remains permanently in that container. As each container receives plates, the documentation associated with that container is updated to show its current configuration, and the container is marked. Container selection for each contract's shipments is made based on the information contained in the permanent records, and is approved by the Manager of Nuclear Materials Management. The process specification, operating procedures, and quality control instructions contain explicit guidance on requirements for the required plate verification and documentation at the time of plate installation. Additional controls exist in the Fuel Assembly Packing area to assure that the correct containers are used. "Correct" means that the container has at least the minimum allowable absorbers for the enrichment of the assemblies to be shipped; any container having more absorbers than required by the assembly enrichment may be used.

TECHNICAL JUSTIFICATION FOR REVISING THE ABSORBER PLATE INSPECTION REQUIREMENTS

The justification for relaxing the absorber plate inspection requirements follows from the conclusions that can be drawn from the following observations. Supporting information, showing calculations for determining area density, and tables showing keff results for the various fuel assembly types, is included in the next section.

Justification

1. **For the design criteria for absorber plate coating:**
   a) **The design minimum area density for Gd_2O_3 per absorber plate side is 0.027 g/cm^2.**

2. **For the absorber coating actually applied:**
   a) **The coating, 32.3 wt% Gd_2O_3, was applied to an actual minimum thickness of 8.25 mils equivalent Gd_2O_3 per side.**
   b) **The area density that 8.25 mils translates to is 0.0984 g-Gd_2O_3/cm^2.**
   c) **The total area density, therefore, for a double-sided absorber plate is 0.1968 g-Gd_2O_3/cm^2.**

3. **For the absorber plates used in all Westinghouse calculations:**
   a) **The area density used was 0.02 g-Gd_2O_3/cm^2. This corresponds to the theoretical "black" density for Gd_2O_3 with respect to thermal neutrons.**
   b) **The total area density, therefore, for the double-sided absorber plates used in the models was 0.04 g-Gd_2O_3/cm^2.**
   c) **This area density translates to a coating thickness of 1.67 mils.**

4. **Results from calculations for the double-sided absorber plates (0.02 g-Gd_2O_3/cm^2 area density per side; 0.04 g/cm^2 total) satisfy NRC requirements.**

5. **Calculations made for the most reactive fuel assembly type using single-sided absorber plates (0.02 g-Gd_2O_3/cm^2 area density total) satisfy NRC requirements. Results indicate that $k_{eff} \leq 0.95$.**

6. **Therefore, because, by design, a single side of an absorber plate contains a Gd_2O_3 area density of at least 0.027 g/cm^2, and because, by actual measurement during application, a single side contains an area density almost five times thicker than the "black" density (0.02 g-Gd_2O_3/cm^2), and because, using approved Westinghouse models with absorber plates with Gd_2O_3 area densities of 0.02 gm/cm^2 for most reactive fuel assembly types, calculated $k_{eff} \leq 0.95$, it follows that it is technically acceptable to conclude that an absorber plate provides satisfactory criticality safety protection based on a detailed visual inspection of the coating on just the visible side.**

<u>Supporting Calculations</u>

1. **The absorber coating that was actually applied to the plates is composed of 32.5 wt% Gd_2O_3, and applied to a *minimum* thickness of 8.25 mils equivalent Gd_2O_3/cm^2. To determine area density (gm Gd_2O_3/cm^2) provided by a coating depth of 8.25 mils, calculate the following:**

   a) **Convert mils to cm:**

      - **mils → 0.00825 inch**
      - **inch → 0.020955 cm**

   b) **Given the volumetric density of Gd_2O_3 = 7.407 gm/cc, determine the actual area density of Gd_2O_3.**

      - **cm * 7.407 g/cc = 0.1552 g/cm2**

   c) **Include the following conservative assumptions to determine final conservative value:**

   d) **Therefore, the area density per side of an absorber plate, including several conservative assumptions, is actually 0.0984 g-Gd_2O_3/cm^2.**

2. **Note that Westinghouse specifications require that the minimum area density applied to any one side of an absorber plate is 0.02 g- Gd_2O_3/cm^2. This corresponds to the area density that is considered "black" for thermal neutron. Also, this is the area density value that has been used in all Westinghouse KENO models for each coated side of every absorber plate.**

3. **Therefore, it is necessary to determine the equivalent mil thickness of Gd_2O_3 that is needed to provide an area density of 0.02 g-Gd_2O_3/cm^2. To determine the actual coating thickness that corresponds to this area density, compute backwards:**

   a) **Compensate for the following conservative assumptions:**

      - **Assume 25% increase in density:**
      - **$g/cm^2 \div 75\% = 0.027\ g/cm^2$**

      - **Compensate for the influence that one plate will have on the other for a double sided Gd absorber plate (~11%):**
      - **$g/cm^2 + 11\%\ (.027\ g/cm^2) = 0.030\ g/cm^2$**

      - **Assume 95% theoretical density for Gd:**
      - **$g/cm^2 \div 95\ \% = 0.0315\ g/cm^2$**

   b) **Again, given the volumetric density of Gd_2O_3 = 7.407 gm/cc, determine the thickness of the coating:**

      - **$g/cm^2 \div 7.407\ g/cc = 0.00425$ cm:**

   c) **Convert cm to mils:**

      - **cm → 0.00167 inch**
      - **inch → 1.67 mils**

   d) **Therefore, the mil thickness Gd_2O_3 required per side to provide area density of 0.02 g-Gd_2O_3/cm^2 is 1.67 mils.**

4. **Previous calculations give k_{eff} results for all type fuel assemblies in shipping containers with different neutron-absorber configuration. The results are presented in Table 1 of Appendix 6-2. These include double-sided Gd_2O_3 coated plates. Each side provides an area density of 0.02 g-Gd_2O_3/cm^2. Therefore, the total area density for the double-sided plate is 0.04 g-Gd_2O_3/cm^2.**

5. **New calculations performed using single-side coating on absorber plates, giving an area density of 0.02 g-Gd_2O_3/cm^2, give the following results:**

Assembly Type	Enrichment wt%	Added Absorbers	KENO $k_{eff} \pm 1\sigma$	95/95 w/ Bias
Type B [vi, vii] also with guide and thimble tubes	5.00	Optional Gd Plates	0.93667 ± 0.00133	0.94586[1]
Type B [vi, vii] also with guide and thimble tubes	4.70	None	0.93919 ± 0.00132	0.94836[1]

1 Analysis CRI-97-006, completed March 10, 1997

APPENDIX 1-7

DESIGN COMPARISON OF THE MCC-5 PACKAGE

TO THE MCC-4 PACKAGE

DESIGN COMPARISON OF THE MCC-5 PACKAGE TO THE MCC-4 PACKAGE

As shown on the various package general arrangement drawings in Appendix 1-2, the following list summarizes the design differences between the MCC-5 (a modified MCC-4 package designed specifically for transportation of VVER-1000 fuel assemblies) and the MCC-4 package (designed to transport a variety of other, standard, fuel assemblies).

1. **Component Weights**: The maximum weight MCC-4 fuel assembly (square lattice) weighs slightly more than the maximum weight MCC-5 fuel assembly (VVER-1000). The MCC-4 package internal structure weighs slightly less than the MCC-5 internal structure. The external structure (shell) weight is identical for both packages, resulting in an equivalent total gross package weight for both packages.

2. **Bottom Support Plate Gussets**: The MCC-4 package utilizes two bottom support plate gussets. The MCC-5 package utilizes four bottom support plate gussets.

3. **Bottom Support Plate**: The MCC-5 package bottom support plate is slightly different from the MCC-4 package to allow proper interfacing of the bottom nozzle support spacer.

4. **Bottom Nozzle Support Spacer**: Unlike the MCC-4 package, the MCC-5 package utilizes a bottom nozzle support spacer to preclude damage to the VVER-1000 fuel assemblies during transport.

5. **Top Nozzle Support Spacer**: Unlike the MCC-4 package, the MCC-5 package utilizes a top nozzle support spacer to preclude damage to the VVER-1000 fuel assemblies during transport.

6. **Top Nozzle Barrel Support**: Unlike the MCC-4 package, the MCC-5 package utilizes a top nozzle barrel support to preclude damage to the VVER-1000 fuel assemblies during transport.

7. **Top Closure Assembly**: The MCC-5 package top closure assembly is slightly different from the MCC-4 package top closure assembly to allow proper interfacing of the top nozzle support spacer.

8. **Clamping Frames and Pressure Pads**: The MCC-4 package clamping frames are shaped to contain two pressure pad assemblies for supporting standard-type, square fuel

assemblies, whereas the MCC-5 package clamping frames contain three pressure pad assemblies for supporting the hexagonally-shaped VVER-1000 fuel assemblies.

9. **Upper Pivot Mounts**: The MCC-4 package upper pivot mounts are identically shaped, but somewhat shorter, than the MCC-5 package upper pivot mounts.

10. **Grid Support Blocks**: Unlike the MCC-4 package, the MCC-5 package utilizes grid support blocks at the fuel assembly grid support strap locations to provide lateral support for the hexagonally-shaped VVER-1000 fuel assemblies.

11. **Optional Absorber Plates**: The optional MCC-4 package absorber plates are flat, whereas the optional MCC-5 package absorber plates are formed to match the grid support blocks for the hexagonally shaped VVER-1000 fuel assemblies. The flat horizontal plates which are optional in the MCC-3 and MCC-4 are required in the MCC-5 under all conditions; the vee-shaped optional plates in the MCC-5 are additional to the full complement of plates used in the MCC-3 and MCC-4.

APPENDIX 2-1

CONTAINER WEIGHTS AND CENTERS OF GRAVITY

MAXIMUM WEIGHTS FOR LOADED SHIPPING CONTAINERS[1]

COMPONENT	MCC-3	MCC-4	MCC-5
FUEL	3300	3870	3700
INTERNALS	1964	3118	3288
SHELL	2280	3545	3545
TOTAL	7544	10,533	10,533

[1] Units of pounds

CENTER OF GRAVITY FOR LOADED SHIPPING CONTAINERS

MCC-3

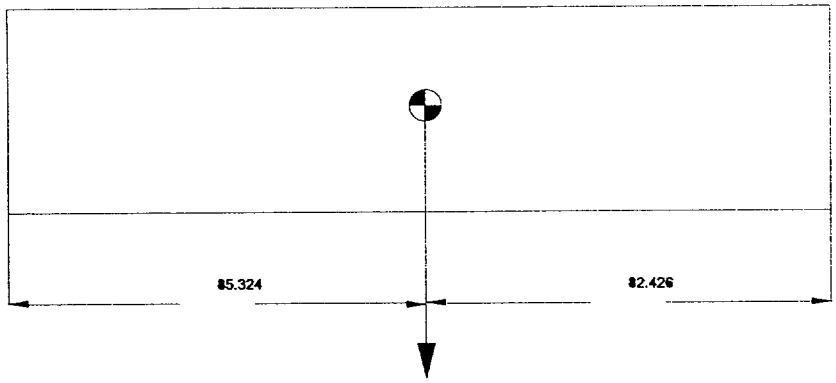

MCC-4

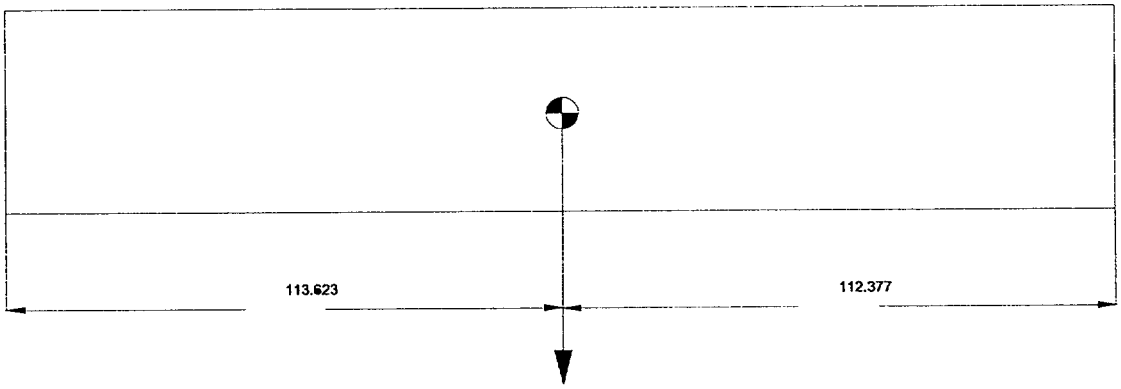

MCC-5

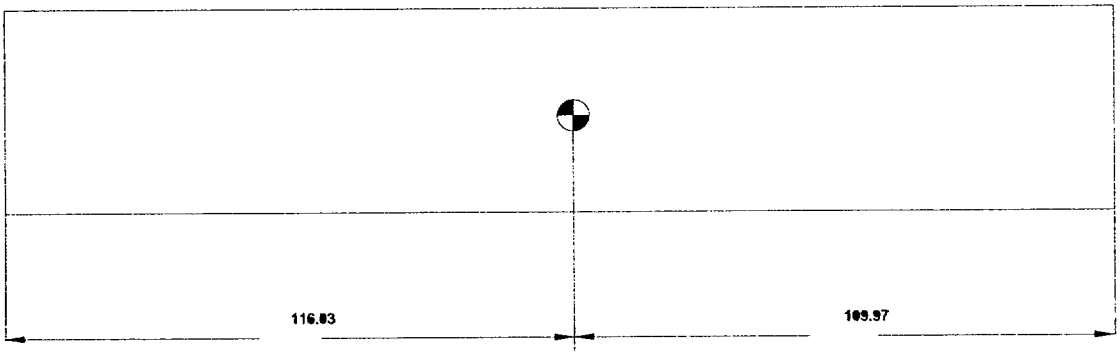

APPENDIX 2-2

CONTAINER LOAD SUSPENSION SYSTEM

CONTAINER LOAD SUSPENSION SYSTEM

INTRODUCTION

The following information is taken from a report submitted by Lord Kinematics* specifically written for the shipping containers of a design quite similar to MCC series containers. Because the load suspension systems are similar, the information is applied to the MCC-4 and MCC-3 shipping containers.

1.0 OBJECTIVE

1.1 The purpose of this report is to summarize the requirements, design and performance of a shipping container suspension system for Westinghouse Electric Corporation XL and conventional 12 ft. nuclear fuel rod assemblies.

2.0 RECOMMENDATION

2.1 The suspension system consists of 24 pieces of Lord part number J-5735-64. There is no change in the suspension system made when used to transport the lighter weight 12 ft. nuclear fuel assemblies. A detailed tabulation of performance data is presented in the Attachment.

2.2 In order to not exceed the design goal shock fragility of 6 G's maximum, the maximum vertical flat drop height is 10" and the maximum rotational drop height is 24".

3.0 DISCUSSION

3.1 The sandwich mounts have a cylindrically shaped elastomer section made in Lord SPE I elastomer. The nominal static radial or shear stiffness of J-5735-64 is 215 lb/in. The axial or compression/tension stiffness is approximately 6.5 times the radial stiffness. SPE I, like other elastomers has dynamic stiffness characteristics quite difference from static stiffness characteristics. The ratio of dynamic to static stiffness for the proposed mount is approximately 1.3. All elastomers are inherently damped and SPE I is no exception. The resonant transmissibility of J-5735-64 is approximately 6, resulting in a loss factor of 0.17. SPE I is a special purpose elastomer having an operating temperature range of -65°F to 160°F. All elastomers exhibit a change in stiffness due to temperature variations. At -40°F, the lowest operating temperature for this application, the proposed mount has a stiffness approximately 1.7 times that at 70°F. At +160°F the proposed mount has a stiffness approximately 0.85 times that at 70°F.

* Lord Kinematics, Shipping Container Suspension System for Westinghouse Electric Corporation XL and Nuclear Fuel Rod Assemblies, June 1, 1978.

3.2 The suspension system consists of 12 pairs of J-5735-64 arranged along the bottom of the suspended unit. Each mount supports an equal share of the total suspended weight in shear. Part number J-5735-64 was selected chiefly for logistics since Westinghouse Electric Corporation has used this part in the past for other nuclear fuel rod assembly shipping containers. It is advantageous to have pitch rotational and vertical translational natural frequencies that are difference so that these two modes are not in phase. It should be noted that a shift in unit c.g. location longitudinally from the proposed location would result in pitch rotational/vertical translational coupling. The longitudinal mount spacing will result in a relatively high pitch rotational natural frequency less likely to be excited by normal transportation vibration environments.

3.3 The computer analyses in the Attachment were performed on Lord's Six-Degree-of-Freedom shock program. The coordinate system used is located at the center of the gravity of the suspended unit. This coordinate system consists of three mutually orthogonal axes obeying the right hand rule. The Z axis is directed vertically outward from the unit center of gravity. The X axis extends longitudinally toward the forward end of the fuel rod assemblies. The Y axis lies in the horizontal plane containing the X axis and is directed in the lateral direction. The stiffness characteristics of each mount is listed in addition to the direction cosine that each stiffness direction makes with the three coordinate axes.

K(1) and K(3) correspond to mount shear stiffness values and are parallel to X and Z axes respectively. K(2) corresponds to the mount compression/tension stiffness value and is parallel to the Y axis. The dynamic to static stiffness ration for each mount is listed in the printout. Eta is the lost factor of the elastomer and is approximately equal to the reciprocal of resonant transmissibility. The computer program does not use loss factor in the solution of system response; consequently, viscous dampers having a damping ratio of .085 were added parallel to K(1), K(2), and K(3) at each mount location so that a damped response could be obtained. It should be noted that a dynamically equivalent 4 mount system was analyzed rather than the 24 mount system since the computer program used is limited to a maximum number of 12 mounts. The development of the dynamically equivalent system is presented in the Attachment.

Six undamped natural frequencies are calculated and if the system is completely uncoupled, the frequencies would correspond to the X, Y, Z translational and roll, pitch, yaw rotational natural frequencies. In order to depict the more complex coupled vibrational modes, a screw analogy is used for every frequency calculated, there is a corresponding point in space through which an invariant axis

passes.

This invariant axis is called a modal axis and its direction cosines are listed in the output. The suspended unit can rotate about this axis and simultaneously translate along it. The lead of screw indicates the distance in inches that the suspended unit travels parallel to the modal axis for one complete revolution about it. If the lead of screw is zero, the suspended unit simply rotates about the modal axis. As the modal axis moves from the center of gravity to a point an infinite distance away from the center of gravity, the vibrational mode associated with that particular frequency changes from pure rotational to pure translational provided that the lead of screw is zero.

The computer program calculates the system transient response to specified initial conditions at the time of impact. System initial conditions for each shock test modeled are calculated in the Attachment. Displacements and accelerations of the suspended unit c.g. for discrete instants of time are calculated for a total duration of 0.3 seconds. Responses are calculated at -40°F, +70°F, and +160°F.

The shipping container suspension system will limit the response of both the XL and 12 ft. nuclear fuel rod assemblies to approximately 6 G's when subjected to 10" vertical flat drops, 7 ft/sec end impacts, and 24" rotational drops. An examination of simulated shock response data for the 12 ft. nuclear fuel rod assembly reveals a peak response of 6.18 G's at -40°F for a 10" vertical flat drop. The computer analyses are based upon assumed infinitely rigid structures interfacing with each mount. In general, structural flexibility results in reduced unit accelerations since some kinetic energy at impact is absorbed and dissipated by these structures before it can be transmitted through the mounts to the unit.

It should be noted that an edgewise rotational drop was analyzed rather than a cornerwise rotational drop. Typically, the edgewise rotational drop is a more severe test and produces larger displacements and accelerations than the cornerwise rotational drop.

ATTACHMENT

DESIGN CRITERIA

Lord Kinematics
Division of Lord Corporation
Erie, Pennsylvania

SHIPPING CONTAINER SUSPENSION SYSTEM DESIGN CRITERIA

Customer: Westinghouse Electric Corporation
Pittsburgh, Pennsylvania

Date 6/01/78

Unit: XL Nuclear Fuel Rod Assembly

1. Suspended Weight: 5187. Lbs.
2. Mass Moments of Inertia (lb-in-sec^2):

   A. Roll - 433.8
   B. Pitch - 31250.
   C. Yaw - 31550.

3. Fragility Factors:

   A. Shock - 6 G's @ -40°F/+70°F/+160°F @ C.G.
   B. Vibration - 6 G's @ -40°F/+70°F/+160°F @ C.G.

4. A. 10" Vertical Flat Drop
   B. 7 ft/sec End Impact
   C. 24" Rotational Drop

5. Vibration Design Requirements:

   N/A

6. Military Specifications which apply:

   MIL-C-5584C Amended

7. Environmental Requirements:

   Operating Temperature Range from -40°F to +160°F

8. Methods of Transportation Used:

   Truck, Rail, Ship, Air

Lord Kinematics
Division of Lord Corporation
Erie, Pennsylvania

SHIPPING CONTAINER SUSPENSION SYSTEM DESIGN CRITERIA

Customer: Westinghouse Electric Corporation
Pittsburgh, Pennsylvania

Date 6/01/78

Unit: 12 ft. Nuclear Fuel Rod Assembly

1. Suspended Weight: 4758. Lbs.
2. Mass Moments of Inertia (lb-in-sec^2):

   A. Roll - 399
   B. Pitch - 22800.
   C. Yaw - 23030.

3. Fragility Factors:

   A. Shock - 6 G's @ -40°F/+70°F/+160°F @ C.G.
   B. Vibration - 6 G's @ -40°F/+70°F/+160°F @ C.G.

4. A. 10" Vertical Flat Drop
   B. 7 ft/sec End Impact
   C. 24" Rotational Drop

5. Vibration Design Requirements:

   N/A

6. Military Specifications which apply:

   MIL-C-5584C Amended

7. Environmental Requirements:

   Operating Temperature Range from -40°F to +160°F

8. Methods of Transportation Used:

   Truck, Rail, Ship, Air

Lord Kinematics
Division of Lord Corporation
Erie, Pennsylvania

SHIPPING CONTAINER SUSPENSION SYSTEM DESIGN CRITERIA

Customer: Westinghouse Electric Corporation
Pittsburgh, Pennsylvania

Date 6/01/78

Unit: XL Nuclear Fuel Rod Assembly

1. Proposed System Comprises: 24 Pieces of Lord P/N J-5735-64
2. Mount Locations and Orientations:
3. Calculated Shock Performance:

A. 10" Vertical Flat Drop

ACCELERATION	DEFLECTION
5.9 G's @ -40°F @ C.G.	2.65" @ -40°F @ C.G.
4.5 G's @ +70°F @ C.G.	3.45" @ +70°F @ C.G.
4.2 G's @+160°F @ C.G.	3.74" @+160°F @ C.G.

B. 7 ft/sec End Impact

ACCELERATION	DEFLECTION
5.6 G's @ -40°F @ C.G.	2.54" @ -40°F @ C.G.
4.3 G's @ +70°F @ C.G.	3.31" @ +70°F @ C.G.
4.0 G's @+160°F @ C.G.	3.59" @+160°F @ C.G.

C. 24" Rotational Drop

ACCELERATION	DEFLECTION
5.8 G's @ -40°F @ C.G.	2.59" @ -40°F @ C.G.
4.4 G's @ +70°F @ C.G.	3.37" @ +70°F @ C.G.
4.1 G's @+160°F @ C.G.	3.66" @+160°F @ C.G.

4. Recommended Minimum Clearances Between Unit and Container:

A. Bottom - 8.0"
B. Top - 4.5"
C. Ends - 4.5"
D. Sides - 4.38"

5. Resonant Transmissibility: 6.0
6. Assumptions: Rigid Unit, Rigid Container

Lord Kinematics
Division of Lord Corporation
Erie, Pennsylvania

SHIPPING CONTAINER SUSPENSION SYSTEM DESIGN CRITERIA

Customer: Westinghouse Electric Corporation
Pittsburgh, Pennsylvania

Date 6/01/78

Unit: 12 Ft. Nuclear Fuel Rod Assembly

1. Proposed System Comprises: 24 Pieces of Lord P/N J-5735-64
2. Mount Locations and Orientations:
3. Calculated Shock Performance:

A. 10" Vertical Flat Drop

ACCELERATION	DEFLECTION
6.2 G's @ -40°F @ C.G.	2.54" @ -40°F @ C.G.
4.7 G's @ +70°F @ C.G.	3.31" @ +70°F @ C.G.
4.4 G's @+160°F @ C.G.	3.59" @+160°F @ C.G.

B. 7 ft/sec End Impact

ACCELERATION	DEFLECTION
5.9 G's @ -40°F @ C.G.	2.43" @ -40°F @ C.G.
4.5 G's @ +70°F @ C.G.	3.17" @ +70°F @ C.G.
4.1 G's @+160°F @ C.G.	3.44" @+160°F @ C.G.

C. 24" Rotational Drop

ACCELERATION	DEFLECTION
6.1 G's @ -40°F @ C.G.	2.52" @ -40°F @ C.G.
4.7 G's @ +70°F @ C.G.	3.28" @ +70°F @ C.G.
4.3 G's @+160°F @ C.G.	3.56" @+160°F @ C.G.

4. Recommended Minimum Clearances Between Unit and Container:

A. Bottom - 8.0"
B. Top - 4.5"
C. Ends - 4.5"
D. Sides - 4.38"

5. Resonant Transmissibility: 6.0
6. Assumptions: Rigid Unit, Rigid Container

APPENDIX 2-3

CALCULATIONS AND EVALUATIONS RELATING TO ASSESSMENT OF NORMAL CONDITIONS OF TRANSPORT

ASSESSMENT OF NORMAL CONDITIONS OF TRANSPORT

The MCC containers satisfy the performance requirements specified in Subpart F of 10 CFR 71 for normal conditions of transport. This regulatory compliance is demonstrated in the following subsections where each normal condition is addressed and shown to meet the applicable regulatory criteria.

2-3.1 Heat

The thermal evaluation of the MCC containers for the normal heat condition specified in § 71.71 (c)(1) is presented in this section. Since there is no internal heat generation, a maximum package temperature of 200 °F will be conservatively assumed.

2-3.1.1 Summary of Pressures and Temperatures

The MCC containers are limited to the transport of unirradiated, low enriched uranium, nuclear reactor core assemblies. During normal conditions of transport, the container will not experience temperatures significantly above ambient temperature. For the normal condition of heat per §71.71(c)(1), the maximum temperature of the MCC container components is less than 200 °F.

The MCC containers are not designed to function as pressure vessels. The fuel assemblies do not generate gasses which could pressurize the MCC container. In addition, the seal between the two halves of the container is only a dust seal and is not a pressure seal. Therefore, the MCC containers will not experience a pressure loading incident to normal transportation.

2-3.1.2 Differential Thermal Expansion

As discussed in Section 2-3.1.1, the outer shell of the MCC containers will operate at a maximum temperature of less than 200 °F during normal transportation. This temperature occurs in the outer shells which are isolated from the internal strongback structures by elastomer vibration isolators. Because of this isolation, no significant effects due to differential thermal expansion will occur between the internal structures and the outer shells.

For the outer shells, the stress due to insolation and 100 °F still air is minimal since there are no constraints on the package. The amount of thermal growth which is expected is determined as follows:

$$\Delta L = \alpha(T_2 - T_1)(L)$$

where: ΔL = Change in package length, in.

α = mean coefficient of thermal expansion
= 6.57×10^{-6} in/in - ◦F for carbon steel at 150 ◦F

T_2 = Maximum package temperature = 200 ◦F.

T_1 = Package initial temperature = 70 ◦F (assumed)

L = Maximum overall package length = 220.0 in.

Solving the preceding equation yields a maximum outer shell thermal growth of 0.188 in. This amount of growth is easily accommodated by the vibration isolators which separate the internal structures and the outer shells.

Based on the preceding results, differential thermal expansion is negligible for the MCC container components.

2-3.1.3 **Stress Calculations**

The MCC containers are transported in a non-constrained, non-pressurized state. Therefore, the containers will not develop any significant stresses due to normal conditions of transport for heat per § 71.71(c)(1).

2-3.2 **Cold**

For the cold condition of §71.71(c)(2), a -40◦F (-40 ◦C) steady state ambient temperature will result in a uniform temperature throughout the package since there is no internal heat generation. The materials of construction for the container are not adversely affected by this temperature condition.

Brittle fracture of the materials used in the MCC containers is not a concern. The critical component of the design (the clamp frame arms) is fabricated from ASTM A240 Type 304 austenitic stainless steel plate. This material does not undergo a ductile-to-brittle transition in the temperature range of interest and therefore, is safe from brittle fracture. The clamp frame systems are also a redundant system. Redundant systems are generally not considered as fracture-critical components because multiple load paths exist. In addition, the thicknesses of the components which use non-austenitic materials are less than 0.4 in. Per NUREG/CR-1815, brittle fracture of Category III materials (which the MCC containers fall under) which are less than 0.4 in. in thickness is not a problem.

2-3.3 **Pressure**

The effect of the reduced external pressure of 3.5 psia (i.e., 11.2 psig internal pressure), per § 71.71(c)(3), is evaluated for the outer shell of the containers. These calculations are very conservative considering the MCC containers are not pressure vessels and differential pressure states will not exist. In addition, the outer shell stiffening angles are conservatively ignored in the calculation. The bounding case used for demonstration is the model MCC-3 container. The circumferential and longitudinal stresses, σ_c and σ_L respectively, in the MCC-3 outer shell are calculated as:

$$\sigma_c = \frac{PR}{t} \qquad \sigma_L = \frac{PR}{2t}$$

where: P = 11.2 psig
R = 20.67 in.
t = 0.089 in.

Substituting the above values results in the following stress levels:

$$\sigma_c = 2.60\ ksi\ \sigma_L = 1.30\ ksi$$

These stress levels will have negligible effect on the outer steel shell which is fabricated from mild carbon steel. Similar results exist for the MCC-4 container.

For the pressure condition of §71.71 (c)(4), the MCC container will be exposed to an external pressure of 5.3 psig. It can be easily demonstrated that the MCC-3 container can withstand this external pressure by conservatively assuming a thin-walled pressure vessel with a length equivalent to the longest span of the outer shell between circumferential stiffeners and neglecting the stiffening effect of the angle flange between the two halves of the outer body. For this analysis, the longest unsupported shell length occurs in the middle of the container upper assembly. Per Code Case N-284, Section III, Division 1, Class MC of the ASME Boiler and Pressure Vessel Code, the outer shell may be analyzed as a shell under axial compression plus hoop compression. For this case (§ - 1713.1.1(b)), the following interaction equation must be satisfied:

$$\frac{\sigma_{\phi s} - 0.5\,\sigma_{heL}}{\sigma_{\phi eL} - 0.5\,\sigma_{heL}} - \left(\frac{\sigma_{\theta s}}{\sigma_{heL}}\right)^2 \le 1.0$$

where: $\sigma_{\phi,} = P(R/t)[(FS)/(2\alpha_{\phi L})]$ $\qquad \alpha_{\phi L} = \sigma_y(10^{-5}) - 0.033$

$\sigma_{\phi s} = P(R/t)[(FS)/(0.8)]$ $\qquad \sigma_{\phi eL} = (0.605)(t/R)E$

$\sigma_{heL} = (C_{heL})(t/R)E$ $\quad C_{heL} = [0.92/(M_\phi - 0.636)]$

$M_\phi = L_\phi/[(R)(t)]^{1/2}$ $\quad P = 5.3$ psig

L_ϕ = Length of unstiffened shell = 41.25 in.

σ_y = Tensile yield strength of shell = 30,000 psi

E = Young's Modulus = 29.0×10^6 for carbon steel

R = Outer radius of shell = 20.62 in.

t = outer shell thickness = 0.089 in.

FS = Factor of Safety = 2.0

Solving the above interaction equation yields a value of 0.668, which satisfies Code Case N-284 for the §71.71 (c)(4) pressure condition. Similar results are obtained for the MCC-4 container.

In summary, the MCC containers can easily withstand the reduced and increased pressure conditions of § 71.71(c).

2-3.4 **Vibration**

The shock mount system of the MCC containers is designed to limit the internal structure to a maximum shock load of 6 g's during normal transportation conditions. For this reason, a static 6 g design load is conservatively used to evaluate the MCC containers for stresses due to normal vibration loads per §71.71 (c)(5).

The stresses in the container outer shells are conservatively calculated by evaluating the container as a simply supported beam supported at its ends, as shown in Figure 2-3.1. The mass of the package is assumed to be evenly distributed along its length. The circumferential shell stiffeners are conservatively ignored in these calculations. For the bounding case, the maximum gross weight of the MCC-3 container (W) is 7,544 lbs. Assuming a uniform 6 g load over the length of the container, the bending stress (σ_b) in the container outer shell is then:

$$\sigma_b = \frac{M(c)}{I_{shell}}$$

where: $M = 6(\omega)L^2/8 = 6WL/8$

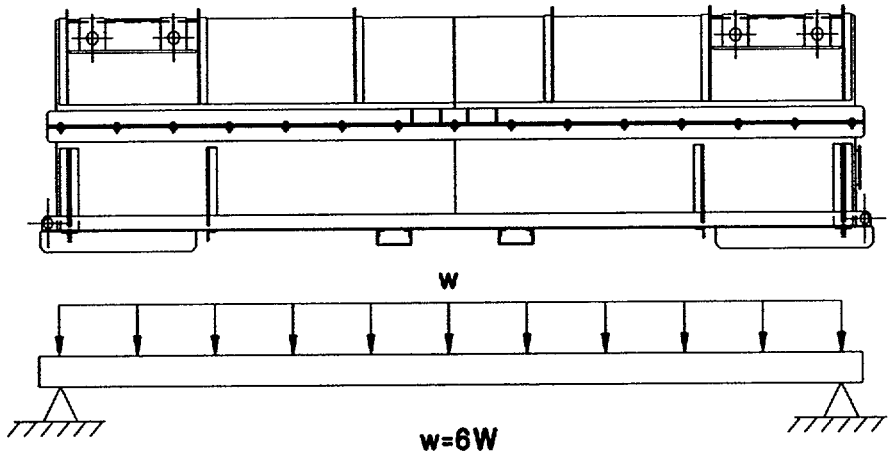

Figure 2-3.1 MCC Outer Shell Vibration Model

ω = Weight per unit length

L = Overall package length = 192.0 in.

c = 20.625 in

$I_{shell} = \pi D^4/64 = 147{,}362\ in^4$

D = Outer diameter of shell = 41.25 in.

Substituting the above values yields a bending stress of 0.15 ksi. The combined membrane plus bending stress (σ_T) for vibration plus pressure (assuming all stresses are directly additive) is 4.05 ksi. The allowable stress, S_a, for the outer shell is 30.0 ksi. Therefore, the outer shell Margin of Safety (M.S.) is:

$$M.S. = (S_a/\sigma_T) - 1 = (30.0/4.05) - 1 = +6.41$$

The clamp frame and clamp frame connections are the critical internal structure components for stresses due to normal operation vibration loads. The clamp frame is conservatively evaluated as a simply supported beam 13 inches in length, which represents the approximate clear span of the clamp frame. The clamp frame is loaded by the accelerated mass of the fuel applied to the clamp frame as a point load. The load is applied at the location of the fuel pad support bolt. The accelerated mass of the fuel is conservatively assumed to be carried equally between six of the seven clamp frames for the MCC-3 container with the bounding fuel assembly weight of 1,650 lbs (the MCC-4 container with heavier fuel assemblies has a total of nine frames and is bounded by the MCC-3 frame loading). This assumption is to account for the effect of the various spacing arrangements of the clamp frames which exist for the different fuel assemblies.

$$F = \frac{(1{,}650\ lbs)(6\ g's)}{6\ clamp\ frames} = 1{,}650\ lbs$$

Assuming simply supported ends with an applied load in the center, the bending stress (σ_b) in the clamp frame is calculated as:

$$\sigma_b = \frac{M(c)}{I_{clamp}}$$

where: $M = F(\ell/2)/2$

$c = 2.0/2 = 1.0$ in.

$I_{clamp} = bh^3/12 = 1.25(2)^3/12 = 0.833\ in^4$

where: b and h are width and height of clamp frame cross section

ℓ = effective clamp frame span = 13.0 in.

Substituting the appropriate values in the above equation yields a bending stress of 6.44 ksi. Because the clamp frames can only be loaded by inertia forces when the package is in the normal orientation, this stress represents the total stress on the clamp frame. No other loads are combined with the vibration load on the internal structure clamp frames.

The allowable bending stress (S_a) for the clamp frame is 30.0 ksi. Therefore the Margin of Safety is:

$$M.S. = (S_a/\sigma_b) - 1 = (30.0/6.44) - 1 = + 3.66$$

The shear load, F_v, on the connection pins is conservatively assumed to be equal to the maximum applied load of 1,650 lbs., and that the full load is carried by one connection. Based on an allowable shear yield stress of 98.1 ksi (0.577 of minimum tensile yield stress for ASTM A564 Type 630 material), the allowable shear strength, F_a, for the clamp frame connection pins in double shear is 18,129 lbs. Therefore, the connection pin Margin of Safety is:

$$M.S. = (F_a/F_v) - 1 = (18129/1650) - 1 = + 9.99$$

The clamp frames connect into pivot mounts which in turn connect to the Unistrut channels attached to the internal structure. The maximum tensile stress in the pivot mounts, due to vibration loads, will occur in the side pivot mount, which is

slightly thinner than the upper pivot mount. The full reaction load of 1,650 lbs. is conservatively assumed to carried by the lower pivot mount. The load, F, in each leg of the pivot mounts is then:

$$F = \frac{1,650}{2} = 825\ lbs$$

Assuming the load is distributed across the width of the connection pins, the bearing stress, σ_B, on the pivot mount is:

$$\sigma_B = \frac{F}{A_B}$$

where: A_B = Bearing Area = (D)(w)

D = diameter of connection pin = 7/16-in.

w = pivot mount bearing surface width = 0.365 in.

Solving for the bearing stress yields a stress level of 5.17 ksi. The allowable bearing stress, S_a, in the pivot mounts is 30.0 ksi. Therefore, the pivot mount Margin of Safety is:

$$M.S. = (S_a/\sigma_B) - 1 = (30.0/5.17) - 1 = + 4.80$$

The load on each of the two Unistrut connection bolts is 825 lbs. This load conservatively assumes that only one pivot mount carries the vibration reaction load and that the load is equally distributed between the two bolts connecting each pivot mount. The manufacturer's recommended allowable tensile load (F_{bolt}) for the P-2381-5 Unistrut stud nuts is 2,000 lbs/stud. The Margin of Safety against pull-out of the two Unistrut bolts is then:

$$M.S. = (2)(F_{bolt})/(F) - 1 = 4000/825 - 1 = + 3.85$$

2-3.5 **Compression**

Per § 71.71 (c)(9), packages which weigh up to 11,000 lbs. (5,000 kg) must be subjected, for a period of 24 hours, to a compressive load applied uniformly to the top and bottom of the package in the position in which the package would normally be transported. The compressive load must be the greater of the following: (i) The equivalent of five times the weight of the package; or (ii) the equivalent of 12.75 kilopascal (1.85 lb/in^2) multiplied by the vertically projected area of the package.

For the MCC-4 container (bounding case), five times the weight of the package is 52,765 lbs. The projected area of the container, A_p, is calculated as:

$$A_P = (D_{max})(L_{max})$$

where: D_{max} = Maximum overall package width = 44.5 in.
L_{max} = Maximum overall package length = 226.0 in.

The projected area is calculated to be 10,057 in^2. Therefore, the total load for a pressure of 1.85 psi is:

$$F_P = (1.85)(10,057) = 18,605 lbs. < 5\,(W) = 52,765\ lbs.$$

Therefore, the controlling load is five times the package weight. The package is transported in a horizontal position, resting on the stacking frames on the bottom ends of the package. Therefore, the maximum stress due to the compression load is a bending stress in the outer shell. The resulting stress in the outer shell is conservatively evaluated by assuming the package acts as a simply supported beam. The bending stress, σ_b, is then calculated as:

$$\sigma_b = \frac{M(c)}{I_{shell}}$$

where: $M = 5(\omega)L^2/8 = 5WL/8 = 1,490,611$ in-lbs

$L = 226.0$ in.

$c = 20.625$ in.

ω = Load per unit length

$I_{shell} = 147,362\ in^4$

The calculated bending stress resulting from a compressive load per § 71.71 (c)(9) is 0.21 ksi. The allowable bending stress for the container shell is 30.0 ksi. Therefore, it can then be concluded that the MCC containers comply with the requirements of this subsection.

APPENDIX 2-4

CALCULATIONS AND EVALUATIONS RELATING TO ASSESSMENT OF HYPOTHETICAL ACCIDENT CONDITIONS

2-4.1

CALCULATIONS

ASSESSMENT OF HYPOTHETICAL ACCIDENT CONDITIONS

Westinghouse MCC containers, when subjected to hypothetical accident conditions specified in § 71.73, meet the performance criteria specified in Subpart E of 10 CFR 71. This compliance is demonstrated in the following subsections where each accident condition is addressed and shown to meet the applicable design criteria previously discussed in Section 2.1.2 of the application.

As stated in Section 2.1.2 of the application, the post accident configuration cannot be more reactive than analyzed in Section 6.0. To prevent it from becoming more reactive, the spacing between fuel assemblies from adjacent packages, when in parallel planes, must not be allowed to be reduced below eight (8) inches. This spacing is accomplished by ensuring that the fuel assemblies are restrained by the strongback and that the outer shell remains intact. If the outer shell was separated from the package, the adjacent fuel package clamp frames could lay between the clamp frames of the adjacent package. The fuel spacing, when the fuel is corner-to-corner, can be slightly closer. The fuel must be restrained such that the gadolinium neutron absorber plates stay between the fuel bundles.

2-4.1 Free Drop

§ 71.73 (c)(1) of Subpart F requires that a package withstand a drop from a height of 30-feet (9 meters) onto a flat, unyielding, horizontal surface. The package is to strike the surface in a position for which maximum damage is expected. Per § 71.73 (b), the initial temperature for the drop is to be the worst case constant ambient air temperature between -20 °F and 100 °F. Brittle fracture of the MCC container materials is not a critical issue through the temperature range of concern as shown in Section 2.6.2. Therefore, the worst case temperature condition for the drop test is 100 °F. This section demonstrates compliance of the MCC containers, with the 30-foot drop test condition, by analysis and prototype testing. The analyses presented determine the ability of the containers to absorb the kinetic energy associated with the 30-foot drop. The prototype testing is confirmation of the package's ability to maintain a subcritical geometry following the 30-foot drop. The drop orientations considered in the analyses and utilized for the prototype tests include the following:

- (Flat) side drop onto package top
- Side drop with slapdown onto package clamp frames
- (Flat) side drop onto package closure

For analytic purposes, the weights of the MCC-3 and MCC-4 containers are considered to be as shown in Section 1.2.1. For purposes of this evaluation, the MCC-3 container, when loaded with its maximum fuel assembly weight of 3,300 lbs., is the bounding case and is utilized for demonstrating regulatory compliance. (See the justification provided in Section 2-4.5)

2-4.1.1 End Drop

The end drop is not a controlling orientation for the MCC containers to maintain a sub-critical geometry. For this orientation, the end of the MCC outer shell and the end supports of the internal strongback will crush. Any residual kinetic energy will be absorbed by axial crushing of the fuel assemblies. Therefore, this axial damage will result in a less reactive geometry for criticality control. In addition, the critical components of the MCC containers, the clamp frames, are redundant (i.e., a single failure does not cause a failure of the package to maintain a sub-critical geometry). Except for the gadolinium oxide absorber plates, the expected deformations and critical load paths of the side drops will be more crucial for the MCC container design to maintain a sub-critical geometry. Demonstration of the gadolinium oxide absorber plates' ability to withstand the impact forces associated with the 30-foot drop events is discussed in Appendix 1-6. Additionally, the prototype containers which were utilized in the drop tests had the gadolinium oxide absorber plates installed. The results of the drop tests are discussed in Appendix 2-4.3.

2-4.1.2 Side Drops

2-4.1.2.1 Side Drop onto Container Top

The internal structure of the MCC-3 container is attached to the outer shell by a series of shock mounts which are intended to limit normal condition transportation events to below 6 g's. Since the shock mount system is relatively soft (with the shear stiffness of the combined shock mounts at 5,160 lb/in), the system will not significantly affect the impact velocity of the internal structure. For conservatism, the internal structure is assumed to impact the drop pad at full velocity. Because of the "softness" of the shock mount system, the outer shell and internal structure may be decoupled and will act independently during the impact from the 30-foot accident drop events.

The deformation of the outer shell assembly due to the 30-foot accident drops is not of critical concern for the function of the MCC containers. As previously discussed, the primary purpose of the MCC container is to maintain a minimum spacing between adjacent packages for criticality control. Of critical concern is the ability of the internal structure to absorb the energy of its accelerated mass without catastrophic failure or deformations which result in less than the allowable criticality spacing. The outer shell deformations are calculated herein to verify the ability of the outer shell to fully absorb the kinetic energy of its accelerated mass due to the 30-foot drop without catastrophic failure.

Outer Shell Assembly Deformations

The kinetic energy associated with the outer shell assembly upon impact is:

$$E_{shell} = W_{shell}(h)$$

where: W_{shell} = weight of the outer shell assembly = 2,280 lbs.

h = drop height = 30 feet (360 inches)

The kinetic energy of the outer shell is 820,800 in-lbs. This energy will be absorbed by the strain energy primarily associated with the deformation of the 2-in. x 2-in. x ¼-in. angle circumferential stiffeners (refer to Figure 2-4.1-1). The energy absorption of the outer shell skin (t = 0.089 in.) is neglected in this calculation.

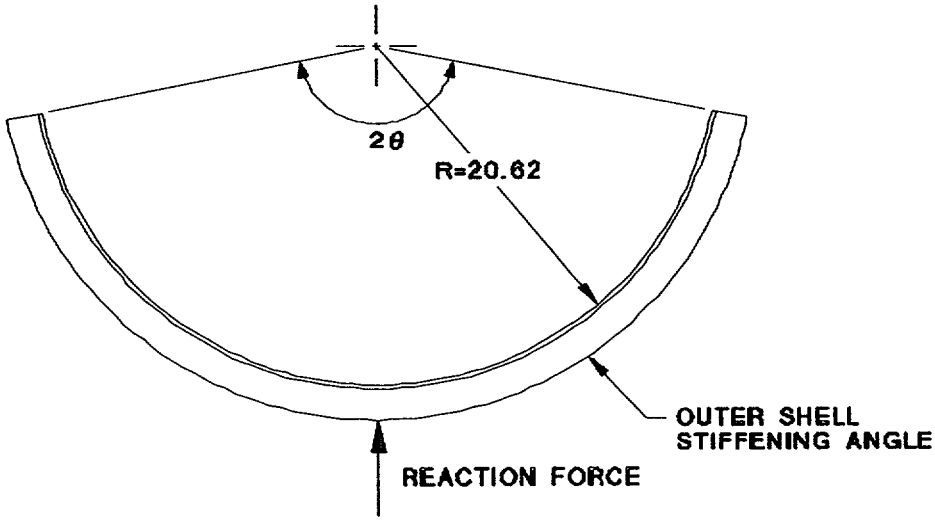

Figure 2-4.1-1 Deformation of Circumferential Stiffener

The initial impact of the outer shell will be on the circumferential stiffeners. The primary energy absorption occurs with the localized buckling of the angle stiffeners. For this condition, the stiffeners can be analyzed as a narrow rectangular beam (length equal to the distance between the stacking brackets, or 10 inches) having fixed ends with a concentrated applied load at the center of the beam. Based on the principles found in Table 34, Case 13, Formulas for Stress and Strain, Fifth Edition by Roark and Young, the force required to buckle the plate ($P\angle$) may be approximated per the following:

$$P_L = \left[\frac{4.43\, b^3 d}{L2}\right]\sqrt{\left(1 - 0.63\,\frac{b}{d}\right) E\, G}$$

where: b = thickness of angle = ¼ - in.

d = height of free edge of angle = 1-¾ in

L = effective length of angle ≈ 10 in

E = Young's Modulus = 29.0×10^6 psi

G = Modulus of Rigidity = 11.5×10^6 psi

Substituting the preceding terms into the above equation determines that the applied force to buckle the angle stiffener is 21,102 lbs. The total force required to buckle all of the stiffeners except the end angles (total number of stiffeners is 4) is 84,408 lbs. Since the end angle stiffeners are located near the end plates of the container, these stiffeners will tend to crush rather than buckle. The force associated with crushing of these angles is given by:

$$F_{L\ crush} = (2)\,\sigma_{flow}\,(A_L)$$

where: σ_{flow} = flow stress = ½ (σ_y + σ_{ult})
= ½(30,000 + 54,000) = 42,000 psi

$A_\angle$ = angle crush area = (¼)(10) = 2-½ in²

Substituting the above values yields a crushing force for the two end angle stiffeners of 210,000 lbs. Using the principle that force multiplied by distance equals energy, the total deformation which is required to absorbed the kinetic energy of the outer shell may be determined per the following:

$$\delta_{crush} = \frac{E_{shell}}{(4)(P_\angle) + F_{\angle\ crush}} = \frac{820{,}800}{[(4)(21{,}102) + 210{,}000]} = 2.79 \text{ inches}$$

The gross deformation is then equal to d_{crush} plus the angle leg length, or 4.54 inches. Therefore, the total outer shell kinetic energy is absorbed by approximately 4-½ inches of deformation of the circumferential stiffeners. Testing of a MCC-3 prototypic container has shown that the circumferential stiffeners deform approximately 3-4 inches for the 30-foot drop onto the container top (refer to Appendix 2-4.3 for details of the drop tests). Since the deformed outer shell

assembly is maintained around the fuel assemblies, the minimum separation distance to maintain a subcritical geometry is still in place.

Internal Assembly Deformations

As noted previously, the internal structure may be decoupled from the outer shell assembly during the accident drops. Therefore, the response of the internal structure to the 30-foot side drop is evaluated by assuming that the kinetic energy associated with mass of the internal structure is absorbed solely by the strain energy of the internal structure deformations.

The kinetic energy associated with the internal structure assembly upon impact is:

$$E_{internal} = W_{internal}(h)$$

where: $W_{internal}$ = (internal structure + fuel assembly weight)
= 5,264 lbs

h = drop height = 30 feet (360 inches)

The calculated kinetic energy of the internal assembly is 1.895 x 106 in-lbs. This energy will be absorbed by the deformation of the following internal structure components (refer to Figure 2-4.1-2):

- Crush of swing bolts
- Crush of clamp frame connections/Unistrut channels
- Crush of fuel assembly grids

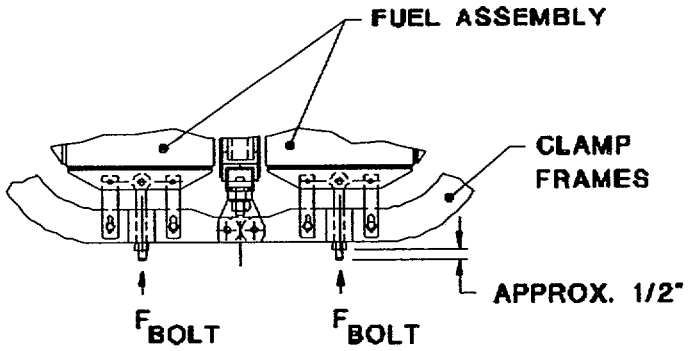

Figure 2-4.1-2 Internal Structure Components

Initial impact of the internal structure is on the swing bolts which extend through the clamp frames. The force associated with the flow of the fourteen swing bolts is calculated as:

$$F_{bolt} = (14)\ \sigma_{flow}\ (A_{bolt})$$

where: σ_{flow} = 42,000 psi

A_{bolt} = tensile area of bolt = 0.1419 in^2

The total force for the flow of 14 swing bolts is 83,437 lbs. Based on a maximum available crush depth of 1-½ inch (end crush plus distance of snubber movement), the energy absorbed by the flow of the swing bolts is calculated as:

$$E_{bolt} = (1.5\ inch)(F_{bolt}) = 125,\ 156\ inch\text{-}lbs$$

The internal structure kinetic energy which remains following the flow of the swing bolts is:

$$E_{remaining} = (E_{internal}) - (E_{bolt}) = 1.77 \times 10^{6}\ inch\text{-}lbs$$

After the swing bolt ends flow, the pressure pads will start to apply impact forces to the fuel assembly grid pads. As the force increases, the snubber arms will slide approximately ½-inch until they contact the clamp frames. At this point, crushing of the fuel assemblies will commence. Compressive impact forces will also be applied to the clamp frame connections to the Unistrut channels. The initial force required to crush the fuel assemblies at the grid locations is approximately 6,000 lbs per pressure pad, or 84,000 lbs total (Ffuel). The 6,000 lbs per pressure pad to crush the fuel (as tested by Westinghouse) is far below the 115,000 plus pounds it would require to flow each snubber. As the fuel assemblies are crushed, the fuel element spacing is reduced until there is, effectively, metal-to-metal contact between all of the fuel elements and the pressure pads. At this point, the fuel assemblies become very stiff and absorb the remaining kinetic energy of the fuel (approximately 1.19 x 106 in-lbs) as strain energy in the assemblies. The maximum applied force at the pressure pads is limited to the force required to flow the snubber arms at each pressure pad location. At all times, there will be a minimum spacing of the arm thickness, plus snubber length plus pressure pad thickness minus any plastic deformation of the snubber, or over four (4) inches per fuel assembly. The snubber plastic deformation is expected to be very small due to the elastic characteristics of the fuel assemblies. The sub-critical geometry is increased (i.e., lower criticality potential) by the crushing of the fuel because the fuel pin-to-fuel pin spacing is reduced, which lowers the moderation potential. This behavior was confirmed in

the prototypical testing of the MCC-3 container (refer to Appendix 2-4.3). Note that the above analysis does not consider the energy absorbed by the flexure of the fuel assemblies between the pressure pads.

The remaining kinetic energy of the internal structure (approximately 496,000 in-lbs) is primarily absorbed by the center wall section and some flexure of the clamp frame at the side pivot mount/Unistrut channel. The upper pivot mount assembly is illustrated in Figure 2-4.1-3.

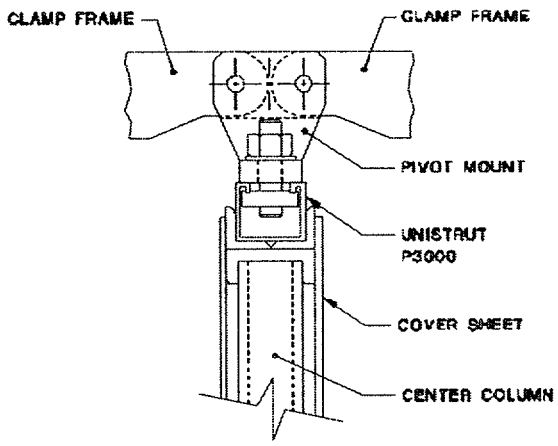

Figure 2-4.1-3 Upper Clamp Frame Attachment Detail

Since the center section is significantly more rigid than the side pivot mount connection, the primary energy absorption will occur in the center wall section. The center wall assembly components will deform according to their relative stiffness. The initial impact to the center wall will first deform the upper pivot mount Unistrut attachment. The potential effective crush area, Astrut, is conservatively calculated based on the contact area with the pivot mount. The force associated with the flow of the Unistrut channels at the seven upper pivot mount locations (F_{strut}) is calculated as:

$$F_{strut} = (7)\ (\sigma_{flow})(A_{strut})$$

where: $\sigma_{flow} = 42{,}000$ psi

A_{strut} = Unistrut effective crush area = 1.16 in^2

From this expression, the force associated with the deformation of the Unistrut channels is estimated to be 341,040 lbs. The maximum available crush depth for the Unistrut channels is ½-inch. Therefore, the energy absorbed by the deflection of the upper Unistrut channel is calculated as:

$$E_{strut} = (F_{strut})\left(\frac{1}{2}\text{ inch}\right) = 170{,}520 \text{ inch-lbs}$$

The remaining kinetic energy of the internal structure will be absorbed primarily by elastic deformation of the main center wall. This kinetic energy, E_{wall} to be absorbed by the center wall deformation is approximately 325,480 in-lbs. Because of the high compressive stiffness of the center wall section (estimated to be greater than 3.0 x 107lb/in), elastic and plastic deformations will completely absorb the remaining energy.

The force associated with the main center wall can conservatively be calculated by assuming an effective width for the cover plates equal to the length of the pivot mount of 5.34 inches. The internal structure center wall is built around six columns fabricated from 1-½ in. x 1-½ in. x ¼-in. rectangular tube, not including the end supports. The crush force of the center wall is calculated by distributing the strength of the six column supports in the center wall evenly to each of the clamp frame locations. Therefore, assuming all deformation as plastic and an effective crushing length of 5.34 inches at each clamp frame location, the center wall crush force, F_{wall} is calculated as:

$$F_{wall} - (7)\sigma_{flow}(A_{wall})$$

where: $\sigma_{flow} = 42{,}000$ psi

A_{wall} = effective crush area of the center wall
$= A_{plate} + A_{columns}$

A_{plate} = effective crush area of cover plates
$= 5.34(0.18)(2) = 1.92 \text{ in}^2$

$A_{columns}$ = effective crush area of column supports
$= (6)(1.25)/7 = 1.07 \text{ in}^2$

Solving the above expression for the force in the wall yields a force of 879,060 lbs. The total deflection of the center wall can be calculated based on the remaining kinetic drop energy to be absorbed. The center wall deflection is calculated as:

$$\delta_{wall} = \frac{E_{wall}}{F_{wall}} = \frac{325{,}480}{879{,}060} = 0.370 \text{ inches}$$

The predicted deformation of the internal wall is acceptable because the clamp frames are in compression at the upper pivot mount. Note that the design of the frame at each pivot mount allows the clamp frames to move relative to the ball-lock and lower connecting pins. This movement allows the clamp frames to bear directly on the inner surface of the pivot mounts without applying shear load to either the ball-lock or connecting pins, thus ensuring that the frames' connectivity to the internal strongback remains intact and continues to restrain the fuel. The center wall structure further encapsulates the gadolinium plates, which ensures criticality control within the MCC package between adjacent fuel assemblies. The ability of the gadolinium absorption plates to withstand the impact of a 30-foot drop event have been demonstrated by prototypical testing (refer to Appendix 1-6).

As the previous calculations demonstrate, the kinetic energy of the 30 foot drop can be conservatively absorbed by the strain energy associated with the deflection of the internal structure components. Note that the preceding analysis is conservative and that actual deformations will be significantly less than predicted here. This conservatism is due to the many different load paths which exist simultaneously within the package and the elastic behavior of these paths.

The actual loadings which the internal supports will see during the drop can be approximated by looking at the crush distance they will experience. As shown above, the total crush of the internals is over three inches. This degree of deformation implies a inertial loading of under 200 g's, which is conservative when considering the structure of the internals and the amount of elastic flexure in the system.

The center wall deformed very little in the actual drop (See Appendix 2-4.3). Stronger than minimum property materials in the test container, and other energy absorbing mechanisms, demonstrate the above analysis to be conservative.

2-4.1.2.2 Side Drop with Slapdown onto Internal Clamp Frames

The container is evaluated for an oblique drop with a slap down on the clamp frames. This orientation will impart the greatest forces on the frames, and if failure occurs, free the fuel. Since the frames are redundant (seven per fuel assembly), a minimum of five clamp frames per assembly would have to fail completely to allow the fuel to move freely and potentially compromise the required spacing.

The impacts, both the initial and the slapdown will occur in localized area at both ends of the container. This will localize the damage but make it more extensive than seen in the above side drops.

Although the internal frame and fuel assemblies will generally behave independently from the outer shell assembly like the other drops evaluated, the concentrated impact area will cause some interaction. In the localized area more of the shell components will be deformed since the loads will not be spread out. Some of the outer shell components beneath the impact region of the internal structure will absorb energy from the internal structure as well as the outer shell assembly. For this reason, the total energy of the system will be evaluated below.

From the scoping analysis performed in Appendix 2-4.2, it has been determined that the container orientation which will impart the maximum inertia forces on the clamp frames is inclined 30° from the horizontal plane. In addition, the container is rotated about its center axis 135° clockwise (refer to Figure 2-4.1-4). This orientation results in direct impact on the corner of the clamp frames on the primary impact as well as the secondary impact. Due to its smaller material sizes, it is expected that the upper end of the internal structure (i.e., end opposite the rotational end) would sustain greater damage than the lower end. Therefore, the orientation which maximum damage is expected would have the initial impact on the upper end of the internal structure. For this drop configuration, the total kinetic energy of the package ($E_{oblique}$) will be as follows:

$$E_{oblique} = W_{MCC}\left[H_{drop} + \left(\frac{L_{MCC}}{2}\sin\theta\right)\right] = 3.08 \times 10^{6} \text{ inch-lbs}$$

where: W_{MCC} = Gross weight of MCC-3 container = 7,544 lbs.

L_{MCC} = Overall Length of MCC-3 container = 194.0 in.

H_{drop} = Drop height = 360 in.

θ = Oblique angle = 30°

Based on the scoping analysis of Appendix 2-4.2, the relative amount of energy which is absorbed for each impact point can be determined. Basing the energy absorbed on the ratio of the impact forces, it is estimated that approximately 42% of $E_{oblique}$ will be absorbed by the initial (primary) impact, with the remainder of the kinetic energy absorbed by the deformation of the MCC container on the slapdown (secondary) impact. The energy absorption for each impact will be discussed separately.

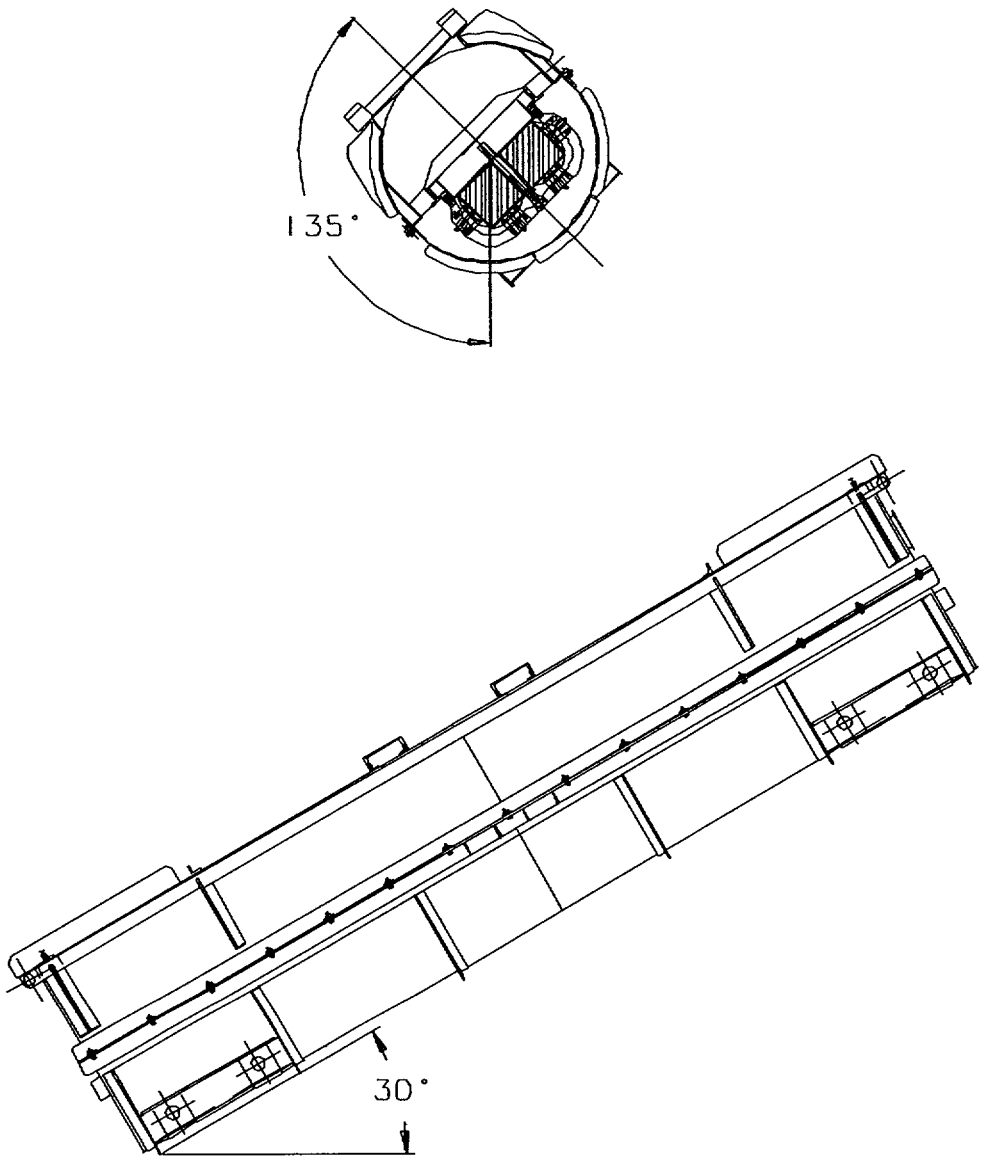

Figure 2-4.1-4 Container Orientation onto Clamp Frames

Initial Impact

For the initial impact of the MCC container, the amount of energy which is estimated to be absorbed is 1.294 x 10^6 -lbs. This energy ($E_{initial}$) absorbed by the following mechanisms:

- Outer shell angle stiffener buckling
- Crushing of outer shell angle stiffener
- Buckling of outer shell end plate
- Straining of elastomer shock mounts by internal structure
- Connecting pin failure for the upper pressure bar
- Plastic hinge formation in angle corner assembly
- Crushing of edge of angle corner assembly
- Buckling of upper pressure bar
- Plastic hinge formation in end clamp frame
- Crushing of the end fuel assembly restraining bolts
- Sliding of the fuel assembly nearest the impact point

The amount of energy which each of these mechanisms will absorb is dependent on their stiffness and their relative location. The following analyses provide an approximate energy distribution based on simple calculations. The analyses is not intended to define the exact damage, but rather to demonstrate that these mechanisms have the capability to absorb the energy without significantly damaging the entire fuel assembly restraint system of the container.

The force require to buckle the outer shell 2-in. x 2-in. x ¼-in. stiffener angle has been previously estimated to be 21,102 lbs (refer to § 2-4.1.2.1). The minimum distance which this force can be applied through is 7-in. Therefore, the energy associated with the buckling of the outer shell stiffener is:

$$E_{buckle} = (21{,}102)(7) = 147{,}714 \text{ inch-lbs}$$

As buckling occurs, the vertical leg of the angle will crush. The maximum crush is equal to the leg length minus the material thickness. The width of the angle segment which will crush is estimated to be approximately 20-in. Therefore, the energy for crushing the angle is expressed as follows:

$$E_{crush} = \sigma_{flow} (1/4 \text{ inch}) (20 \text{ inches}) \delta_{crush}$$

where $\sigma_{flow} = 42{,}000$ psi

$$\delta_{crush} = \text{leg length} = 1.75 \text{ in.}$$

Solving for the crush energy yields 367,500 in-lbs. The total energy absorption of the stiffening angle is then the sum of the two mechanisms:

$$E_L = E_{buckle} + E_{crush} = 515{,}214 \text{ inch-lbs}$$

The buckling of the outer shell assembly end plate may be approximated by a fixed-edged plate with a compressive load applied uniformly. The critical unit buckling stress (s_{cr}) for this case is presented Table 35, Case 10b, Formulas for Stress and Strain, Fifth Edition by Roark and Young:

$$\sigma_{cr} = K \frac{E t^2}{f^2(1-\nu^2)}$$

where: E = Young's Modulus = 29.0×10^6 psi

t = thickness of end plate = 0.134 in.

r = outer radius of plate = 20.62 in.

K = shape factor = 7.22

ν = Poisson's ratio = 0.3

Substituting the preceding values into the above expression yields a compressive unit stress of 9,717 psi, which acts over the 20-inch length of the crush area. Therefore, the total force on the end plate is:

$$F_{end} = \sigma_{cr}(20 \text{ inch})\, t = 26{,}041 \text{ lbs}$$

The energy absorbed by the end plate buckling through the crush distance of 7-in. is then:

$$E_{end} = (7 \text{ inch})(F_{end}) = 182{,}287 \text{ inch-lbs}$$

At the instant of impact, the eighteen elastomer shock mounts will be strained by the inertia of the internal structure. From bench tests, it has been determined that the strain energy of a single shock mount is approximately 1,750 in-lbs per inch of deflection. Therefore, the total strain energy of the shock mounts is:

$$E_{elastic} = (18)(1{,}750)\delta_{internal} = 220{,}500 \text{ inch-lbs}$$

where: $\delta_{internal} = 7\text{-in.}$

Following the straining of the elastomer shock mounts, the upper corner of the top closure assembly of the internal structure will impact the inside surface of the outer shell assembly. The top closure assembly components which will deform and absorb energy consists of a 2-in. x 2-in. x 3/16-in. angle, a 1.5-in. x 2.5-in. x ¼-in. tube, the upper ½-in. diameter connecting pin, and the upper 1.0-in. x 1.5-in. x 13-¼ in. pressure bar. The deformation and energy absorption of each of these separate pieces will be discussed individually.

The initial failure of the top closure assembly is expected to be the connecting pin. This pin is loaded in double shear for the drop orientation considered. Using the distortion energy theory, the maximum shear stress which will cause failure is 0.577 of the ultimate strength. Therefore, the failure load for the pin is expressed as follows:

$$F_{pin} = 2\left[0.577(\sigma_{ult})\left(\frac{\pi}{4}\right)d^2\right]$$

where: $\sigma_{ult} = 54{,}000$ psi

d = pin diameter = ½-in.

The resultant force required to fail the connecting pin is 12,245 lbs. This force will act through a distance equal to the pin diameter. Therefore, the energy absorption of the pin is:

$$E_{pin} = F_{pin}(d_{pin}) = 6{,}123 \text{ inch-lbs}$$

Following the pin failure, the edge of the 2-in. x 2-in. x 3/16-in. angle will develop a plastic hinge as well as crush through the thickness of the angle. For plastic hinge formation, the bending stress will be equal to the plastic hinge stress:

$$\sigma_{plastic} = (SF)\,\sigma_y = \frac{M_{plastic}}{Z_{\angle}}$$

where: $\sigma_y = 30{,}000$ psi

SF = Plastic hinge shape factor $\approx$ 1.25 for angle
$M_{plastic}$ = plastic hinge moment = $F_{plastic}(d)$

$$Z_{\angle} = 0.190 \text{ in}^3$$

d = effective moment arm = 2.59 in.

Solving the above equation for the force required to form a plastic hinge gives a value of 2,751 lbs. This force will act through a distance of approximately 1-in., which will absorb:

$$E_{hinge} = F_{hinge}(1\text{-inch}) = 2{,}751 \text{ inch-lbs}$$

The materials in the corner of the top closure assembly which will flow are the outer shell skin, the rectangular tube, and the 2-in. x 2-in. x 3/16-in. angle with the 1-½ in. x 1-½ in. x ¼-in. connection plates. The exact area of contact is dependent on the amount of flow and the impact angle. In addition, some of the material will bend out of the way rather than flow. For analytical purposes, an area of 3 in^2, which is slightly larger than the cross sectional area of the tube plus the angle, is assumed to be the average contact area. The crush depth (δ_{crush}) is estimated to be approximately 1-½ in. Thus, the energy associated with this material flowing/crushing is:

$$E_{flow} = \sigma_{flow}(3 \text{ inch}^2)\,\delta_{crush} = 231{,}714 \text{ inch-lbs}$$

where: $\sigma_{flow} = 42{,}000$ psi

The total energy associated with the corner angle assembly is then:

$$E_{corner} = E_{hinge} + E_{flow} = 234{,}465 \text{ inch-lbs}$$

Buckling of the upper pressure bar can be determined from classical buckling expressions. Since the slenderness ratio of the pressure bar is low, the buckling force (F_{buckle}) will be based on the parabolic formula:

$$F_{buckle} = A\left(\sigma_y - K\left(\frac{l}{k}\right)^2\right)$$

where: $\sigma_y = 30{,}000$ psi

A = Cross-sectional area = 1.5 in^2

$K = (\sigma_y/2)^2(1/nE)$

E = Young's modulus = 29.0 x 10^6 psi

l = unrestrained length of pressure bar = 12.13 in.

k = radius of gyration of pressure bar = 0.434 in.

n = end-condition factor = 1.0 (fixed-fixed ends)

The calculated buckling force for the pressure bar is 44,307 lbs. This force will act through a distance equal to the crush of the corner assembly or 1.5 in. Therefore, the energy absorbed will be:

$$E_{buckle} = F_{buckle}\ \delta_{crush} = 66{,}461 \text{ inch-lbs}$$

As the corner of the container collapses, the end clamp frame can be deformed. The clamp frame can be modeled as an arch which is pinned and free to translate at the ends (refer to Figure 2-4.1-5). The freedom to translate at the ends is due to the relatively weak Unistrut stud nuts (when compared to the strength of the clamp frames). Therefore, the pivot mounts will provide little constraint and the frames will rotate about the snubbers. Per Advanced Mechanics of Materials by Seely and Smith, the plastic bending stress ($\sigma_{plastic}$) in a curved beam (arch) can be expressed as follows:

$$\sigma_{plastic} = K \frac{M_{plastic}}{Z_{frame}}$$

where: $\sigma_{plastic} = SF\ \sigma_y = 45{,}000$ psi

SF = Shape factor for plastic hinge
= 1.5 for rectangular section

$$M_{plastic} = \tfrac{1}{2} F_{plastic} \left[R \sin \left(\frac{1}{2}\theta\right)\right]$$

R = Radius of frame curved section
= 5.47 in.

K = Correction factor for curved beams
1.14 for inside surface (controlling)

Z_{frame} Section modulus for inner surface
= 0.894 in^3

θ = angle of curved frame section = 90 °

Solving the above expression for the force required to develop a plastic moment in the clamp frame arm yields a value of 18,253 lbs. This load is conservative compared to an actual test of the frame described in Appendix 2-4.4. This force will act through a distance of no less than 2-in. Therefore, the energy associated with the plastic hinge formation in the clamp frame is:

$$E_{frame} = F_{plastic}(\delta_{frame}) = 37{,}046 \text{ inch-lbs}$$

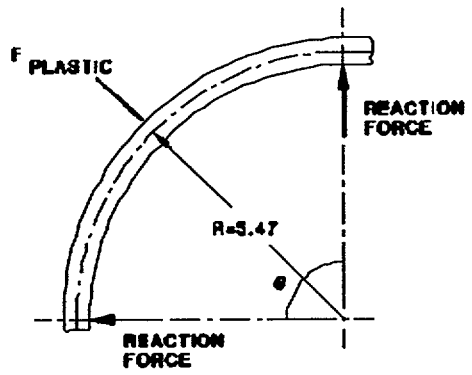

Figure 2-4.1-5 Clamp Frame Plastic Hinge Model

Performing a summation for the absorbed energy and subtracting this summation from the initial energy yields the remaining kinetic energy (E_r) which must be absorbed:

$$E_r = E_{initial} - (E_{\angle} E_{end} + E_{elastic} + E_{pin} + E_{corner} + E_{buckle} + E_{frame})$$

From the above summation, the remaining energy which must be absorbed is 31,904 in-lbs. This energy will be absorbed by the buckling of the fuel restraining bolts and the sliding of the fuel assembly closest to the impact point. The sliding of the fuel assembly requires the overcoming of the pressure pad preload forces times the frictional coefficient of the polyethylene sheeting-on-fuel grid spacer, which is assumed to be 0.35. Each pressure pad is preloaded to a nominal value of 1,000 lbs., with fourteen pressure pads per assembly. Therefore, the energy absorbed by the frictional sliding per linear inch of movement of the fuel is:

$$E_{friction} = (14)(0.35)(1{,}000) = 4{,}900 \text{ inch-lbs/inch}$$

The force required to buckle the four fuel restraining bolts will be based on the parabolic buckling formula for columns, since the slenderness ratio of the bolts is low:

$$F_{bolts} = 4\left[A\left(\sigma_y - K\frac{l}{k}\right)^2\right]$$

where: σ_y = 30,000 psi

A = cross-sectional bolt area = 0.1419 in^2

K = $(\sigma_y /2p)^2(1/nE)$

E = Young's modulus = 29.0 x 10^6 psi

l = maximum unrestrained length of bolts = 4.5 in.

k = radius of gyration of bolt = 0.106 in.

n = end-condition factor = 1.2 (fixed-rounded ends)

From this expression, the force required to buckle the four fuel restraining bolts is 16,356 lbs. The total force required to slide the fuel and buckle the bolts is:

$$F_{total} = F_{fuel} + F_{bolts} = 21{,}156 \text{ lbs}$$

The required deflection to absorb the remaining energy of the initial impact can now be determined :

$$\delta_{fuel} = \frac{E_r}{F_{total}} = 1.50 \text{ inches}$$

Because the length of the fuel restraining bolts is larger than the required deflection, the fuel assembly will not bottom out on the top closure assembly. Furthermore, this deflection does not have any adverse affect on the ability of the container to provide the required spacing for criticality control.

Since the total deformation required to absorbed the energy from the initial impact is localized, the overall function of the MCC containers will not be impaired by this drop orientation.

Secondary Impact

For the secondary impact of the MCC container, the amount of energy which is estimated to be absorbed is 1.786×10^6 in-lbs. This energy ($E_{secondary}$) will be absorbed by the following mechanisms:

- Outer shell angle stiffener buckling
- Crushing of outer shell angle stiffener
- Buckling of outer shell end plate
- Straining of elastomer shock mounts by internal structure
- Crushing the edge of the bottom support and spacer plates
- Plastic hinge formation in clamp frames
- Crushing of the fuel assembly nearest the impact point
- Crushing of swing bolts

For the slapdown impact, the MCC container will be nearly horizontal at the time of impact. However, for conservatism, it will be assumed that the container will be inclined at a slight angle ($\approx 5°$) from the horizontal plane. This inclination will limit the amount of contact surface, and thus impart maximum damage to the container due to the secondary impact. At a 5° angle, three angle stiffeners will be impacted. The maximum amount of crush for the secondary impact will be based on the ratio of the secondary and initial kinetic energies, times the initial crush:

$$\Delta_{secondary} = \frac{E_{secondary}}{E_{initial}} \Delta_{initial} = 9.66 \text{ inches}$$

where: $\Delta_{initial} = 7\text{-in.}$

This crush will occur at the end of the outer shell assembly which contacts the impact surface. At the other two stiffener locations, which are 30-in. and 66-in. from the end stiffener angle, the amount of crush will be equal to 6.60 in. and 2.93 in. respectively. The forced required to buckle an outer shell stiffener angle has been previously determined to be 21,102 lbs. The total energy associated with the buckling of the three angle stiffeners is then:

$$E_{\angle\ buckle} = (21{,}102)(9.66 + 6.60 + 2.93) = 404{,}947 \text{ inch - lbs}$$

The crushing of the angle stiffener will only occur at the end stiffener. The energy associated with this mechanism has been previously determined to be 367,500 in-lbs. Therefore, the total energy absorbed by the angle stiffeners will be the sum of the above:

$$E_{\angle} = E_{\angle buckling} + E_{\angle\ crush} = 772{,}447 \text{ inch - lbs}$$

The force associated buckling of the outer shell end plate has been determined for the initial impact. For the secondary impact, the energy absorbed will be:

$$E_{plate} = (9.66)(F_{plate}) = 251{,}556 \text{ inch-lbs}$$

The elastic strain energy of the elastomer shock mounts will be approximately equal to the initial impact energy:

$$E_{elastic} = (18)(1{,}750)\delta \text{internal} = 220{,}500 \text{ inch-lbs}$$

$$\text{where: } \delta_{internal} = 7\text{-in.}$$

The energy absorbed by the formation of a plastic hinge in the three clamp frames is different for each frame since the container is inclined. It is estimated that the end clamp frame will deform a total of 3-in., with the other two clamp frames having about a ½-in. and 1-in. less deflection respectively. Therefore, the energy absorbed will be:

$$E_{frames} = F_{plastic}\ (3 + 2.5 + 2) = 136{,}898 \text{ inch-lbs}$$

$$\text{where: } F_{plastic} = 18{,}253 \text{ lb.}$$

Prior to the formation of the plastic hinge in the clamp frames, the fuel will be crushed in the areas under the pressure pads. The initial fuel assembly crush force per pad has been determined to be 6,000 lbs (see page 6). Since only three clamp frames (six pressure pads total) will be affected in the secondary impact, the energy absorbed by the fuel crush will be:

$$E_{fuel} = (6)(6{,}000)(\delta \text{fuel}) = 36{,}000 \text{ inch-lbs}$$

$$\text{where: } \delta_{fuel} = 1\text{-in.}$$

Additional energy absorption will occur by the crushiung of the ends of the swing bolts. From page 2.16, the energy absorption per bolt has been estimated to 8,940 in-lbs. For the secondary impact event, approximately four of the swing bolts will be crushed. Therefore, the energy absorbed by the bolts is:

$$E_{swing\ bolts} = (4)(8{,}940) = 35{,}760 \text{ inch-lbs}$$

Following the energy absorption of the above mechanisms, the bottom support and spacer plates will impact and crush, absorbing the remaining energy. The remaining energy to be absorbed (E_r) will be:

$$E_r = E_{secondary} - \left(E_{\angle} + E_{plate} + E_{elastic} + E_{frames} + E_{fuel} + E_{swing\ boltss}\right)$$

From this summation, it is found that the bottom support and spacer plates must absorb 369,557 in-lbs. The bottom support plate is a ¾-in. thick carbon steel plate while the spacer plate is a ½-in. thick austenitic stainless steel plate. The amount of material crush which will be required to absorb the remaining energy can be determined from the relative flow strengths of the two materials.

$$Volume_{crush} = \frac{E_r}{\sigma_{flow\ ave}} = 8.18\ inch^3$$

where: $\sigma_{flow\ ave} = (0.75/1.25)(\sigma_{flow\ cs}) + (0.50/1.25)(\sigma_{flow\ ss})$
$= 45{,}200$ psi

$\sigma_{flow\ cs} = 42{,}000$ psi (carbon steel)

$\sigma_{flow\ ss} = 50{,}000$ psi (stainless steel)

Assuming a 45° impact on the support and spacer plates, the required crush depth to absorb the remaining energy is approximately 2-½ inches. This depth of crush is highly localized and will have no effect on the ability of the MCC containers to provide the required spacing to maintain a sub-critical geometry.

The above analyses demonstrate the capability of the container and payload to absorb the energy of the slapdown event without failing all of the clamp frames which restrain the fuel assemblies and provide the required minimum spacing for criticality control. The analyses demonstrate that the kinetic energy can be absorbed in localized areas of the container which correspond to the areas of impact. These areas, which sustain substantial damage, do not compromise the restraint of the fuel assemblies and the subsequent required spacing. The localized areas of the container (i.e., the ends) will sustain damage, leaving the undamaged areas of the container to restrain and maintain the spacing required for criticality control. The center clamping frames and the outer shell will basically remain undamaged after the event, as the above analyses indicate. This condition was confirmed by prototypic testing of the MCC-3 container. The testing, which is discussed in Appendix 2-4.3, demonstrated much less damage than was predicted by the analyses. The clamp frames on the initial impact end sustained very little damaged and did not deformed. This configuration left four of the seven frames fully capable to restrain the fuel an provide the required spacing. The outer shell closure, as expected, was not significantly damaged with the majority of the outer shell fully intact to assist in maintaining the required spacing.

The reduced damage of the test unit indicates that the kinetic energy was dissipated by other means. Possible reasons for the differences include: 1) the material properties of the test unit were significantly stronger that the minimum values utilized in the analyses, and 2) more of the energy was dissipated in elastic flexure of the various components, such as the center wall, the cork fuel protectors, the various components of the strongback, the fuel assemblies, and the outer shell assembly. Any of these mechanisms could affect the amount of damage and the subsequent forces experienced by the components.

2-4.1.2.3 Side Drop onto Package Closure

The side drop onto the package closure evaluates the ability of the package to remain intact under the most severe conditions. The main purpose of the side drop onto the package closure is to ensure the top and bottom segments of the outer shell do not separate. The damage to the outer shell and internal structure is expected to be maximized in the side drop onto the package top and the side drop onto the clamp frames. The outer shell and internal structure's ability to fully absorb the kinetic energy of the 30-foot drop has been demonstrated in the preceding sections. Therefore, the energy absorption capacity of the outer shell and internal structure will not be explicitly demonstrated again in this section.

The outer shell upper and lower segments are connected with thirty (MCC-3) or fifty (MCC-4) ½-in. T-bolts. The package closure failure mechanisms evaluated in this section include:

- Failure of the T-bolts
- Failure of the shell connection flange

The fuel as stated earlier, is unrestrained. The middle arms remain fully intact to maintain spacing. The damaged areas will have crushed the fuel making it less reactive. The basic structure will remain intact, confining both the fuel and the gadolinium plate in the pre-drop geometry.

2-4.1.2.3.1 Side Impact on Closure

The MCC container response to a side impact is dependent on the stiffness of the outer shell. The ends of the container and the support cradle are much stiffer than the center section. Hence, the separation loads from the outer container impact and the payload impact are not transmitted to the non-impacted side bolts (refer to Figure 2-4.1-6). The adequacy of the T-bolts can be determined by looking at each section.

The adequacy of the T-bolts on the non-impacted center section of the container can be reviewed by determining the maximum load which can be transmitted to the T-bolts.

For analysis purposes, the center section can be broken up into segments, approximately 40 inches in length, with a stiffening angle on each lid segment (refer to Figure 2-4.1-7).

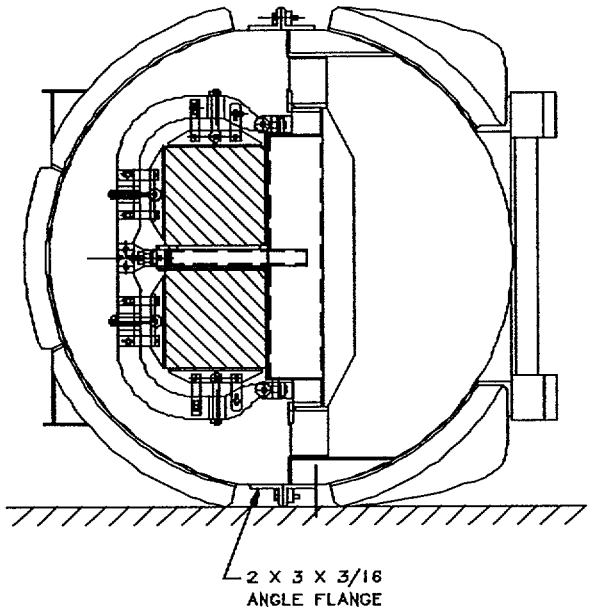

Figure 2-4.1-6 Side Drop onto Package Closure

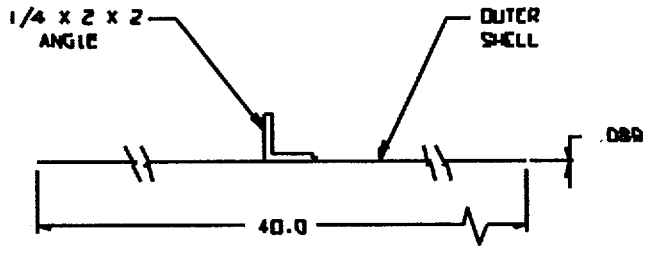

Figure 2-4.1-7 Outer Shell Center Section Model

The cross sectional area is made up of a 0.089-in. plate and a ¼ x 2 x 2 angle. The moment of inertia for this section ($I_{section}$) is calculated to be:

$$I_{section} = I_{\angle} + (y_{\angle} - y)^2 (A_{\angle}) + I_{plate} - + (y_{plate} - y)^2 (A_{plate})$$

$$y = \frac{(A_{\angle})(y_{\angle}) + (A_{plate})(y_{plate})}{(A_{total})} = 0.175 \text{ inch}$$

where: y = centroid location of section

$y_{\angle}$ = centroid of angle = 0.669 in.

y_{plate} = centroid of plate section = 0.0445 in.

$A_{\angle}$ = Area of angle = 0.94 in²

A_{plate} = Area of plate = 3.56 in²

$A_{total} = A_{\angle} + A_{plate} = 4.50$ in²

$I_{\angle}$ = Section Modulus of angle = 0.34 in^4

I_{plate} = Section Modulus of plate = $bh^3/12 = 2.35 \times 10^{-3}$ in^4

Where b and h are the width and thickness of the plate

From the above expressions, $I_{section}$ is found to be 0.632 in^4. The maximum transmitted load due to the impact of the shell is determined from the maximum moment (M_A) and the maximum tension force (T_A), using Table 17, Case 13 of Formulas for Stress and Strain, Fifth Edition by Roark and Young.

$$M_A = w(R)^2 \left(2 - \frac{K_4}{2}\right)$$

$$T_A + \frac{w R}{2}(K_4)$$

where: R = Radius to Centroid = 20.711 in.

w = weight per linear circumferential inch

$K_1 = 1 + \alpha + \beta = 1.0173$

$K_2 = 1 - \alpha + \beta = 1.0167$

$K_4 = K_2/K_1 = 0.999$

$\alpha = (I_{section}) / (A_{total}\, R^2) = 3.27 \times 10^{-4}$

$\beta = [(F)(E)(I_{section})]/[(G)(A_{total})\,(R) = 0.017$

E = Young's Modulus = 29.0×10^6 psi

G = Modulus of Rigidity = 11.5×10^6

F = Shape Factor = 1.0 (conservative)

A plastic hinge in the outer shell/stiffener angle will be formed, which will allow the shell to deform. This hinge will form when the bending stress approximately equals 1.25 times the yield stress, or $\sigma_{plastic} = (30{,}000) = 37{,}500$ psi (at a distance c from the neutral axis to the point of highest stress, 1.914 inches). Equating this plastic hinge stress to M_A allows the force w to be determined:

$$w = \frac{2\sigma_{plastic}\, I_{section}}{3c(R)^2} = 19.24 \text{ lbs/inch}$$

Substituting the circumferential load (w) into the equations for the bending moment M_A and tension force T_A equals 12,383 in-lbs and 199 lbs. respectively. These loads are reacted by the T-bolts (refer to Figure 2-4.1-8). For each shell section, the T-bolts are spaced at 16.88 inches. This spacing results in 2.37 bolts per section (40.0/16.88) which will react these loads. The load in each T-bolt (P_{bolt}) is determined as follows:

$$P_{bolt} = \frac{M_A/d + T_A}{2.37} = 7{,}050 \text{ lbs.}$$

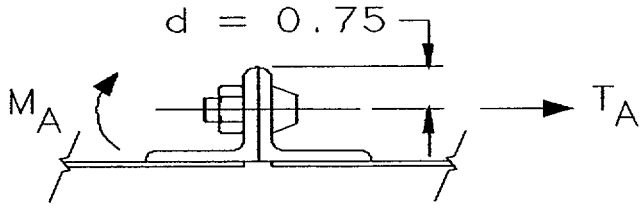

Figure 2-4.1-8 Outer Shell T-Bolt Reactions

The T-bolts are ½ - 13 UNC threads and have a minimum tensile strength of 125.0 ksi. The bolt ultimate capacity ($P_{capacity}$) is then:

$$P_{capacity} = A_t\,(125{,}000) - 17{,}737 \text{ lb.}$$

where: A_t = Bolt tensile stress area = 0.1419 in²

The resultant Margin of Safety for the T-bolts is:

$$\text{M.S.} = (17{,}737/7{,}050) - 1 = +1.51$$

The maximum transmitted load would not change due to the application of the payload force. That force would still have to be transmitted to the T-bolts by a similar mechanism. Since the transmitting mechanism is limiting, the T-bolts cannot be loaded additionally.

Center impact side T-bolts can be evaluated by reviewing the applied loads. Adjacent and perpendicular to the sealing angle flange in the center portion are two stiffening angles for the lid. There are no similar sections for the lower half. When the sealing flange is impacted, both the outer shell and the internal structure apply a separation load to the sealing flange. Since the bare sealing flange strikes the impact surface, the impact loads will be high.

The capacity of the T-bolts has been calculated above as 17,737 lbs. The capacity of the 0.31-in. x 2-in. x 3-in. sealing flange angle to transmit the load to the T-bolt is found by equating the maximum applied potential bending stress to the plastic hinge stress of 45.0 ksi (1.5(30.0 ksi)). The resultant moment is then reacted by a T-bolt.

$$M_{bolt} = \frac{\sigma_{plastic}\, I_{flange}}{c}$$

where: M_{bolt}= Maximum applied potential moment = $F_{bolt}\,(d)$

I_{flange} = Moment of inertia for a 16.88 inch stay
= 1/12 (16.88)(.31)^3 = 0.043 in^4

d = distance between bolt centerline and edge of sealing flange = 0.75 in.

c = distance to extreme fiber = 0.31/2 = 0.155 in.

F_{bolt} = Force in T-bolt, lbs.

Solving for F_{bolt} produces a maximum potential force of 16,645 lbs. This applied potential force is close to the minimal capacity of the T-bolt (16,645 lbs vs. 17,737 lbs). Because of the relative closeness of these two values, there may be some bolt failures in center section on the impacted side. This condition was experienced in the prototypic drop tests of the MCC-3 container. However, there are additional T-bolts which will not fail and thus, the outer shell assembly will remain around the fuel assemblies.

2-4.1.2.3.2 End Bolts on Impacted Side

Toward the ends of the package, in the region adjacent to the support cradle and stacking frame, the stiffeners are reinforced and symmetrical about the flange. This configuration reduces the rotation due to the separating force on impact. The stiffener angles protect the T-bolts from experiencing the separating moment and prevents failure of the T-bolts (refer to Appendix 2.4.3).

2-4.1.2.3.3 End Bolts on Non-impacted Side

The end sections are very stiff compared to the center section because of the end plates of the shell and the axial compression of the end sealing flange. These components ensure that most of the energy of impact is transmitted to the T-bolts (refer to Figure 2-4.1-9).

For this analysis, it is assumed that only the end shell is effective and that a 18-inch section acts upon the T-bolts. For simplicity, it is further assumed that the weight is uniformly distributed. For one-half the MCC-3 outer shell assembly, the weight is w_{shell} = 1140 lbs., which equates to a weight per section (w_{ss}) of 109.59 lbs ([18/187.25][1140]).

To estimate the impact force, it is assumed that the kinetic energy of the outer shell assembly is absorbed by the flow of the sealing flange. The amount of flange crush (δ_{ss}) is estimated as follows:

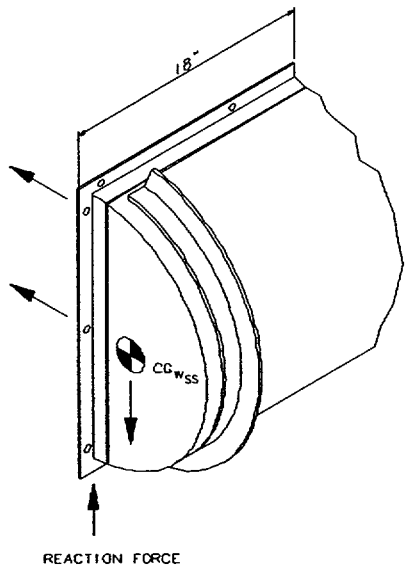

Figure 2-4.1- 9 Outer Shell End Assembly Model

$$\delta_{ss} = \frac{E_{ss}}{\sigma_{flow} A_{flange}}$$

where: $\sigma_{flow} = 42{,}000$ psi

A_{flange} = Flow area of upper and lower flanges
$= 2\,[(18)(.31)] = 11.16$ in^2

E_{ss} = Kinetic Energy of section
$= 360(w_{ss}) = 39{,}452$ in-lbs

Based on the above values, the estimated sealing flange crush is 0.084 in. Ratioing this deflection to the drop height gives the approximate g loading of the impact.

$$G_{impact} = \frac{\Delta_{drop}}{\delta_{ss}} = \frac{360}{0.084} = 4{,}286$$

Although possible, this impact load is exceedingly high. Since other mechanisms may absorb kinteic energy, such as bending of the angle, one-half of the above value will be used for calculation purposes (i.e., $G_{impact} = 2{,}143$).

The T-bolt loads increase linearly from the initial contact point. The load in the T-bolts may be found by summing moments about the impact point:

$$F_{bolt}\left[3(43.75) + (22.25)\left(\frac{22.25}{43.75}\right)\right] = \left[\frac{(20.531)(2)}{\pi}\right](G_{impact})w_{ss}$$

From the above equation, the T-bolt force (F_{bolt}) is found to be 21,531 lbs., which is larger than the T-bolt capacity. When adding in the force of the payload, the force on the T-bolts will be larger.

The upper shell will stay attached to the lower portion of the outer shell assembly of the container. The T-bolts in the center will remain intact on the non-impacted side while the bolts toward the ends of the outer shell will maintain integrity on the impacted side.

2-4.1.3 Corner Drop

The primary function of the MCC container is to maintain the criticality spacing of the fuel. In accordance with this purpose, the corner drop analysis is not a controlling drop orientation for the MCC container. The resulting deformations and deceleration loadings of the side drop discussed in Section 2-4.1.2 bound the corner drop results.

2-4.1.4 Oblique Drops

The primary function of the MCC package is to maintain the criticality spacing of the fuel. In accordance with this function, only the oblique drop which would cause the most severe slap-down effects on the package is evaluated. The resulting deformations and deceleration loadings of the side drop with slap down onto the clamp frames is evaluated in Section 2-4.1.2.2.

2-4.1.5 Summary of Results

As discussed in the preceding sections, the MCC containers will survive the crucial 30-foot accident drops. The containers are expected to be damaged as the kinetic energy of the accident drops is absorbed by the strain energy associated with the deformation of the container. The internal structure and the outer shell assembly are generally expected to act independently during the accident drops, each deforming to absorb its own kinetic energy. This behavior is due to the very soft shock mount system which connects the two separate components. Although damage is expected, failure of the container to remain substantially intact and provide the required spacing for criticality control will not occur. The fuel will maintain its relative position in the structure and maintain the minimum required criticality spacing of 8 inches for the crucial fuel orientation. The maximum deformation to the package components is 4 inches which will occur during the 135° orientation side drop. These results closely correlate with the results recorded in the hypothetical accident tests performed on a prototypical MCC-3 container, which is discussed in Appendix 2-4.3.

2-4.2

EVALUATION OF DROP ANGLE

JUSTIFICATION OF OBLIQUE DROP ANGLE

The performance tests to demonstrate the structural adequacy of the Westinghouse MCC containers under the hypothetical accident requirements of 10 CFR 71.73 requires that a specimen be able to sustain a free fall from a height of 30-feet onto a flat, unyielding horizontal surface, striking the surface in a position for which maximum damage is expected. To comply with this requirement, it is necessary to evaluate which orientation would possibly produce the maximum damage to and/or failure of the package. For the MCC containers, failure is defined as not providing adequate spacing or restraint to the fuel assemblies which would result in a criticality event. The most probable failure which would result in an unsafe criticality geometry is failure of the clamp frames which restrain the fuel assemblies. To propagate this potential failure, the maximum forces from both the primary and secondary impacts would be required to apply the loads to the clamp frames.

At an inclined angle of 90° from the horizontal, the MCC container would be impacting the surface in the longitudinal axis orientation. This orientation would potentially result in crushing the fuel and would not impact any significant loads to all of the clamp frames. At 0°, the package would not experience any additional impact loads from a secondary impact caused by rotational acceleration following a primary impact. Therefore, it is clear that in order to impart the greatest forces onto the clamp frames and normal to the fuel assemblies, the package must be orientated between 0° and 90° as measured from the horizontal.

To determine which angle should be utilized in evaluation of the package, a simplistic model of the MCC internal strongback structure was modeled using the Shipping Cask Analysis System (SCANS) program. The MCC SCANS model consisted only of the internal structure, since the MCC outer shell and the internal structure can be decoupled (note that the impact angle for the internal structure will be slightly less than the initial angle of the outer shell assembly). The SCANS model was then analyzed at various orientations from 15° to 60°, in increments of 15° using various linear stiffnesses for the "impact limiters" (i.e., the end clamp frame/attachment brackets/fuel bundle).

The results of the various computer runs of the SCANS model are summarized in Figure 1. In reviewing this data, one can see that the vertical g's due to the primary impact increase as the package inclination increases, for a specified stiffness. However, the vertical g forces due to the secondary impact are very similar for the 15° and 30°orientations, but decrease as the angle is increased. Note that the actual MCC package will have a stiffness which is more represented by the lower stiffness value rather than the higher values.

For the above reasons, the total maximum vertical g forces which will be imparted to the MCC clamp frame will occur when the package is oriented approximately at the 30° orientation. Therefore, this orientation was utilized in the MCC container evaluation for compliance to 10 CFR 71.73.

FIGURE 1

WESTINGHOUSE MCC CONTAINER

SUMMARY OF VERTICAL G's FOR VARIOUS OBLIQUE ANGLES

SCANS Model Output

Angle	*Package Stiffness kips/in*	*Primary Impact*	*Secondary Impact*
15°	5.0	14.1	22.6
30°	5.0	17.2	22.5
45°	5.0	18.0	21.1
15°	10.0	19.8	32.1
30°	10.0	22.1	31.9
45°	10.0	25.9	29.7
15°	20.0	28.3	45.5
30°	20.0	31.6	45.1
45°	20.0	37.0	41.7
15°	50.0	45.2	72.1
30°	50.0	50.5	71.4
45°	50.0	59.1	65.5
15°	100.0	64.2	102.1
30°	100.0	71.7	100.9
45°	100.0	84.1	92.3
15°	200.0	91.0	144.2
30°	200.0	101.8	142.5
45°	200.0	119.3	130.0

2-4.3

EVALUATION OF TEST RESULTS

TESTING OF THE MCC CONTAINER

INTRODUCTION

The MCC-3 container was drop tested to confirm the survivability of the container. Three accident condition tests were performed on three separate containers. These tests were selected to demonstrate the container's ability to meet the structural requirements following the accident events.

The tests demonstrated that the package would meet the following criteria:

1) Integrity of clamp frames.

2) Minimum spacing would be maintained.

3) The outer shell assembly would remain around the internal structure.

The integrity of the clamp frames is required to ensure that the fuel assemblies will maintain their relationship to the gadolinium plates and will maintain their spacing relative to other containers.

Minimum spacing is required to maintain a sub-critical geometry. The minimum required spacing is four (4) inches between the edge of a fuel assembly and the edge of another container holding fresh fuel in a plane parallel to the assembly -- for a total minimum fuel-to-fuel separation of eight (8) inches.

The outer shell assembly must be maintained around the internal structure for spacing purposes, and to assure the contents can only be exposed to full-density water (flooding) moderation. Without the shell, the clamp frames and snubbers, which act as spacer blocks, could be placed adjacent to each other which would result in the required spacing not being maintained.

The three drop orientations chosen to demonstrate the container's ability to satisfy these conditions were: 1) a side drop onto the package top; 2) a side drop with slapdown onto the internal clamp frames; and 3) a side drop onto the package closure. The side drop onto the package top loads up the frames and its connection points. It also attacks the snubbers and swing bolts. The slapdown applies the maximum crush force to the fuel, clamp frames, and connection points in localized areas. The drop onto the closure applies the maximum load to the T-bolts which hold the two halves of the outer shell together.

PACKAGE CONFIGURATION

All drops were performed using an MCC-3 container with a modified payload. The

payload weight was increased to ensure that the maximum load per clamp frame and per closure bolt would be tested. The worst case condition not only bounded the possible configurations for the MCC-3 container, but also bounds the MCC-4 container. **(See the justification provided in Section 2-4.5.)** Both fuel compartments contained simulated fuel assemblies. The weights of the dropped packages were 4,244 pounds for the empty package and 3,300 pounds for the fuel assemblies. The total weight of each test container was 7,544 pounds.

DROP TEST FACILITIES

All three tests were performed at the Oak Ridge National Laboratory drop facility.

Impact (Target) Pads

There are two drop test facilities which have been used to test packages. The smallest facility is the old test facility that utilizes a concrete pad with an impact surface of armor plate. This facility has been modified recently to provide a larger impacting surface than was available in the original pad.

The concrete and steel in the pad weighs approximately 40 tons; its top surface is approximately 11-ft x 10-ft and has an 8-ft square armor plate surface embedded in it. A larger impact surface was added to the pad as part of the recent modification. Several pieces of armor plate 6-in thick were added, which effectively cover the entire pad and overhang about 2-ft in one direction. The additional armor plate is welded to the original plate and adds approximately 60 tons. However, it has a significantly larger effective mass, since the bulk of the pad rests on a 3-ft diameter concrete column which was sunk into bedrock approximately 7-ft below grade. An illustration of this pad is shown in Figure 1.

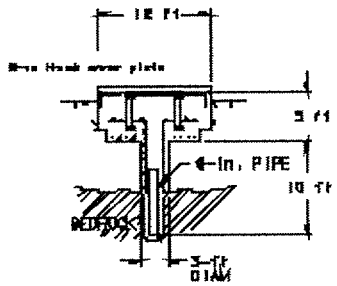

Figure 1 Sectional View of the Small Drop Pad

DAMAGE SUMMARY

All of the containers performed well in the tests. In general, the damage/deformation was less than what was expected. The clamp frames' geometry was preserved and the overall spacing was maintained. Sufficient T-bolts survived the drop tests to ensure that the outer shell assembly would not be separated from the fuel assemblies and the internal structure. Details of each test are provided below.

In all cases, very little global damage occurred to the fuel assemblies or the internal structure. The center wall deformed very little, thus ensuring that the gadolinium plates would remain intact and functional.

SIDE DROP ONTO CONTAINER TOP

Refer to Figures 2-4.3-1 through 2-4.3-8.

The container demonstrated an adequate margin of safety against loss of fuel retention. The overall damage to the container was less than what was expected. The total deformation of the top cover was approximately 4-inches. There was a noticeable affect of the ends and stiffener angles. At the ends, the stiffener angle folded. In the center, the angles deformed more, but did not fold. The deformed shape of the angles was similar to flattening of an arch. It was very evident that the internal structure bottomed out by the imprints of the clamp frames on the top shell cover.

An interesting phenomenon which occurred was the localized shearing of the lid outer shell. The location of one stiffener angle was offset slightly from a frame. The stiffener angle was driven in and the frame out, shearing the shell. This effect was a local occurrence which would be impossible to duplicate over the length of the outer shell lid. In all cases, there are more clamp frames than stiffening angles.

The fuel restraint system held the fuel assemblies in position. All of the clamp frame connections retained their connectivity to the strongback. There was only a slight deformation of one Unistrut channel at one end. The snubbers limited the flow of the pressure pad swing bolts. Their undamaged presence demonstrated that the required spacing would be maintained as long as the outer shell assembly remained intact. The clamp frames did not noticeably deform. The fuel assemblies crushed approximately ½ to 1-inch.

SIDE DROP WITH SLAPDOWN ONTO INTERNAL CLAMP FRAMES

Refer to Figures 2-4.3-9 through 2-4.3-18.

The container was dropped at an inclined angle of 30°, relative to the horizontal plane, and was rotated about its longitudinal axis 135° clockwise, to ensure that the impact point would occur on the corner of the fuel.

Significant damage occurred to the outside of the container. The initial impact corner deformed in approximately 6-inches. The slapdown corner deformed approximately 7-inches. The stacking support angle was completely crushed and flattened on both ends. The internal structure impacted the outer shell and punched several holes in each of the corners.

Most of the kinetic energy on the initial impact end was absorbed by deforming the top closure assembly. The end fuel restraining bolts deformed significantly and one connecting pin was sheared. The end clamp frame was only slightly deformed. The fuel assembly closest to the initial impact point was crushed very little.

The middle clamp frames were damaged very little, with only a slight crush and bending of the adjustable swing bolts. The center section of the fuel assembly had insignificant amount of crush.

As expected, the damage on the slapdown end was more significant. Three clamp frames were deformed inwardly with most of the damage occurring on the outer two. The bottom support structure punched through the outer shell and struck the impact surface. This condition resulted in a relatively high g loading, but limited the deformation of the fuel. As can be seen in the photographs, the end plate was only slightly damaged, indicating that a majority of the energy had already been absorbed. For this reason, dropping the container with a reversal of the ends would not result in significantly more damage. Due to the deformation of the clamp frames, the top pivot mount stud nuts partially pulled out of the Unistrut channel. This situation is not a concern because the fuel assemblies remained restrained by the fact that the connection to the adjacent frame remained intact. In addition, the undamaged center frames would have provided sufficient restraint to maintain spacing even if the end frames had completely failed. The lower pivot mount connections remained connected, although there was significant deformation of the Unistrut channel on the deformed clamp frames. The lower pivot mount connection on the most severely deformed frame remained attached to only one side of the Unistrut channel. The fuel assemblies under the pressure pads were crushed approximately ½ to 1 inch.

SIDE DROP ONTO PACKAGE CLOSURE

Refer to Figures 2-4.3-19 through 2-4.3-27.

The side drop onto the closure demonstrated the adequacy of the closure T-bolts. It is required for the top and bottom shells to stay connected to the internal structure inside. This is required to maintain the sub-criticality spacing since without the outer shell assembly, the clamp frames and snubbers, which act as spacers, could be located side-by-side, thus reducing the spacing by one half. This is also required to assure that contained fuel assemblies can only be exposed to full-density water moderation (flooding), and not to partial-density water moderation (sprays, etc.).

Fifteen of the thirty T-bolts either pulled through the shell sealing flange or failed in tension. None of the T-bolts failed in shear. The six guide pins, which have closer tolerances than the T-bolts, did not shear either. The location of the T-bolt failures varied, depending on the construction of the container. On the impact side, six bolts failed. The majority of these failures were in the center section where the shell has the minimum amount of reinforcement. The outer shell, with the internal shock mount bracket, deformed and applied a high bending moment in the closure flange area. This prying action was resisted by the T-bolts until failure occurred. In general, this condition did not occur towards the ends where the major reinforcement which would resist this bending moment is located. The bending of the shell was demonstrated by the fact that the center section of the container, which is loaded by the fuel assemblies, deformed downward about 2-½ inches on the non-impacted side, relative to the ends. The remaining T-bolts failed on the ends and towards the ends on the non-impacted side. These failures were the result of the stiff ends, and reinforcement in these locations, transmitting the separation load from the weight of the shell and payload, pushing the shell apart. The moment is reacted by the bolts on the far side of the container.

By having two different mechanisms working in the container, catastrophic failure of fasteners is avoided. This behavior ensures that there is a large margin against having the outer shell assembly fail in such a manner that the internal structure will separate from the outer shell.

The internal structure impacted initially on the shock mounts and then rotated to spread the load between the shock mounts and the frames contacting the external shell. The load on the shock mounts crushed the mounting bracket such that the connecting bolts punched into the outer shell. The frames also indented into the outer shell. The loads were sufficient to cause the trunnion block on the uprighting pivot to fail. Once this

failed, the strongback and fuel assemblies slid out of the side swing bolt (different than the adjusting fuel swing bolts) connections and became free.

The impact on the frames, with the subsequent load transmittal to the center wall, as well as the non-impacted frames, caused some yielding in the Unistrut pivot mount connections to the center wall. All of the frames remained connected to the adjacent frame so that restraint of the fuel assemblies was maintained. The majority of the yielding of connections occurred in the center section where the deformation of the outer container was the greatest, allowing the most deformation of the internal to occur. The center clamp frame pried its lower pivot mount connection out of the Unistrut channel. This failure is due to a stiffening angle on the outer shell being located adjacent to the frame. During impact, the frame was driven in and the frame out, shearing the shell, which allowed the frame to see a higher impact than if the shell and angle were there to deform and soften the impact. Due to the redundant nature of the frames, this single failure does not prevent the package from fulfilling its requirements.

The adjustable swing bolts were bent slightly. There was very little damage to the frames or to the snubber blocks. There was a small amount of crush to the fuel assembly of about ½-inch, but no compromise of the required spacing occurred.

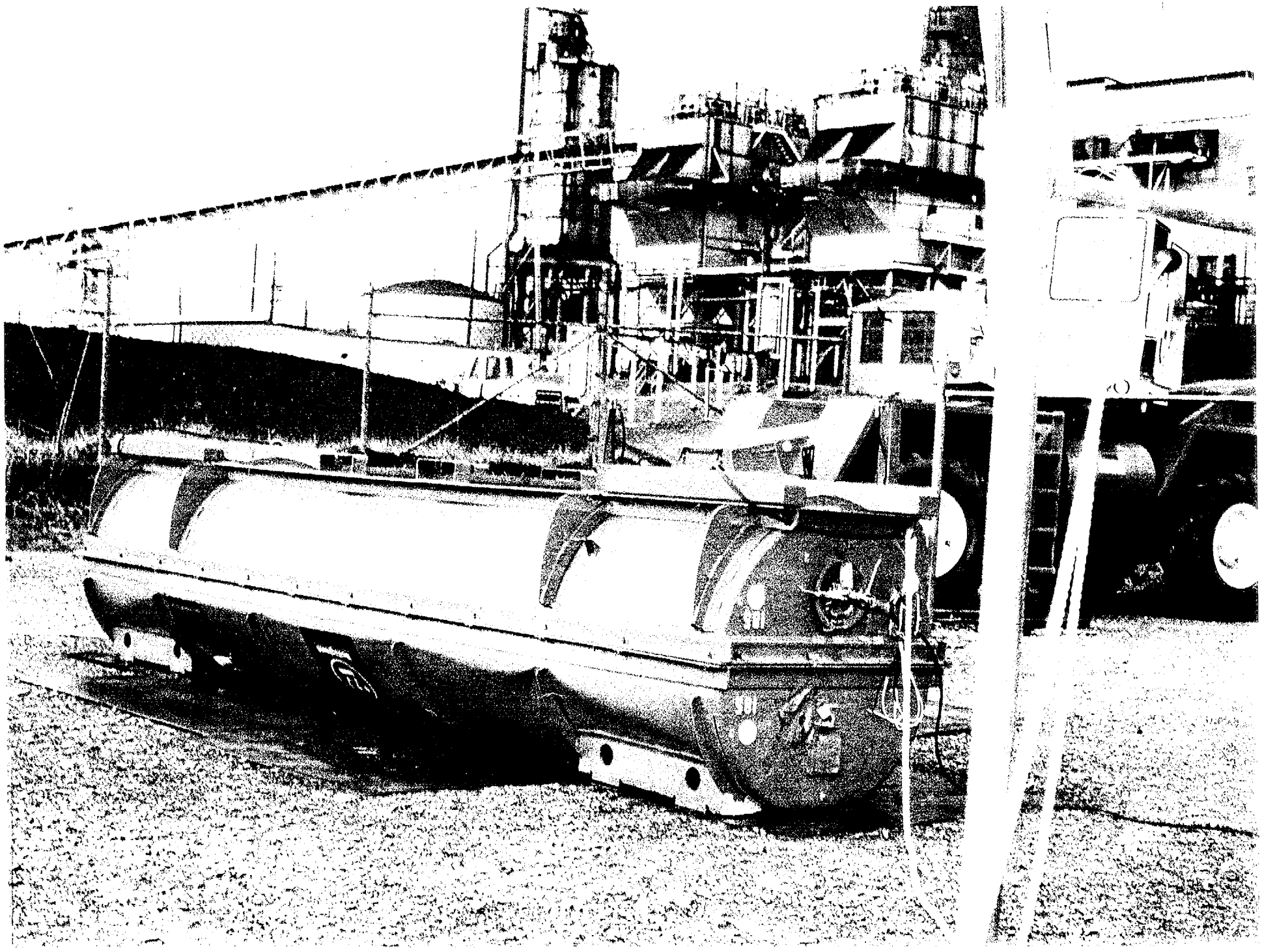

FIGURE 2-4.3-1 SIDE DROP ONTO CONTAINER TOP

FIGURE 2-4.3-2 SIDE DROP ONTO CONTAINER TOP

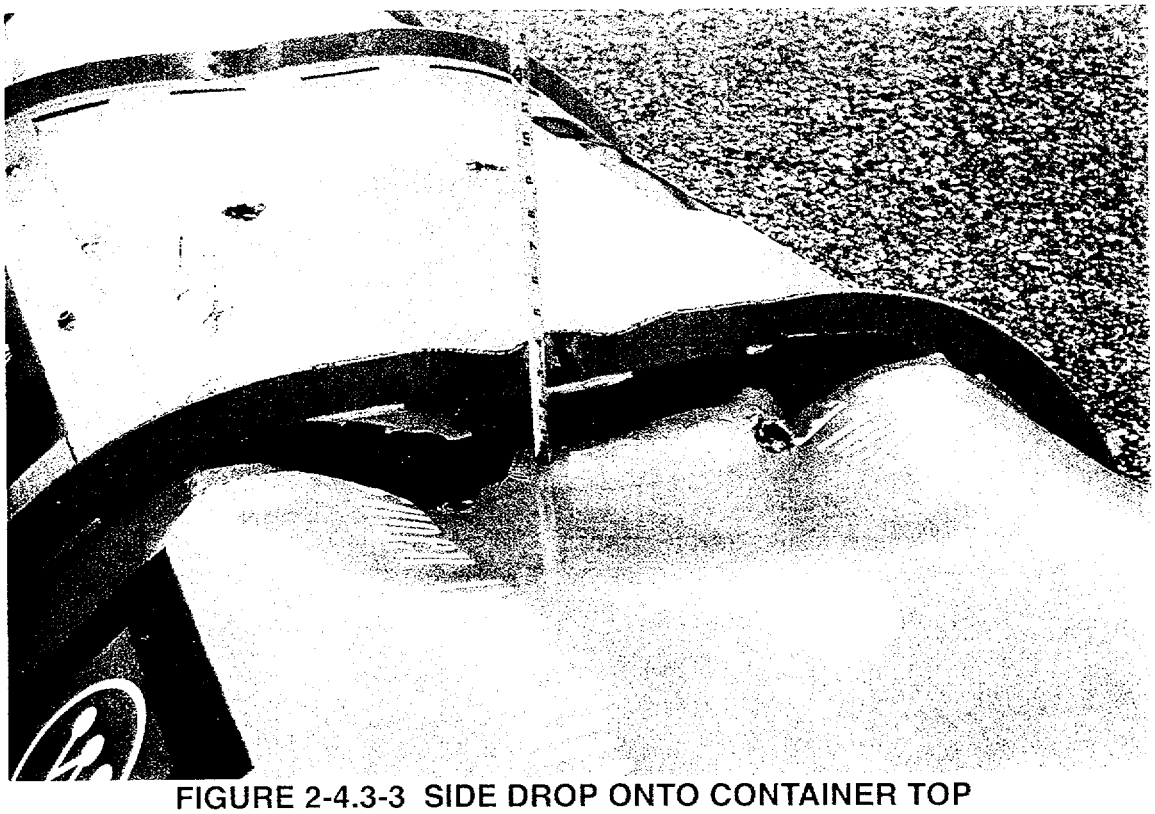

FIGURE 2-4.3-3 SIDE DROP ONTO CONTAINER TOP

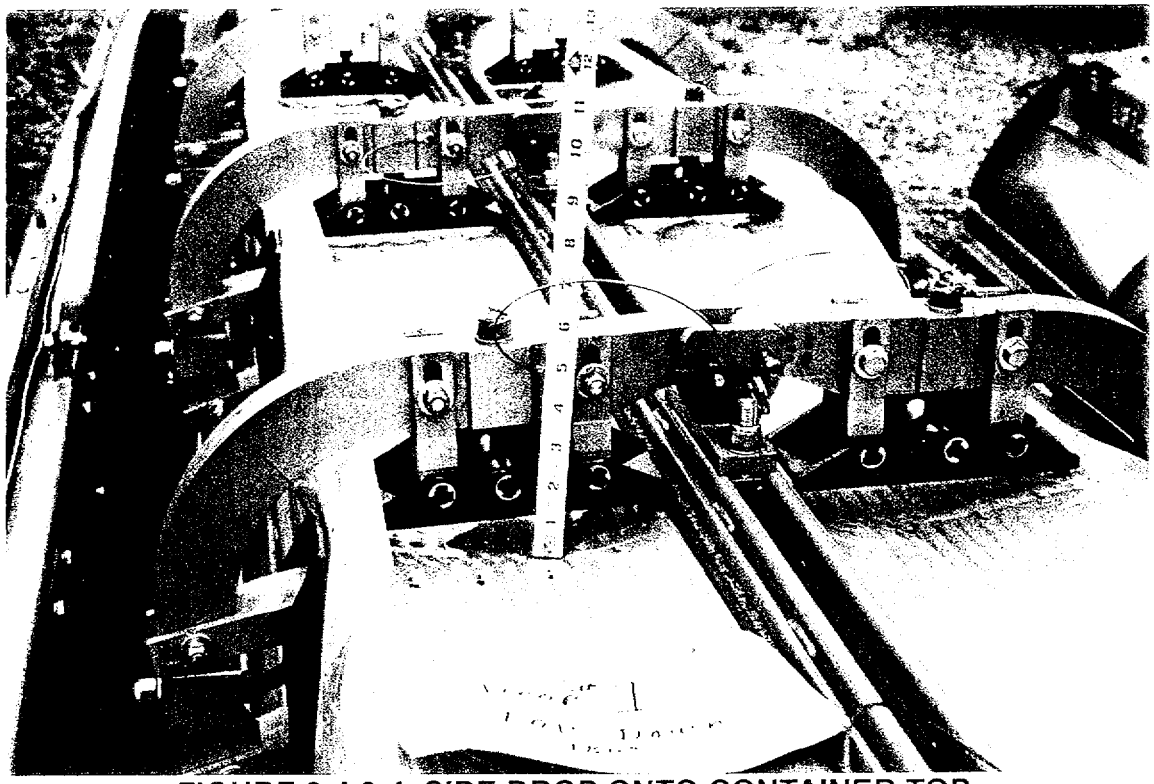

FIGURE 2-4.3-4 SIDE DROP ONTO CONTAINER TOP

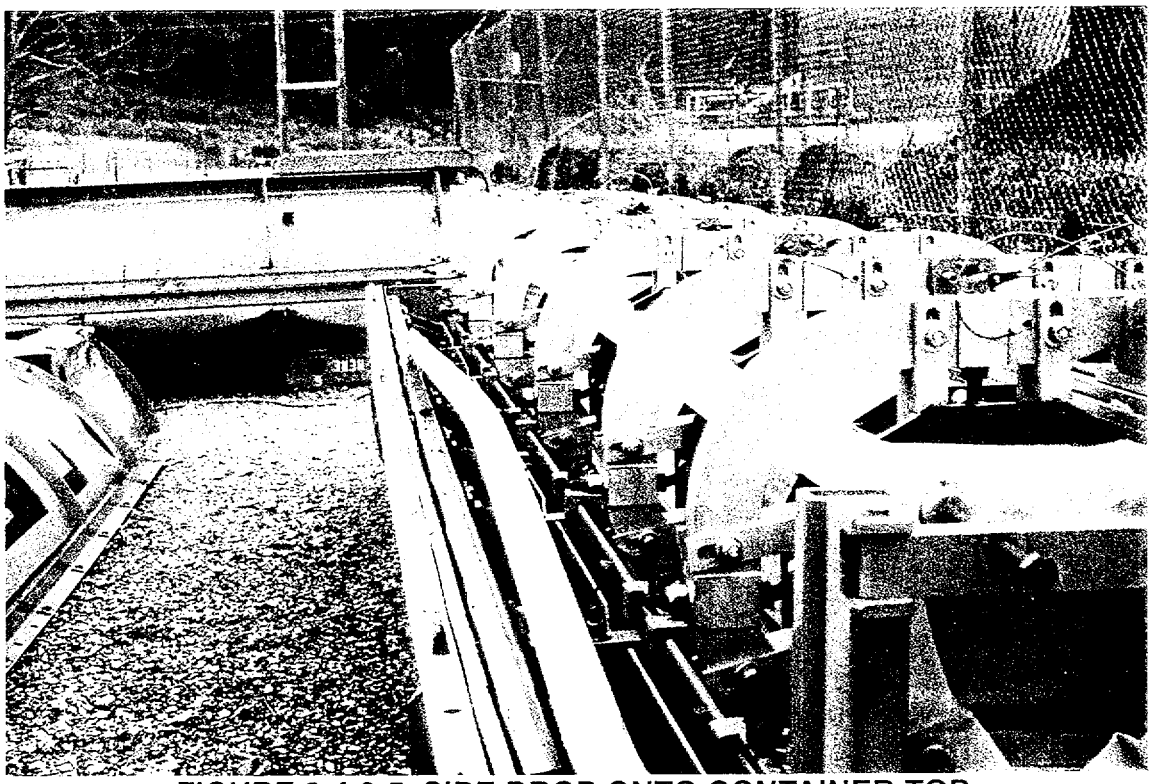

FIGURE 2-4.3-5 SIDE DROP ONTO CONTAINER TOP

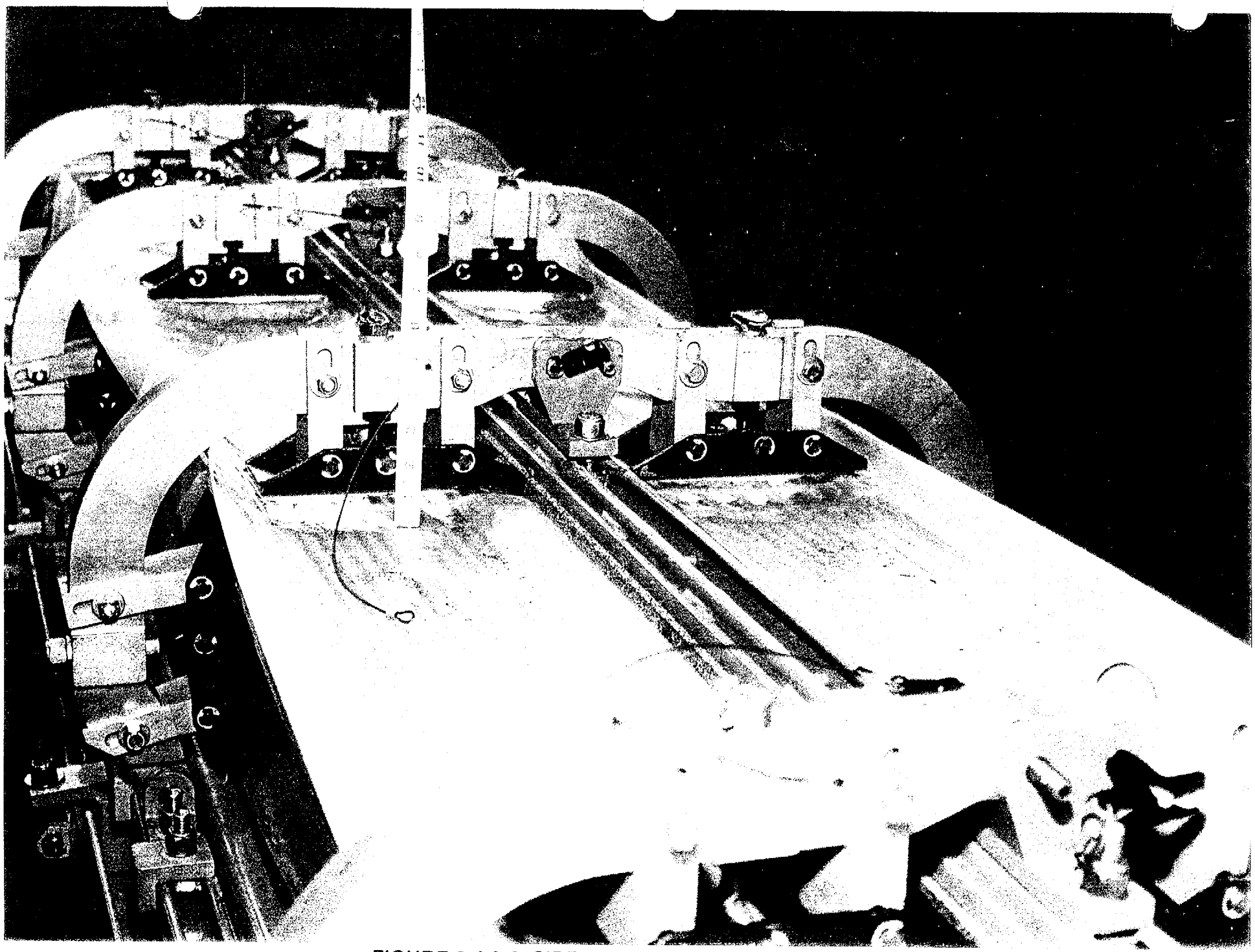

FIGURE 2-4.3-6 SIDE DROP ONTO CONTAINER TOP

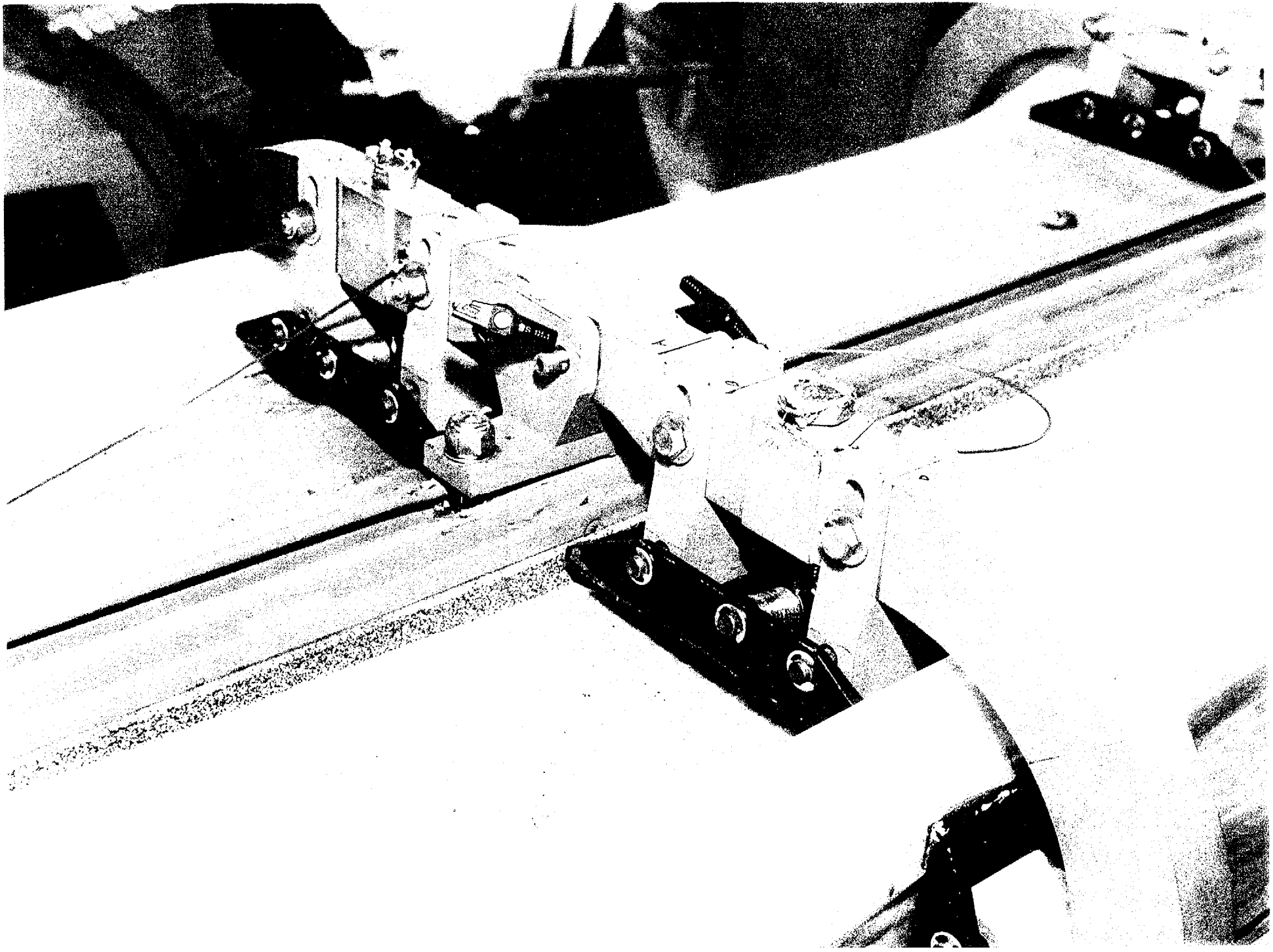

FIGURE 2-4.3-7 SIDE DROP ONTO CONTAINER TOP

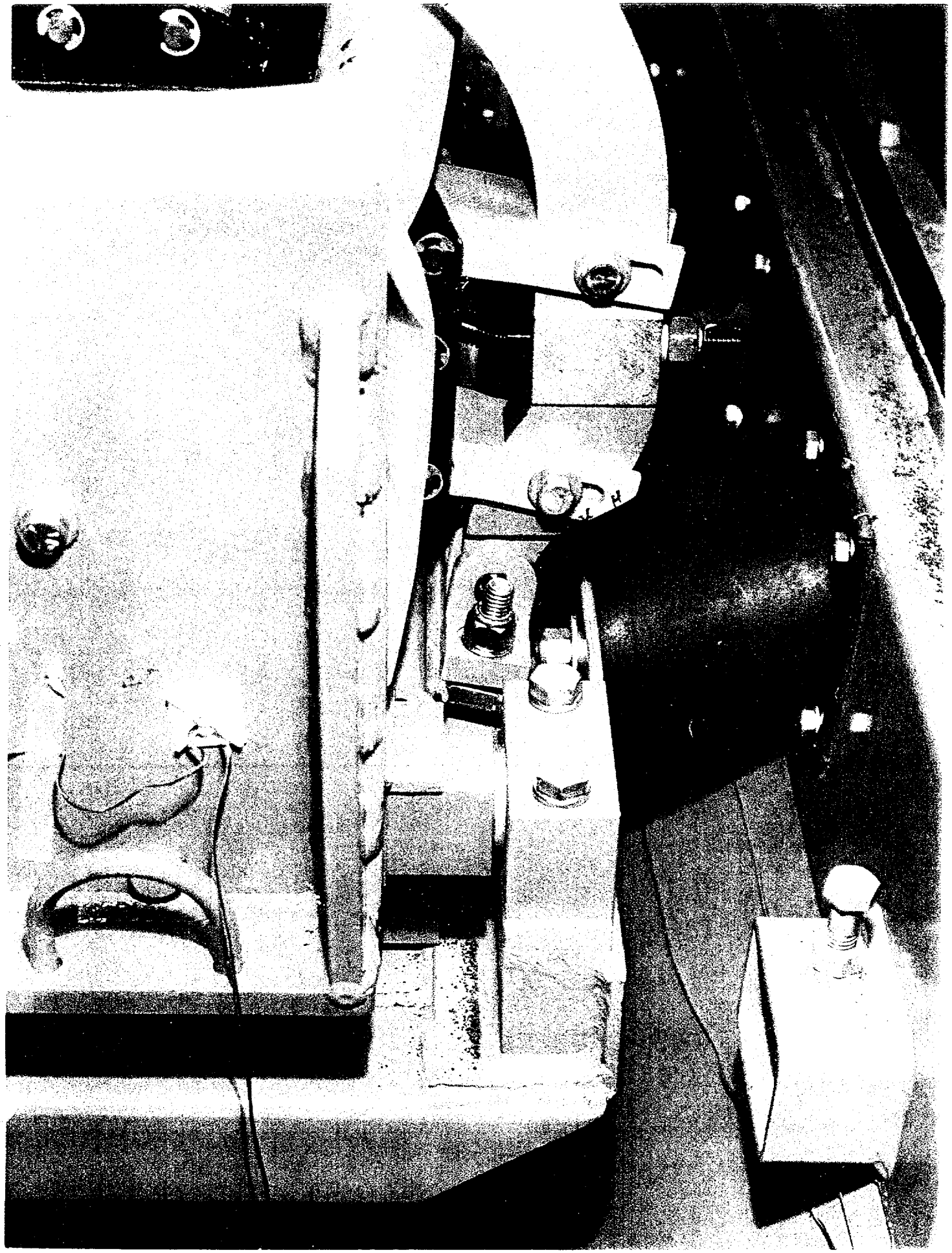

FIGURE 2-4.3-8 SIDE DROP ONTO CONTAINER TOP

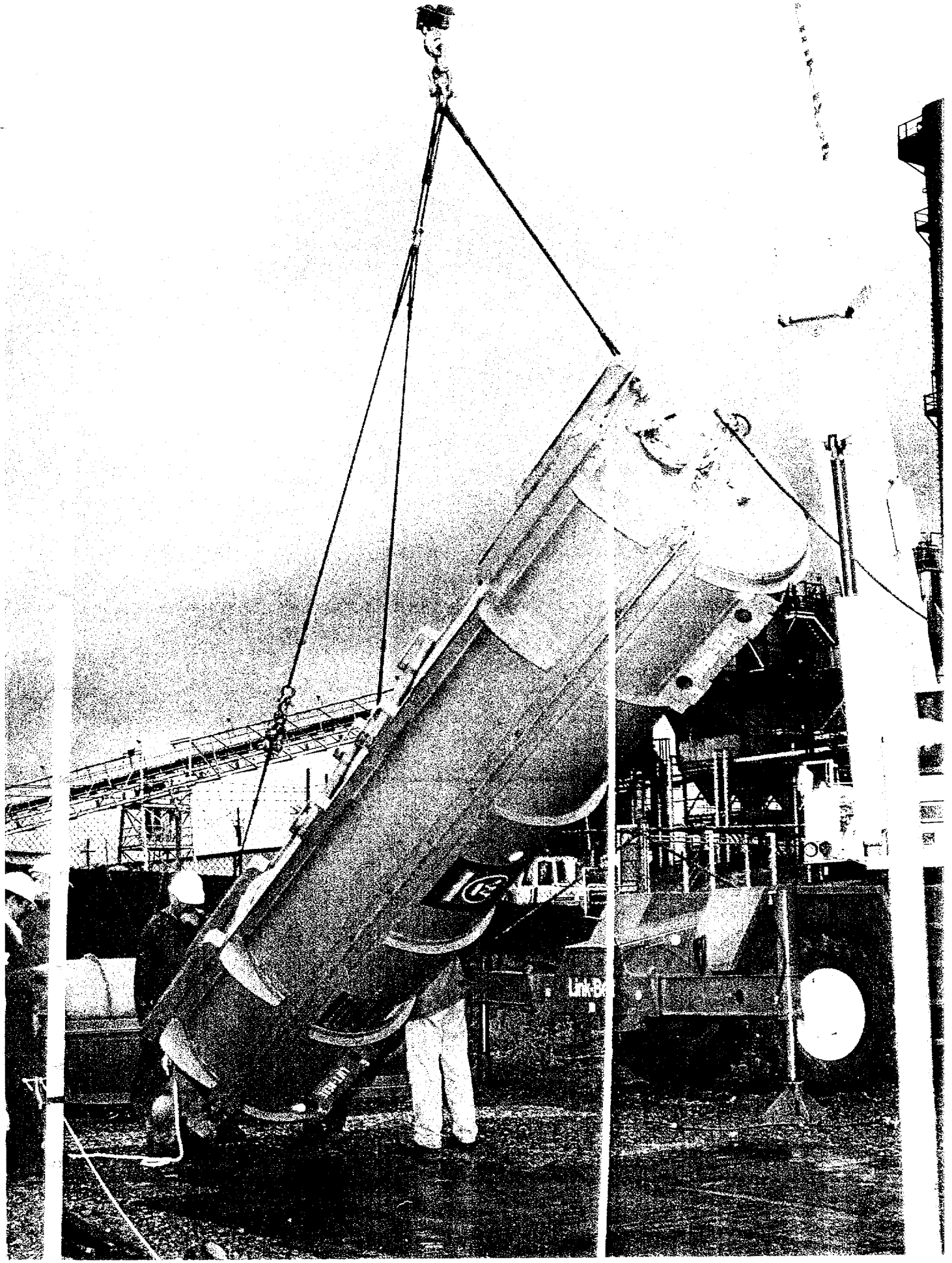

FIGURE 2-4.3-9 SIDE DROP W/SLAPDOWN ONTO CLAMP FRAMES

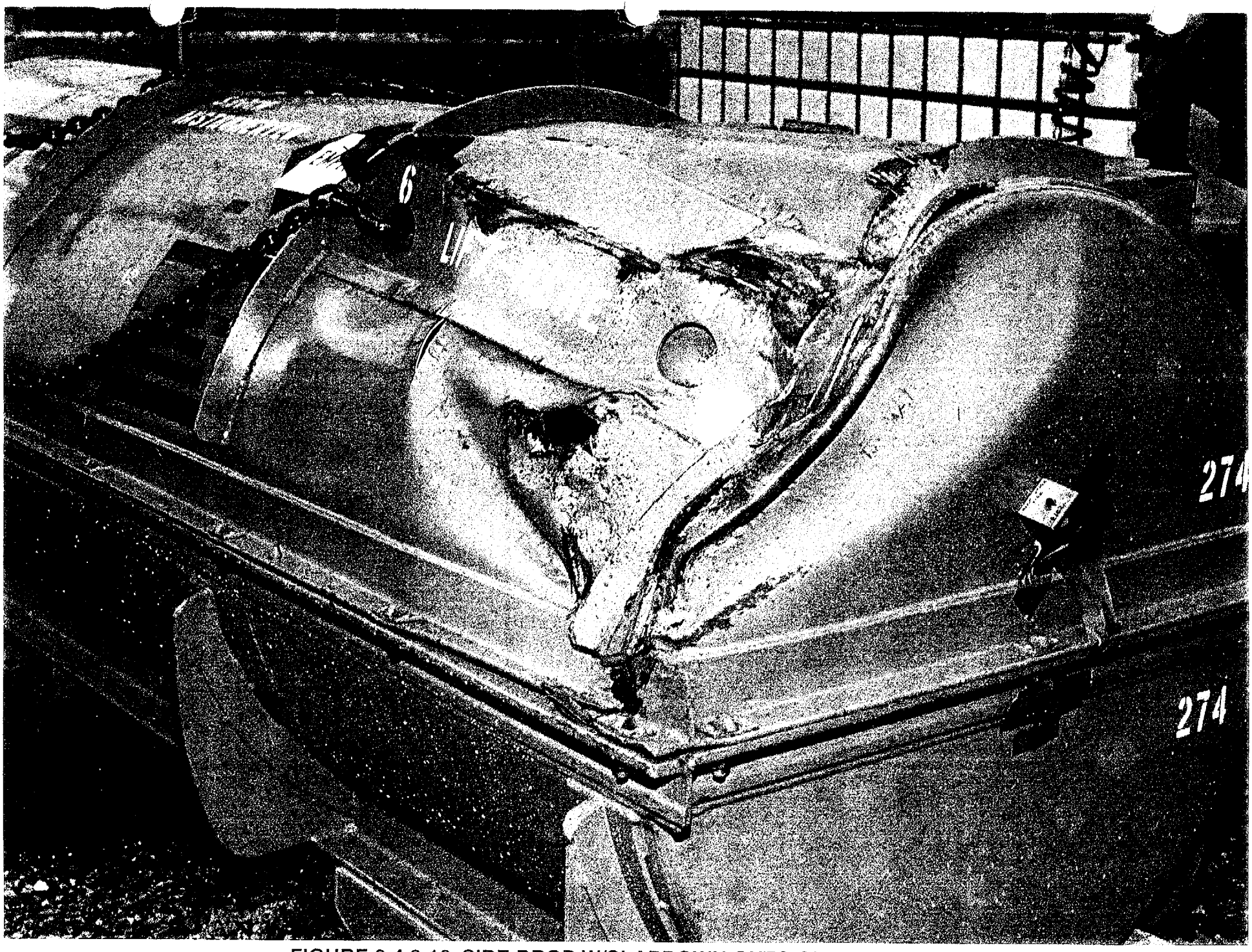

FIGURE 2-4.3-10 SIDE DROP W/SLAPDOWN ONTO CLAMP FRAMES

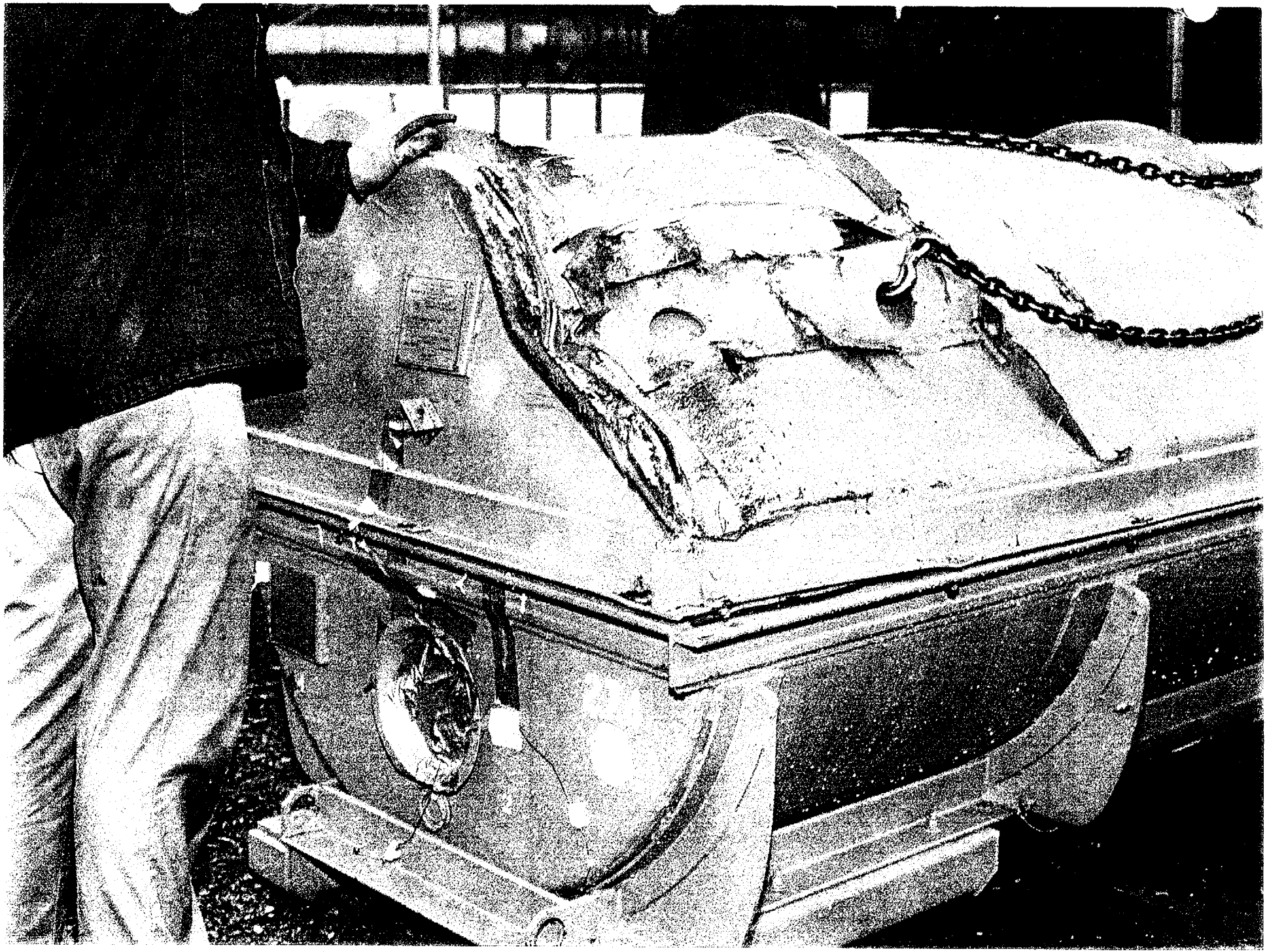

FIGURE 2-4.3-11 SIDE DROP W/SLAPDOWN ONTO CLAMP FRAMES

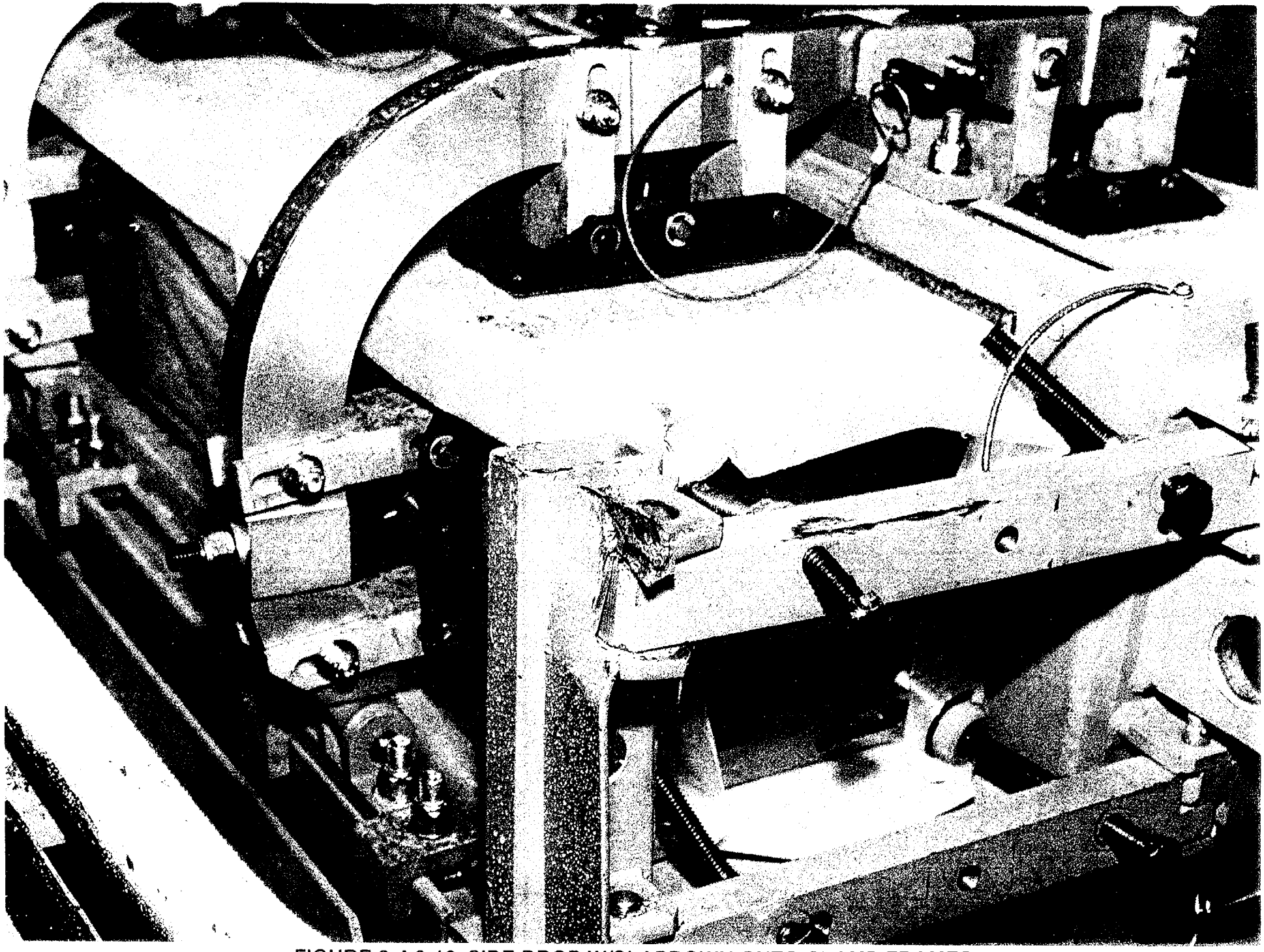

FIGURE 2-4.3-12 SIDE DROP W/SLARDOWN ONTO CLAMP FRAMES

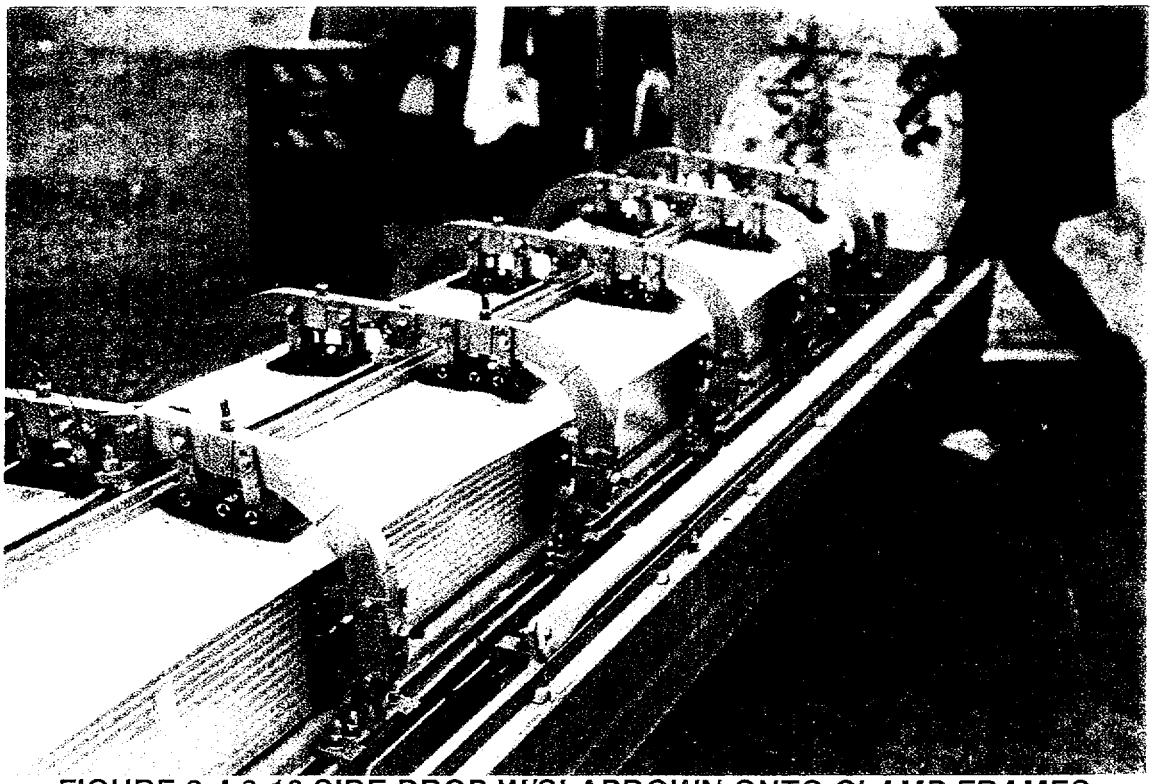

FIGURE 2-4.3-13 SIDE DROP W/SLAPDOWN ONTO CLAMP FRAMES

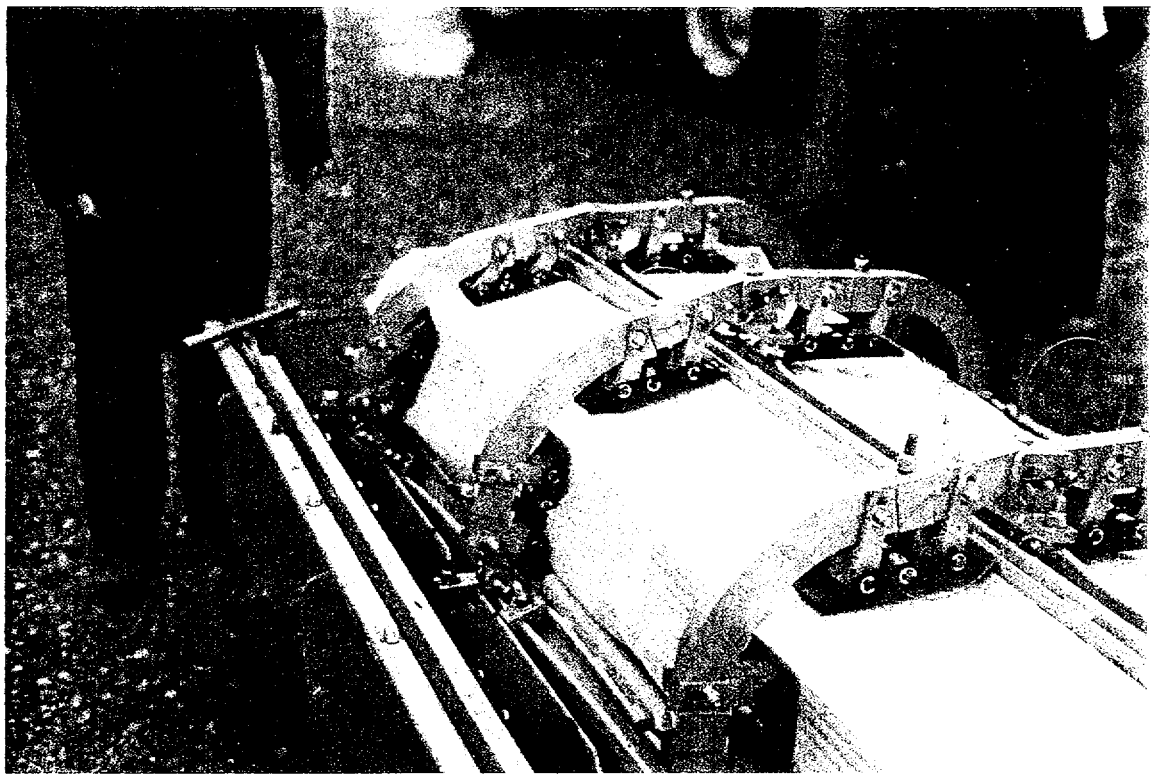

FIGURE 2-4.3-15 SIDE DROP W/SLAPDOWN ONTO CLAMP FRAMES

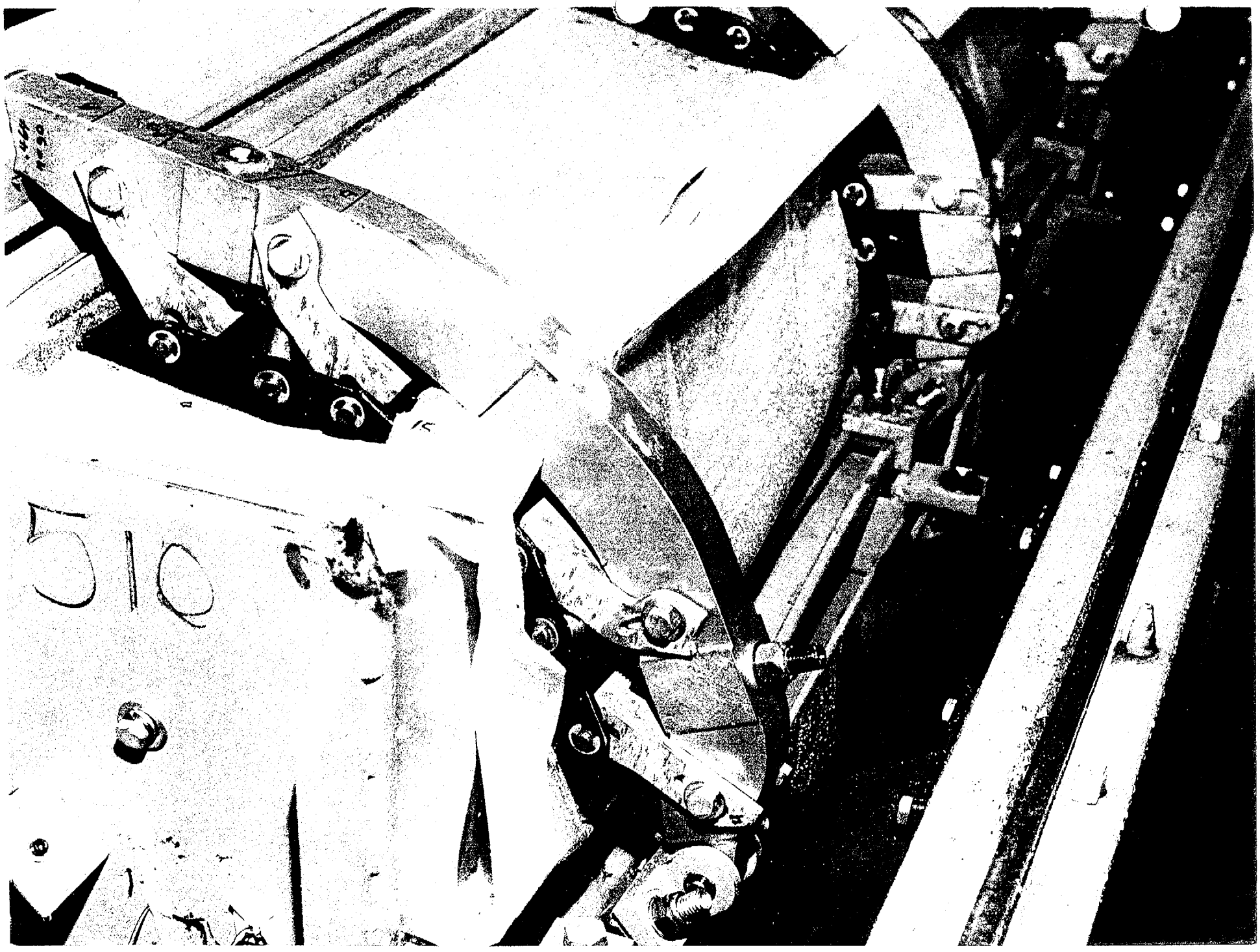

FIGURE 2-4.3-14 SIDE DROP W/SLAPDOWN ONTO CLAMP FRAMES

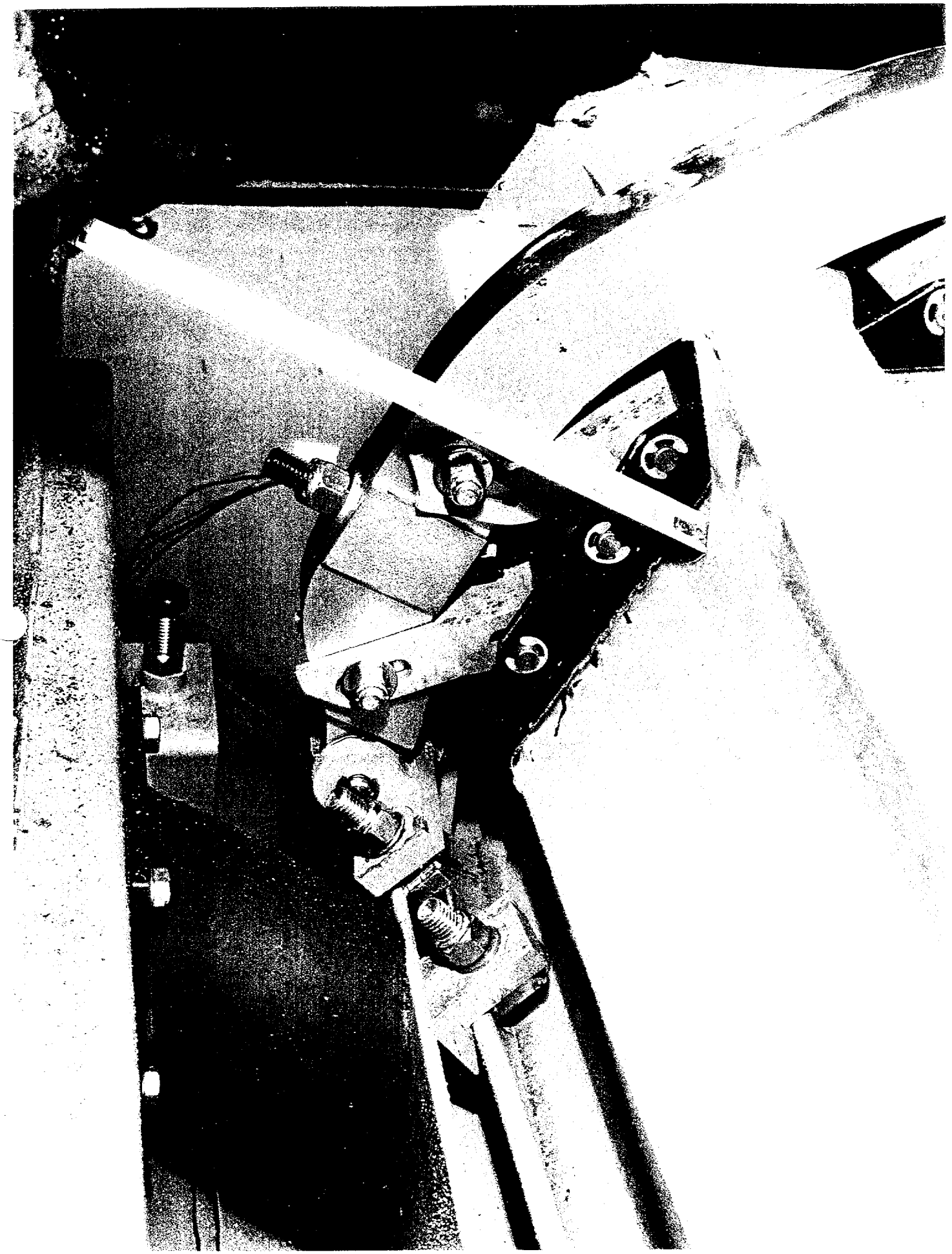

FIGURE 2-4.3-16 SIDE DROP W/SLAPDOWN ONTO CLAMP FRAMES

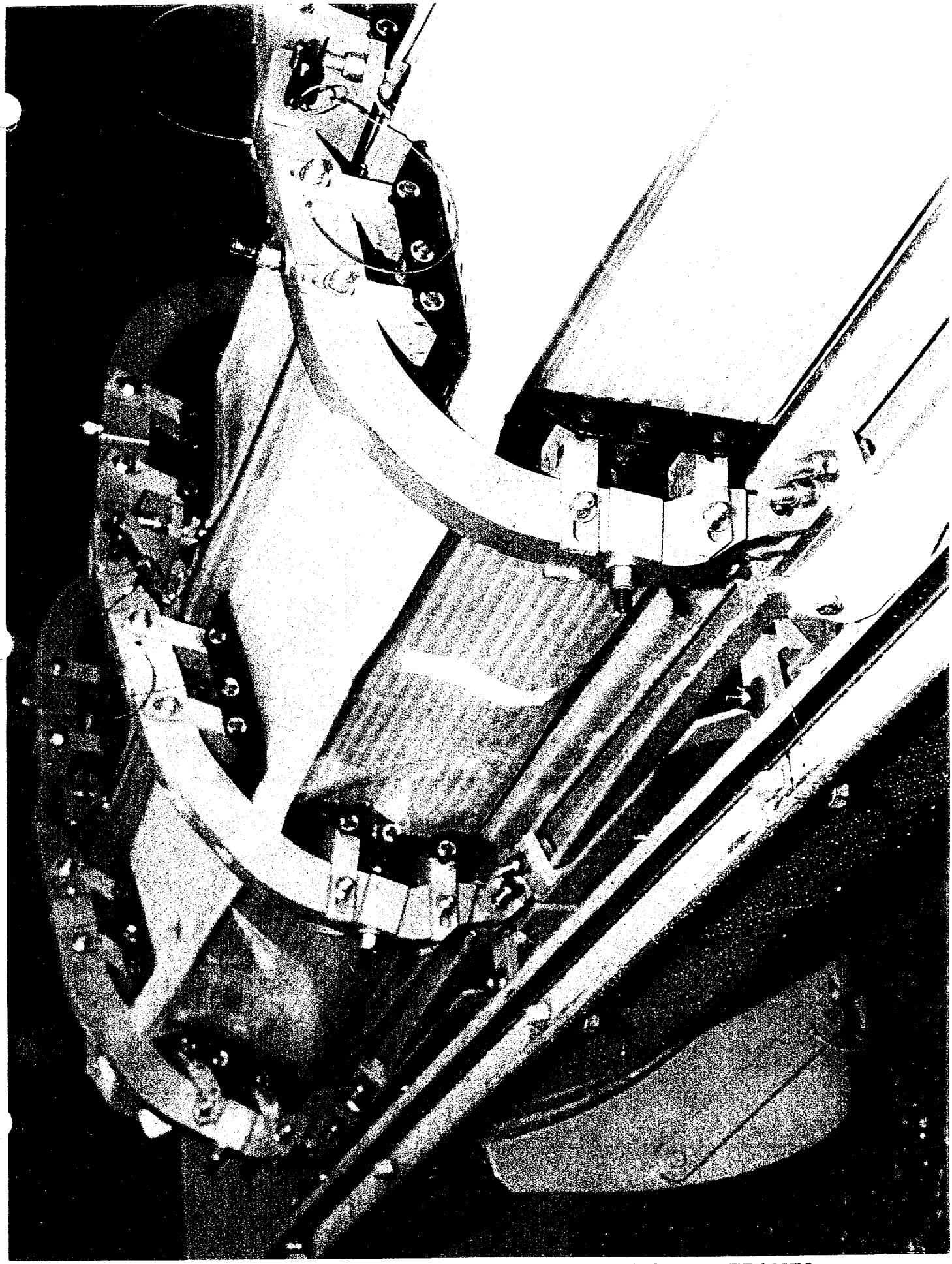

FIGURE 2-4.3-17 SIDE DROP W/SLAPDOWN ONTO CLAMP FRAMES

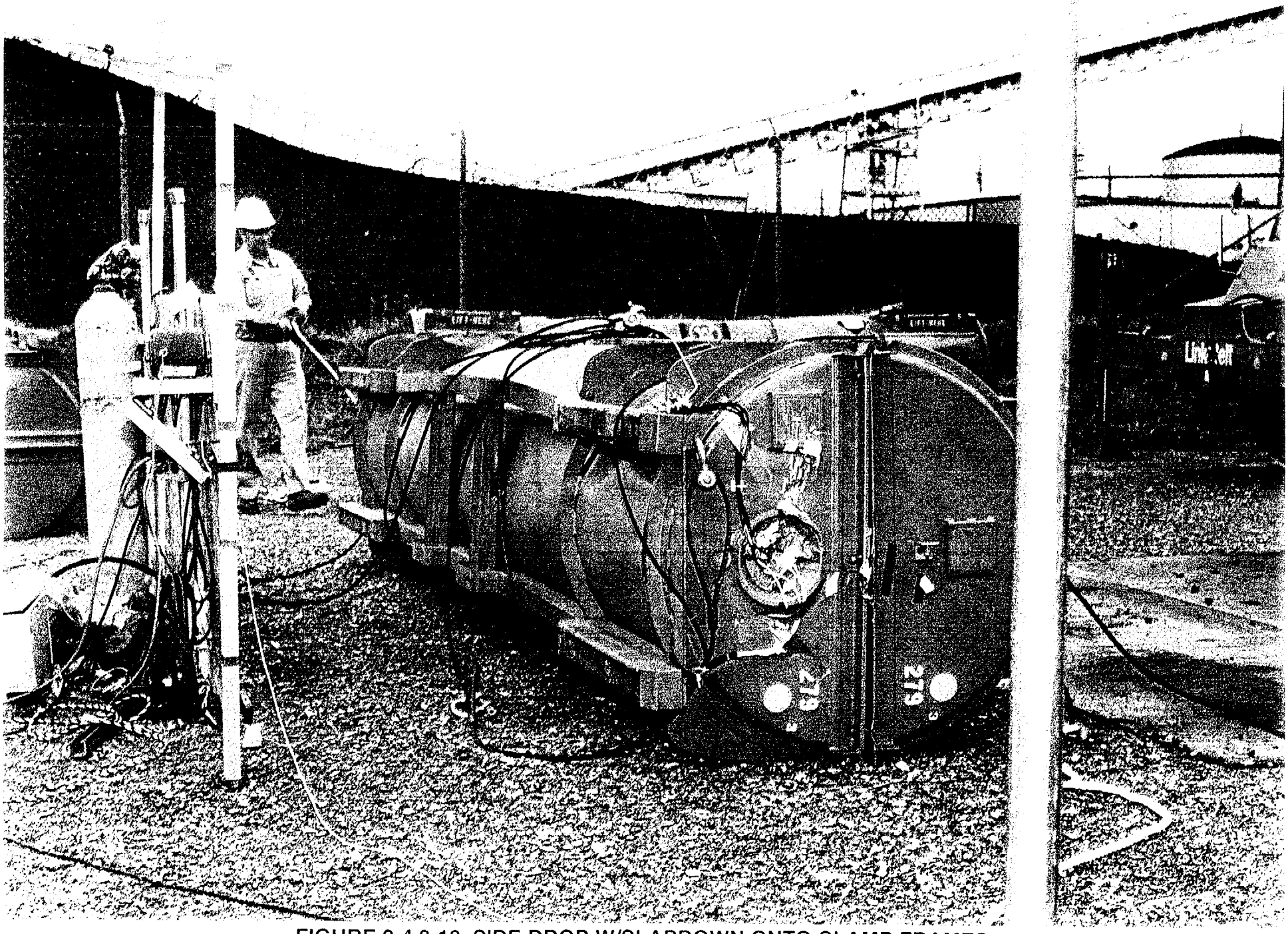

FIGURE 2-4.3-18 SIDE DROP W/SLAPDOWN ONTO CLAMP FRAMES

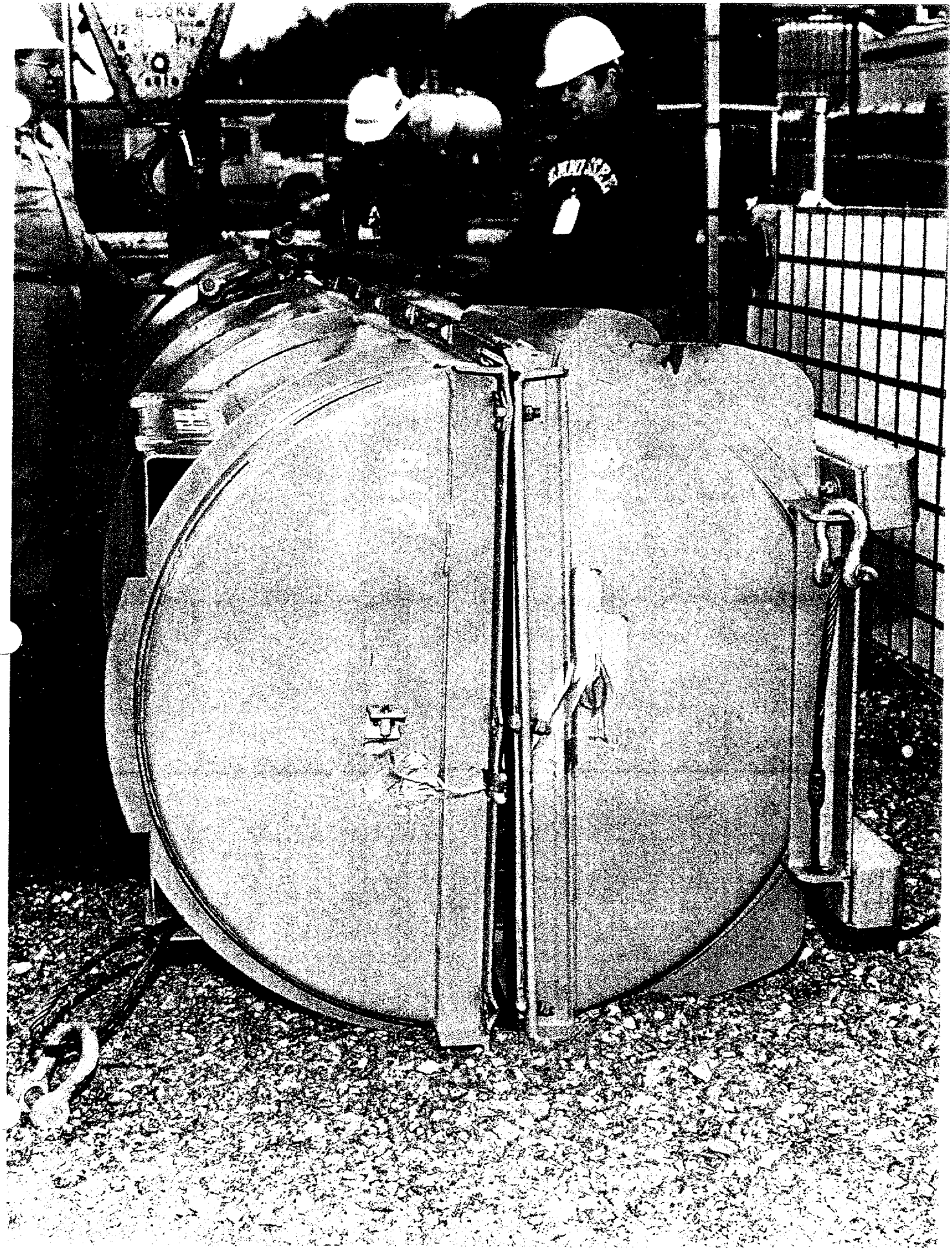

FIGURE 2-4.3-19 SIDE DROP ONTO PACKAGE CLOSURE

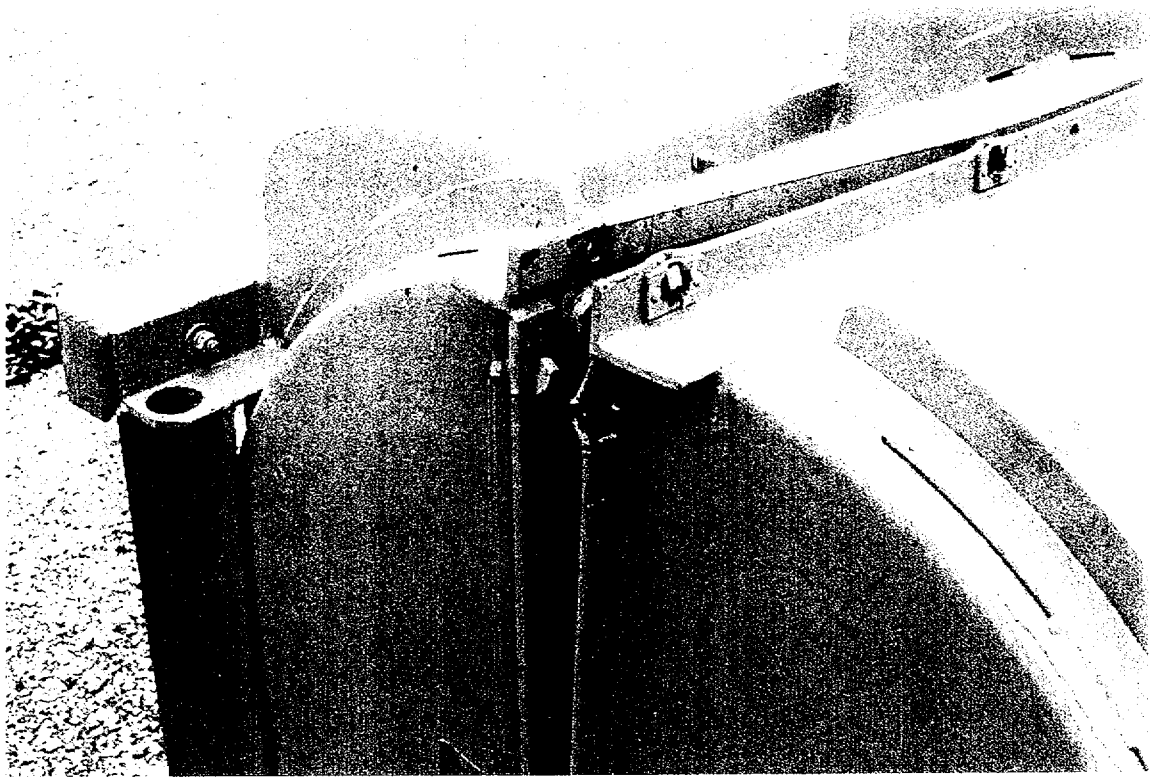

FIGURE 2-4.3-20 SIDE DROP ONTO PACKAGE CLOSURE

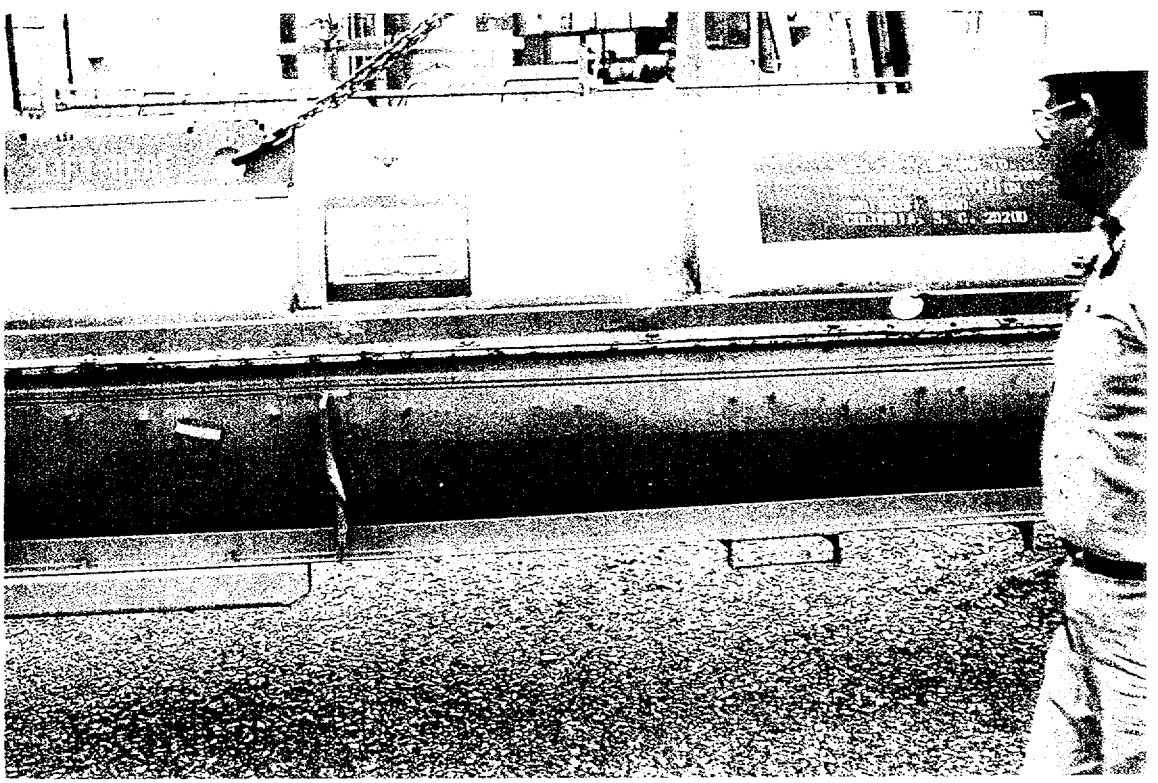

FIGURE 2-4.3-21 SIDE DROP ONTO PACKAGE CLOSURE

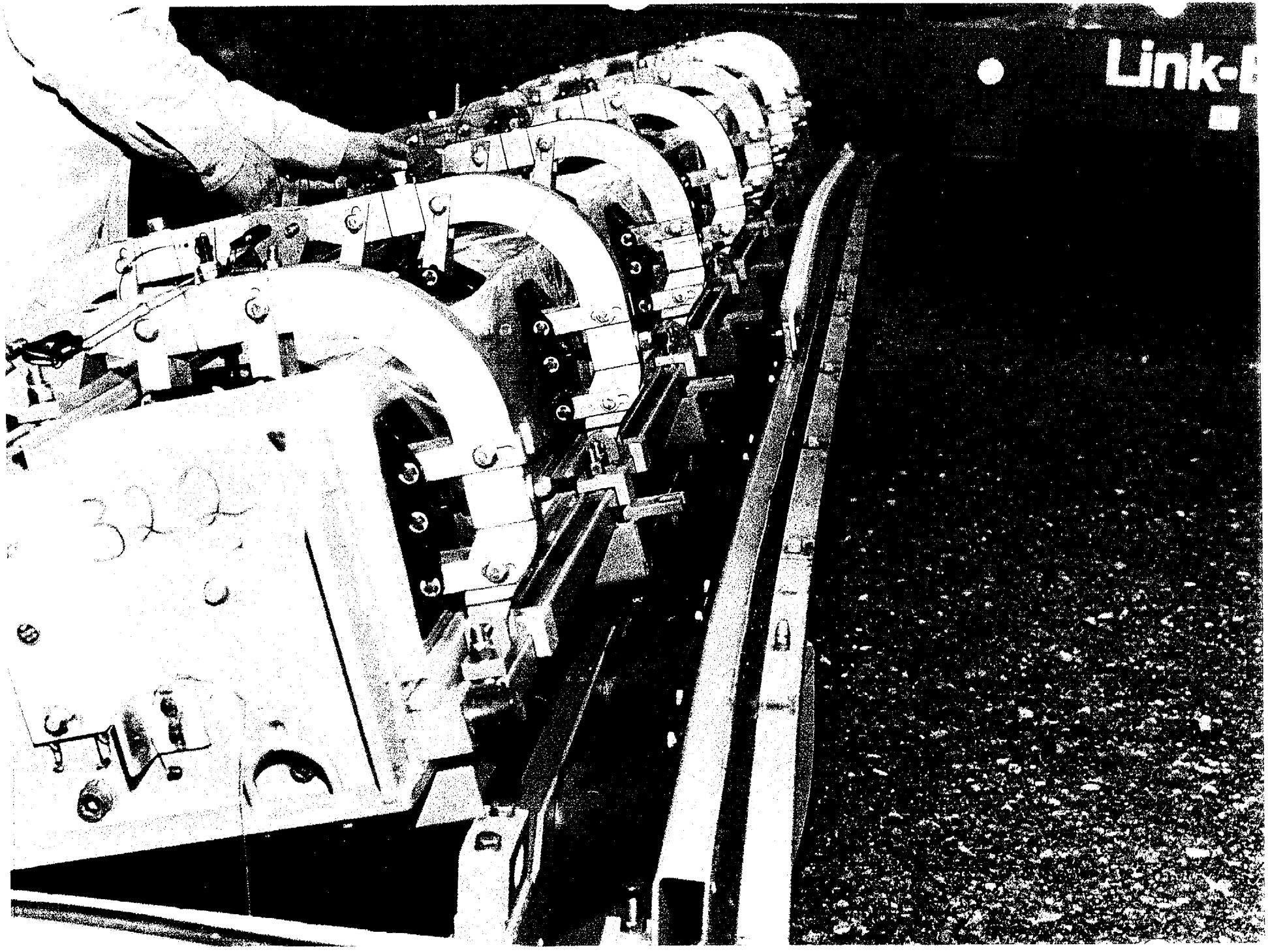

FIGURE 2-4.3-22 SIDE DR ONTO PACKAGE CLOSURE

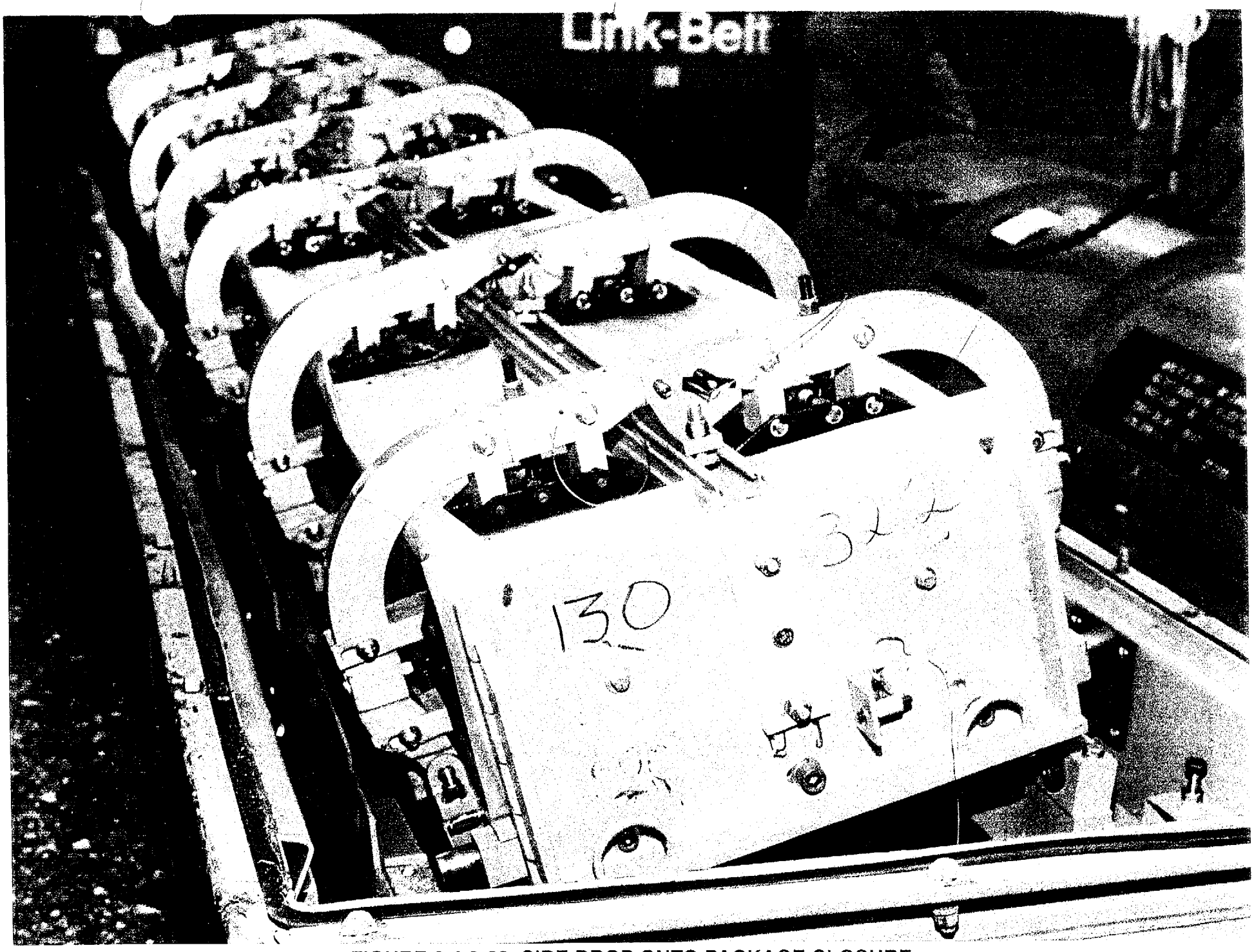

FIGURE 2-4.3-23 SIDE DROP ONTO PACKAGE CLOSURE

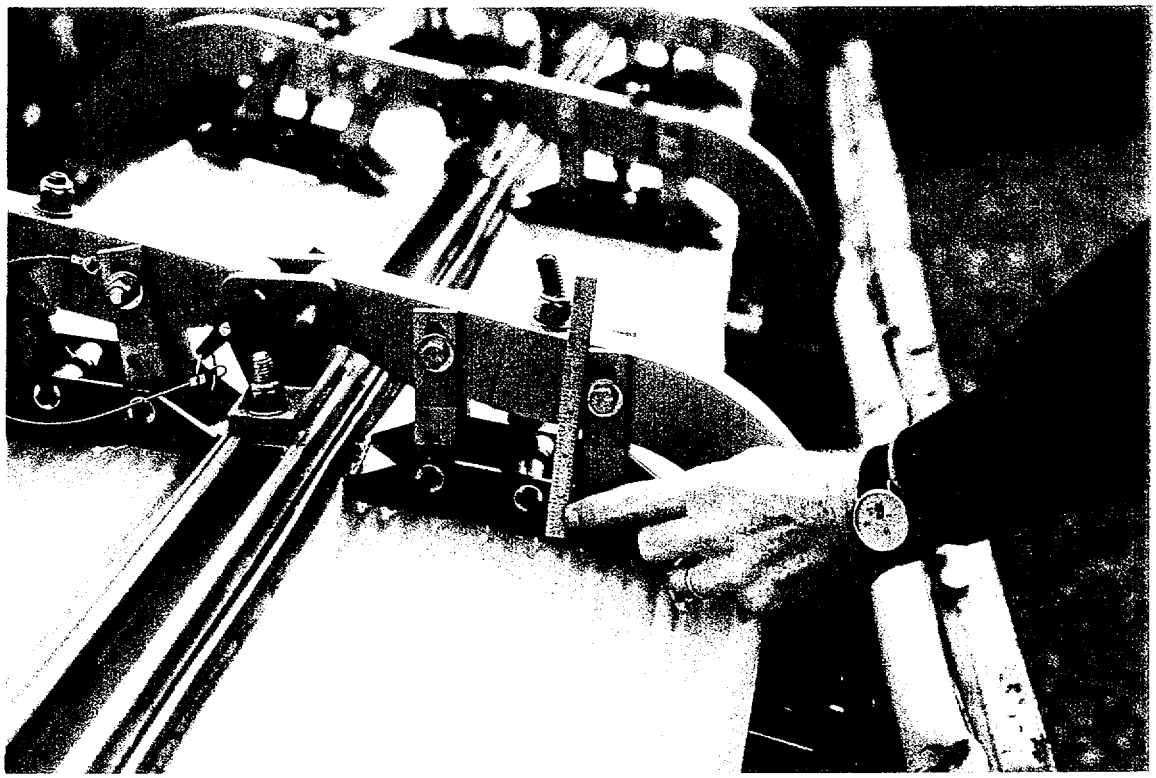

FIGURE 2-4.3-24 SIDE DROP ONTO PACKAGE CLOSURE

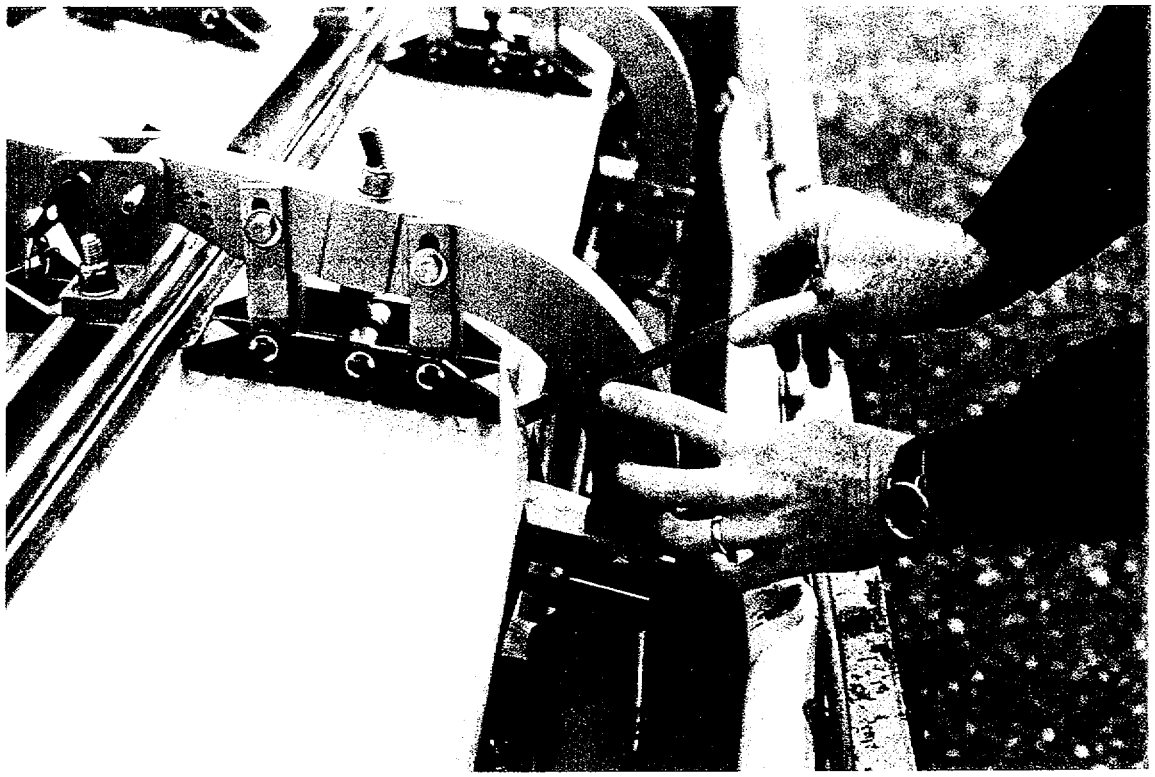

FIGURE 2-4.3-25 SIDE DROP ONTO PACKAGE CLOSURE

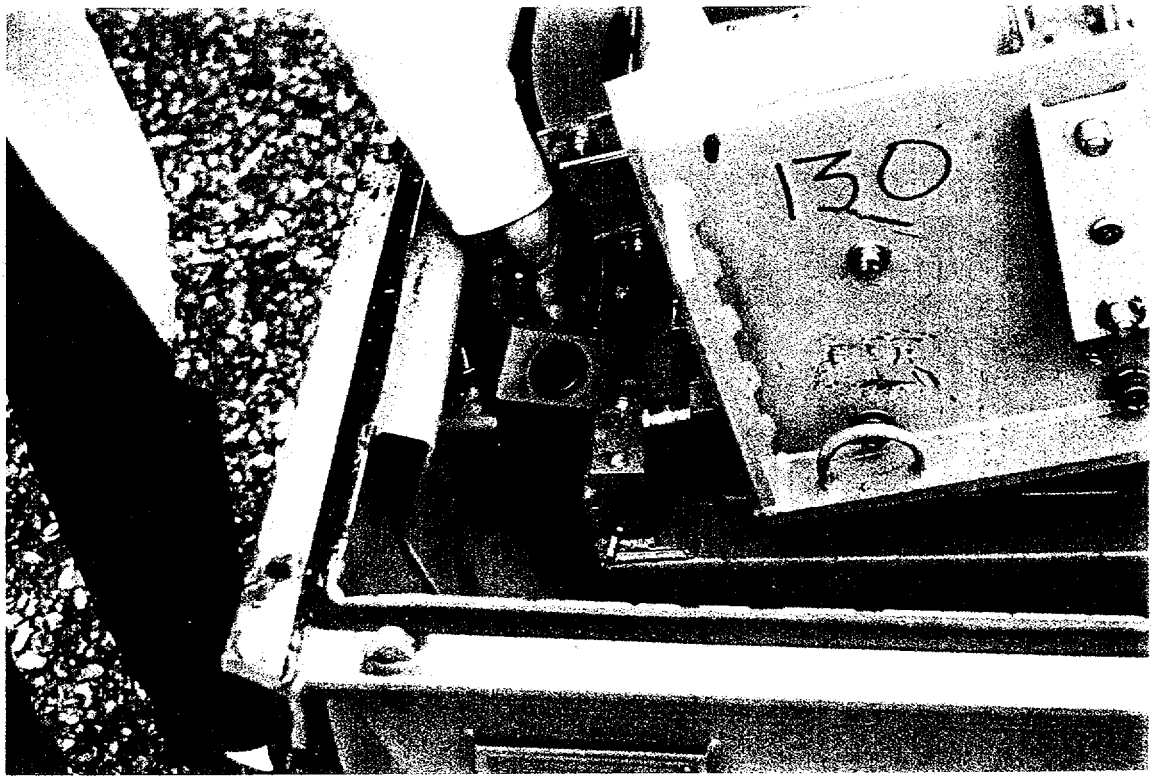

FIGURE 2-4.3-26 SIDE DROP ONTO PACKAGE CLOSURE

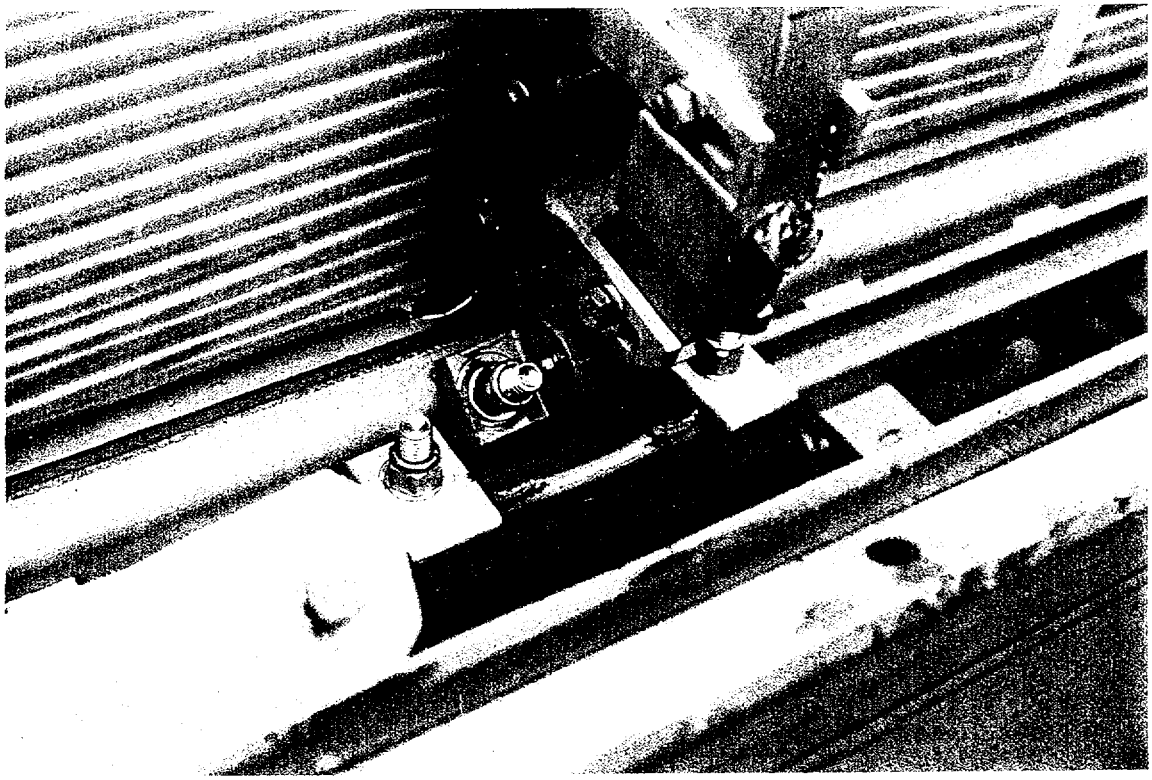

FIGURE 2-4.3-27 SIDE DROP ONTO PACKAGE CLOSURE